Maynooth University
National University of Ireland Maynooth

The Application of Robotics and Computer Vision to Post-Process Evaluation of Dairy Powder Rehydration

Behrad Mozafari

A dissertation submitted for the degree of Doctor of Philosophy

Maynooth University, Department of Electronic Engineering
Teagasc, Department of Food Chemistry & Technology

November 2024

Name of the Head of the Department: Prof. Gerry Lacey

Name of the Supervisors:

Dr Rudi Villing (Maynooth University)
Dr Norah O'Shea (Teagasc)

This thesis has been prepared in accordance with the PhD regulations of Maynooth University and is subject to copyright. For more information see PhD Regulations (December 2022)

Abstract

High rehydration quality is essential for infant formula (IF) powder. Existing rehydration tests lack objectivity and reproducibility. Furthermore, current studies into improving the objectivity of rehydration tests lack both integrated platforms and systematic analysis of end-user rehydration behaviour.

This thesis evaluated an automated approach to measuring the IF Powders rehydration quality. It was hypothesised that the approach would provide a better understanding of how human-like bottle agitation and powder physicochemical properties impact rehydration quality. First, a previously-developed robotic sample preparation prototype was integrated with a computer vision system to estimate sediment height, foam height, and number of white particles in rehydrated IF powders. Secondly, these estimates were compared to ratings from eight participants and modified laboratory reference tests. Finally, bottle agitations from ten participants were characterised using computer vision, and human-like robotic agitations were statistically learned.

The platform exhibited significant correlations with participants' ratings (> 0.68), modified reference tests (0.79 and 0.55 for sediment height and white particles, respectively), and platform duplicate measurements (> 0.87). While white particle correlation may necessitate further research, the results suggest the potential to provide automated objective results across laboratories. The platform's novel ability to monitor sediment height over time was used to develop a predictive model for rapid screening of dispersibility. The learned swirl agitation resulted in a lower foam height and higher sediment height than shake agitation suggesting that different end-users' rehydration styles may yield different rehydration qualities. Results also showed that participants applied less energy and lower amplitude to agitation in the swirl style than shake style. Taken together, these findings could inform future updates to international guidelines on powder rehydration (e.g., WHO).

The thesis contributions include: (i) the development of an objective automated platform, (ii) the improvement/development of reference/benchmarking tests, (iii) providing insights into rehydration, and (iv) characterising/learning human bottle agitations.

Declaration

I declare that this thesis is my own work and has not been submitted in any form for another degree or diploma at any university or other institution of tertiary education.

Information derived from the published or unpublished work of others has been acknowledged in the text and a list of references is given.

Sponsors

This research was supported by the Walsh Scholarship Programme co-funded by Teagasc (the Irish Agriculture and Food Development Authority) and Abbott Nutrition, and the MU HEA COVID-19 Costed Extensions Fund for three months, offered by the Higher Education Authority and the Department of Further and Higher Education, Research, Innovation and Science.

Publications

Journal Papers

- Mozafari, B., O'Shea, N., Fenelon, M., Li, R., Daly, D.F. and Villing, R., 2024. An automated platform for measuring infant formula powder rehydration quality using a collaborative robot integrated with computer vision. Journal of Food Engineering, 383, p.112229. https://doi.org/10.1016/j.jfoodeng.2024.112229

Peer-reviewed Conference Papers

- Mozafari, B., O'Shea, N., Fenelon, M. and Villing, R., 2022, June. Towards Image Processing-based Quantification of White Particles in Reconstituted Infant Formula. In 2022 33rd Irish Signals and Systems Conference (ISSC) (pp. 1-6). IEEE. https://www.doi.org/10.1109/ISSC55427.2022.9826210

Peer-reviewed Conference Abstracts

- B. Mozafari, R. Villing, M. Fenelon, N. O'Shea, 2023, November. Modification of Powder Rehydration Sediment Tests Tailored for Image Analysis Purposes. In 2023 SDT 80th Anniversary Conference: Digitalisation of Processing in the Dairy Industry. https://doi.org/10.1111/1471-0307.13066
- B. Mozafari, R. Villing, M. Fenelon, N. O'Shea, 2022, November. Image Analysis for Sediment Quantification in Rehydrated Infant Formula. In 2022 36th EFFoST International Conference (The European Federation of Food Science and Technology conference) (p. 541).

Journal Papers in Preparation

- Mozafari, B., Villing, R., Fenelon, M., Li, R., Daly, D.F. and O'Shea, N., Exploring the Impact of Infant Formula Powder Properties on Rehydration Quality Using an Automated Platform.

Acknowledgement

I am grateful that I had the opportunity to, once again, pursue my research aspirations. My family and grandparents have provided every possible support throughout my journey without any questions. I love you.

This interdisciplinary project required considerable patience, trust, and communication from my supervisors. I sincerely thank them for granting me the freedom to research. Their contributions and detailed feedback were essential to the success of this project.

The peaceful environment provided by my landlady was crucial to the success of this research. I will always be grateful for her kindness. Diane, thank you!

I would like to express my sincere gratitude to my friends, Anna, Aoife, Arianna, Barry, Caroline, Fatima, Grevet, Guangya, Homa, Hussain, Isaiah, Mark, Miriam, Ricardo, Rizwan, and my colleagues, Claire, David, Deirdre, Eoin, Farhad, Gayle, Honey, Iwana, Laura, Magdalena, Marion, Mark, Martina, Nigel, Noel, Nooshin, Nurdan, Philip, Runjing, Sarah, Sheila, Siobhán, Tanaka, Treasa, and Yonas. I am grateful for the breakfast chats with Dave, Ger, Gerard, and Mossie. I also thank Lindsey, Malcolm, Laura, Edel, Lynda, Josephine, Tom, Kim, and Katarzyna who cook, bake, or serve food with love.

I would like to express my gratitude to the welcoming staff of Fermoy Library. The positive environment they have cultivated in the library helped me to formulate my research ideas in Chapter 5. Thank you, Angela, Gemma, Lynda, and Majella.

During my time in Fermoy, I was also a member of two famous old groups. I am grateful to Fermoy Rowing Club, Orla, and Stephen; the peaceful Blackwater River became a place of profound thoughts. Also, thank you, Colette, Orla, Katherine, Tris, Jacqui, and other members of the vibrant and well-organised Fermoy Musical Society.

Finally, I am grateful for the time and effort that participants spent on this study.

Table of content

List of Figures

List of Tables

Glossary

D10, D50, D90: The diameter of an equivalent sphere below which 10%, 50%, or 90% of the particles are smaller by volume.

D[4, 3]: The volume-weighted mean diameter of particles in a distribution.

Degrees of Freedom: The number of independent movements possible in a mechanism or robot.

End Effector: The part of the robot at the end of the arm that interacts with the environment to perform specific tasks (e.g., grippers or welding torches)

Acronyms

Cobot: Collaborative Robot

CFD: Computational Fluid Dynamics

CI: Confidence Interval

CV: Computer Vision

DoF: Degrees of Freedom

DS: Dissolved Solids

DMP: Dynamic Movement Primitives

FFT: Fast Fourier Transform

GMM: Gaussian Mixture Model

HSI: hyperspectral imaging

HMM: Hidden Markov Models

IF: Infant Formula

IMU: Inertial Measurement Unit

ISO: International Organization for Standardization

IWMP: Instant Whole Milk Powder

LfD: Learning from Demonstrations

LOOCV: Leave-One-Out Cross-Validation

L*a*b*: Lightness (L*), green-red (a*), blue-yellow (b*)

MEMS: Micro-Electromechanical System

ML: Machine Learning

NRMSE: Normalised Root Mean Square Error

PAT: Process Analytical Technologies

PCA: Principal Component Analysis

PSD: Particle Size Distribution

RGB: Red, Green, Blue

RMSE: Root Mean Square Error

ROI: Region of Interest

RPM: Revolutions Per Minute

SDP: Slowly Dissolving Particles

SMEs: Small and Medium-sized Enterprises

SOP: Standard Operating Procedure

SW: Sediment Weight

TTS: Target Total Solids

WHO: World Health Organisation

WP: White Particles

Nomenclature

$\boldsymbol{A_i}$**:** Amplitude of the representative signal

$\boldsymbol{B}$**:** Bottle coordinate system (representing human hand)

$\boldsymbol{C}$**:** Camera coordinate system

$\boldsymbol{EE}$**:** End Effector coordinate system

$\boldsymbol{\mathcal{F}\{x(t)\}}$**:** Fast Fourier Transform

$\boldsymbol{F_{fa}}$**:** Feature components of frequency and amplitude

$\boldsymbol{f_i}$**:** Frequency of the representative signal

$\boldsymbol{K}$**:** Number of components in the GMM

$\boldsymbol{k^*}$**:** Index of the GMM component that best represents most of the agitation cycles

$\boldsymbol{m}$**:** Selected number of top frequencies from the magnitude spectrum of a signal

$\boldsymbol{M}$**:** Number of data points in a single demonstrated agitation cycle

$\boldsymbol{N}$**:** Number of demonstrated agitation cycles

$\boldsymbol{\mathcal{N}(F_{fa}|\mu_k, \Sigma_k)}$**:** Gaussian distributions with means μ_k and covariances Σ_k

$\boldsymbol{P(k|F_{fa,i})}$**:** Posterior probability of component k given the frequency and amplitude features of cycle i.

$\boldsymbol{\phi_i}$**:** Average of the phase of the representative signal

$\boldsymbol{R}$**:** Robot base coordinate system

$\boldsymbol{S}$**:** Scaling matrix

$\boldsymbol{T}$**:** transformation matrix

$\boldsymbol{T_i}$**:** Tags ($i = 1, \dots, 5$) coordinate system

$\boldsymbol{TCP}$**:** Tool Centre Point coordinate system

$\boldsymbol{(v_x, v_y, v_z)}$**:** Bottle linear velocity in axes x, y, and z

$\boldsymbol{W}$**:** World coordinate system

$\boldsymbol{w_k}$**:** Weights of the GMM model

$\boldsymbol{(\omega_x, \omega_y, \omega_z)}$**:** Bottle angular velocity in axes x, y, and z

$\boldsymbol{WObj}$**:** Work Object coordinate system

$\boldsymbol{X(f)}$**:** Signal in frequency-domain

Chapter 1: Introduction

1.1. Background and motivation

Infant formula (IF) powder is a source of nutrients for infants when breastfeeding is not an option (Renfrew et al., 2003; WHO, 2009). It is designed to mimic breast milk's nutritional profile and health benefits (Martin et al., 2016; Thompkinson and Kharb, 2007). Therefore, IF undergoes extensive quality control to ensure compliance with national and international standards (Martin et al., 2016).

A key powder property is its ability to completely and quickly dissolve in water when rehydrated by an end-user to form a homogenous solution (Crowley et al., 2016; Selomulya et al., 2023). However, it is challenging to achieve this ideal behaviour (Hogekamp and Schubert, 2003). Various rehydration stages influence powder rehydration, including wettability, sinkability, dispersibility, and solubility (Forny et al., 2011). The quality of rehydration stages depends on several factors, including water temperature, energy input during mixing or agitation, powder manufacturing methods (the processing steps and conditions used to produce the powder), and the composition and structure of the produced powder (Fitzpatrick et al., 2016; Forny et al., 2011). Powders with poor rehydration quality can exhibit several undesirable rehydration attributes such as sedimentation, excessive foam formation (Sharma et al., 2012), and persistent undissolved particles (Toikkanen et al., 2018) in the prepared mixture.

Powder rehydration tests used for quality assurance may be conducted using either standardised or in-house methods (Pisecky, 2012; Schuck et al., 2016). These tests are designed to measure powder rehydration stages or attributes such as dispersibility, wettability, solubility, and sediment volume (Sharma et al., 2012). However, these methods are primarily based on manual sample preparation and visual inspection, introducing subjectivity and poor reproducibility (Munir et al., 2017). Therefore, their results may vary depending on the energy input and agitation technique

(Schober and Fitzpatrick, 2005), and the subjective interpretation of the mixture post-rehydration (Munir et al., 2017). It is necessary to standardise measurements using an automated and quantitative approach to allow objective comparisons between different powders (Munir et al., 2017).

A powder that rehydrates well in a laboratory setting must also rehydrate well when prepared by an end-user (e.g., at home) (Fang et al., 2008). Therefore, during rehydration tests, it is important to consider the realistic conditions under which the powder is expected to dissolve (Jeantet et al., 2010; Richard et al., 2013). In some studies, the end users' preferences are taken into account when rehydrating the powder (e.g., Lloyd et al., 2019). However, despite certain studies attempting to quantify end-user error regarding the amount of powder or water used (Rosenkranz et al., 2024) or the water temperature (Grant et al., 2024), there has been no systematic evaluation of human bottle agitation to determine whether end-user agitation style affects rehydration quality. Additionally, bottle agitation preferences may be influenced by national or international recommendations for safe powder rehydration (Farrent et al., 2021; WHO, 2007), or by cultural and geographical habits (O'Shea et al., 2021). Quantifying end-user bottle agitation parameters (e.g., agitation energy, frequency, and amplitude) and understanding their impact on rehydration is a research gap that should be addressed to provide measurable insights for regulatory bodies (such as FDA and WHO) to improve their recommendations to end-users on optimal rehydration practices (cf. Farrent et al., 2021; WHO, 2007). A study of end-user bottle agitations would allow manufacturers to better understand powder rehydration behaviour based on end-user needs. It also helps in optimising production processes and evaluating batch consistency by objectively replicating end-user bottle agitation movements (e.g., using robotics). The number of studies characterising realistic agitations during powder rehydration is currently limited, and none appear to have been conducted around infant formula powder. Therefore, the importance of characterising bottle agitations during IF powder rehydration is understudied despite the fact that IF is a powdered food intended primarily for infants, who have

sensitive digestive systems (Bakshi et al., 2023), and deviations from optimal rehydration practices could adversely affect nutrient delivery (Farrent et al., 2021; Renfrew et al., 2003).

To address the subjectivity issue, some researchers have explored alternative methods for assessing rehydration quality. These include light transmission technology for sediment height measurement (Ji et al., 2016b), turbidity sensing (Gaiani et al., 2005) and static light scattering (Mimouni et al., 2009), FBRM (focused beam reflectance measurement) and ERT (electrical resistance tomography) (Xu et al., 2024) for monitoring the rehydration process, and computer vision (CV) for dispersibility (Ding et al., 2020b). Fang et al. (2008) suggest that these techniques, particularly those which incorporate a mix of emerging technologies, can be more objective, reliable, and reproducible than traditional qualitative methods, and can provide more insights into how powder rehydration quality can be increased.

Chapman (2003) suggested that robotics can increase productivity and efficiency by automating laborious and repetitive laboratory procedures in the food, agriculture, and pharmaceutical industries. Robots are expected to be employed more often in laboratories as they become “benchtop” or smaller, more affordable, and more modular (Chapman, 2003). In addition, several CV algorithms have been developed for the automatic inspection, classification, and quality assessment of food products (Aggarwal and Mohan, 2010; Farrera-Rebollo et al., 2012; Salazar-González et al., 2018; Villanueva et al., 2015). In contrast, only a limited number of studies have examined the use of robotics or CV in the analysis of IF powder rehydration (Ding et al., 2020b; Lloyd et al., 2019).

1.2. Research Objectives

The purpose of the work described in this thesis was to develop and validate an automated rehydration platform using robotics and CV system to assess the rehydration attributes of IF powders. The hypothesis was that CV algorithms could be used to objectively quantify foam height, sediment height, and undissolved particles, after standardised robotic rehydration, with repeatability approaching that of manual visual inspection.

The key research questions addressed were:

1. Is it possible to develop an automated platform that rehydrates the IF powder in a commercially available baby bottle, automatically captures images, and uses CV algorithms to quantify key rehydration attributes? The purpose of using a commercially available baby bottle is to provide similar conditions (e.g., fluid dynamics) to those presented by the end-user during rehydration.
2. Is there a relationship between automatically quantified rehydration attributes and traditional laboratory measurements conducted for characterising rehydration performance? It is expected that the answer to this question will provide insights into whether and how automated measurements can complement or replace traditional laboratory tests for foam, sediment, and unhydrated particles. Additionally, interpretation of the possible relationships between the automated measurements and the traditional measurements may provide new insights into the rehydration process.
3. Is it possible to develop a predictive model that estimates traditional measures solely based on automatically quantified rehydration attributes? Considering that such a prediction occurs simultaneously with estimating the rehydration attributes, it may be possible to save time or resources by providing predictive insights about the time-consuming laboratory tests.
4. Is it possible to characterise human bottle agitation behaviour using emerging technologies? It has been reported that different people may scoop different amounts of powder when given the same instructions. But what about agitation? Does bottle agitation, particularly agitation energy, differ significantly between individuals when the same instructions are given? If this is the case, it may impact the level of rehydration.
5. Is it possible to generate “human-like” bottle agitations with the robotic platform? Are the automated measurements of rehydration quality attributes similar after the robot performs human-like swirl and shake agitations? It would be ideal if there were no significant

differences, however, any possible difference may highlight the need for promoting (by regulatory bodies) agitation styles that facilitate the dissolution of powders.

1.3. Thesis scope

The scope of the thesis was limited to the following:

1. Only stage-1 infant formula powder was considered for rehydration.
2. Throughout the thesis, deionised water with a fixed volume and temperature was used as the liquid medium for rehydration. The volume and temperature of the water was controlled manually, not by the automated platform. However, the experiments were strictly controlled to ensure consistency in water volume and temperature (cf. Gribble et al., 2017). It was not within the scope of this thesis to examine the impact of changing water temperatures and volumes on rehydration.
3. Even though some pilot plant powders were used in this study as donations, no investigation was conducted on the effect of processing parameters on rehydration, and all discussions concerning this are based solely on laboratory physiochemical analyses of the produced powders. The scope of this thesis does not include the analysis of the direct relationship between the processing parameters and the rehydration attributes.
4. Only one type of commercially available baby bottle was used to rehydrate powder by the robot.
5. The scope of this thesis included the design and development of the whole vision system (including selecting all hardware components, developing software and algorithms, and integrating them with the robot, as a “benchtop” solution), and the development of “human-like” robotic agitations. The robot for the development of the automated platform was not selected as part of the current thesis. Although this robot could follow the learned bottle agitation paths, due to its motor torque limits, it could not match the frequency of the acceleration change in the learned trajectories. However, it could perform scaled-up versions

of these paths to achieve the same agitation energy as the learned trajectories. Furthermore, the robotic agitations used in Chapters Three and Four were those that had been developed by O'Shea et al., (2021). However, the programme was improved for the robot to communicate with the developed vision system and to rotate the bottle in front of the camera.

6. The automated measurements were based solely on the visible manifestations of rehydration attributes, and the robot used only an RGB camera as its only sensor. Investigations of the use of other types of cameras (such as thermal or hyperspectral cameras) or other types of lighting (such as ultraviolet or infrared) was outside the scope of this thesis.
7. This thesis investigated the effects of swirl and shake agitations on infant formula preparation, as described in the WHO white paper (WHO, 2007). Although there may be a variety of agitation movements in different countries (such as the figure eight agitation) (O'Shea et al., 2021), examining their effects was beyond the scope of this study.
8. It was outside the scope of the current thesis to investigate people's agitation preferences across different demographics. The participants who demonstrated bottle agitations were not intended to represent a specific group of people, such as parents or caregivers, or people from different cities or countries.

1.4. Thesis contributions

This thesis contributed to a better understanding of the rehydration process on the following fronts:

1. The development of an objective rehydration evaluation platform. The platform developed through chapter three was, to the best of our knowledge, the first automated rehydration analyser that combined robotics and a CV system.
2. The development of modified laboratory tests for benchmarking and evaluating the performance of the automated platform. The modified sediment weight test, in particular, performed better than traditional tests in the collection of finer fractions of sediment that would normally pass through the sieve in traditional tests.

3. The development of digitally-generated reference images in a systematic manner for participants' ratings of white particles. The method for developing these images or the images themselves may be useful in future studies. In the past, these images could not represent the range of observations that could be made in a laboratory environment, and they were created subjectively.
4. Obtaining deeper insights into rehydration using the automated platform and comparing its results with those of the laboratory tests. In particular, flowability was identified as an important factor in rehydration process. The powder's "flowing" is the first step in the rehydration process, before it is wetted.
5. Developing a predictive rehydration model for dispersibility (as an estimation and more rapid method than the standard test) based solely on automated measurements obtained from the developed platform. The platform could monitor sediment height changes over time for the first time in the literature and use this information in conjunction with sample colour for predicting sample dispersibility as a rapid screening method.
6. Characterising human bottle agitations and obtaining key end-users' agitation parameters for shake and swirl agitation styles. This study is the first to provide insight into the variability of agitation parameters, in particular the amount of energy applied by individuals. Researchers have already highlighted the importance of unintentional errors in rehydration, such as powder scooping behaviour or the water temperature.
7. Developing an in-house method for learning the dominant bottle agitation behaviour of participants for swirl and shake styles. Despite the natural diversity of agitation patterns in humans, this method provided a single representative agitation pattern for both swirl and shake styles. It enabled the robot to perform human-like agitations in a reproducible and objective manner. It was demonstrated for the first time in the literature that human-like swirl

agitation results in less dissolved solids than human-like shake agitation. According to the results, shake agitation increases the likelihood of powder rehydration by end-users.

1.5. Thesis outline

This thesis consists of six chapters intended to accomplish the following objectives:

- Chapter 1 (Introduction): provides an overview of the thesis including its objectives and research questions, scope, contributions, and structure.
- Chapter 2 (Literature review): reviews the latest research on understanding the requirements for ideal rehydration and emphasises the necessity of quantifying it, particularly by using an objective and automated method. This chapter includes a review of the latest applied solutions for objectively measuring rehydration of infant formula powders, dairy powders, food powders, or a wider range of powders, such as pharmaceutical powders. Furthermore, the latest robotic research in performing "human-like" movements was reviewed to determine whether these techniques could be applied to robotic powder rehydration agitations.
- Chapter 3 (Platform development): focuses on developing an automated rehydration and quality estimation platform by integrating a collaborative robot (cobot) and in-house CV system. In this chapter, details are provided on how the cobot mixed IF powder with water in a commercially available baby bottle and captured images of the resulting mixture. Additionally, it contains the method for developing three CV algorithms and applying them to the cobot-captured images of the prepared formula to estimate foam height, sediment height, and the number of undissolved particles. The chapter also evaluates the algorithms' performance against the ratings of eight participants on a random selection of the same images used by the automated platform.
- Chapter 4 (Platform evaluation) aimed to link the novel and objective estimates obtained using the platform developed in Chapter Three to traditional testing methods. The chapter involved:

(i) evaluating whether the automated quality ratings generated by the platform are consistent with the traditional laboratory measurements used to characterise rehydration performance; and (ii) developing a predictive data-driven model to estimate established measures solely based on automated quantification of rehydration attributes. In this chapter, two of the traditional tests needed modification to improve their resolution. The relationship between automated estimates and traditional measures provided new insights into the rehydration process.

- Chapter 5 (Towards standardised characterisation and robotic replication of human bottle agitation) sought to gain new understanding of end-user behaviours during rehydration, which is a critical consideration when developing standardised rehydration quality measurement methodologies. The chapter involved using a camera and an IMU sensor to record ten participants' hand movements during bottle agitation. IMU data were only recorded as a contingency measure and proved unnecessary as the camera data were of sufficient quality for analysis. The key attributes of human bottle agitations were identified. A learning from demonstration technique was developed for the robot to mimic the dominant pattern in human swirl and shake bottle agitations, yielding statistically learned "human-like" robotic agitations. Finally, the chapter used the CV algorithms developed in Chapter 3 to compare the effects of different "human-like" agitations on rehydration. Further study of this difference in rehydration quality would benefit both companies and regulating bodies.
- Chapter 6 (Concluding remarks): summarises the findings of the PhD and suggests avenues for future research.

Chapter 2: A review of quality assessment of infant formula powder rehydration using emerging technologies

A manuscript based on this chapter is being prepared for submission to Trends in Food Science & Technology as:

- *Mozafari, B., Villing, R., and O'Shea, N., A review of quality assessment of infant formula powder rehydration using emerging technologies*

2.1. Introduction

Most food powders must be mixed with water or other liquids before consumption (Fitzpatrick and Ahrné, 2005). Rehydration, however, is a complex process impacted by a wide variety of parameters (Richard et al., 2013), and identifying these parameters and understanding their interrelationships is challenging (Hogekamp and Schubert, 2003; Selomulya et al., 2023). It has been suggested that the use of emerging technologies for monitoring various aspects of rehydration can prove useful in gaining a better understanding of powder rehydration (Fang et al., 2008).

The present chapter provides an overview of the application of emerging technologies in two aspects of rehydration: i) mixing, and ii) evaluating the quality of the prepared mixture. Particularly, it reviews studies that attempt to make mixing methods more realistic and reproducible as well as methods for objectively evaluating rehydration quality. When applicable, this review is expanded to include dairy, food, or other similar (e.g., pharmaceutical) powders, and conclusions are drawn regarding potential applications in infant formula powder. The purpose of this expansion is to overcome the limitations of existing studies, especially for the rehydration of infant formula powder (the limitation may have resulted from inherent challenges associated with food digitalisation, such the volatility of the sector's requirements (Demartini et al., 2018)).

The chapter begins with highlighting some current limitations in understanding rehydration and highlighting the review questions. Robotics and image analysis are then discussed as emerging technologies that are trending in current literature on food digitalisation (Demartini et al., 2018; Meenu et al., 2021). Robot Learning from Demonstration, which is a technique that has become increasingly popular in robotics research (Ravichandar et al., 2020), is discussed as a possible tool for performing realistic mixing. Then the chapter concludes with final remarks and a discussion of the potential benefits of integrating emerging technologies (Fang et al., 2008; Munir et al., 2017) to address current research challenges.

2.1.1. Importance of studying powder rehydration

Most materials manufactured by process industries are in the form of particles (Seville et al., 2012). Mixing powders with liquids is an important research topic for a wide range of applications (Nelson, 2012). For example, in the food (Selomulya et al., 2023), drugs (Khadka et al., 2014), and fertiliser (Duan et al., 2023) industries, understanding powder rehydration mechanism is critical to ensuring that materials (e.g., nutrition or drugs) can be delivered as intended during powder design (e.g., expected delivery time and dilution).

In the food industry, drying has been a traditional method of improving the efficiency of processing, packaging, storage (increased shelf-life and less occupied space), and easier transportation of products (Rahman, 2020). The powdered form of dried food is popular since it occupies even less space which makes storing and transporting food products easier (Bhandari et al., 2013; Skibsted et al., 2010). As a result, throughout history, a wide variety of food powders (e.g., flour made from different grains, milk powder, salt, and spices) have been developed for industrial or domestic use (Bhandari et al., 2013; Kelly et al., 2003).

2.1.2. Food powder rehydration

Domestic and industrial applications of food powders are broad, and in most cases, the powders must first be dissolved in a liquid medium (e.g., water) before use (Fitzpatrick and Ahrné, 2005). Food powders may contain oil and other ingredients that are not water-soluble, which may make water interaction difficult (Hogekamp and Schubert, 2003). It is therefore necessary to investigate how different food particles may be given the opportunity to interact with water and become rehydrated (Bhandari et al., 2013; Hardy et al., 2002). The rehydration process can be affected by liquid and mixing conditions, as well as the chemical composition and physical structure of the food powder (Richard et al., 2013). For different food powders, there may be a different mixing energy or water temperature required for a quick and complete rehydration, depending on how much fat or protein is present in the powder (Fitzpatrick et al., 2016).

Food powder rehydration is considered to be a complex process (Parthasarathi and Anandharamakrishnan, 2014). The process has mainly been classified into three (Ji et al., 2016b) to four (Fang et al., 2008; Ji et al., 2016b; Schober and Fitzpatrick, 2005) stages, namely wetting, sinking, dispersing, and dissolving (Figure 2-1). Assuming that the liquid and mixing conditions remain unchanged, the powder performance at each of the four stages is often considered to determine its rehydration quality (Schuck et al., 2012). However, due to their overlap, observing these stages independently is difficult (Selomulya et al., 2023).

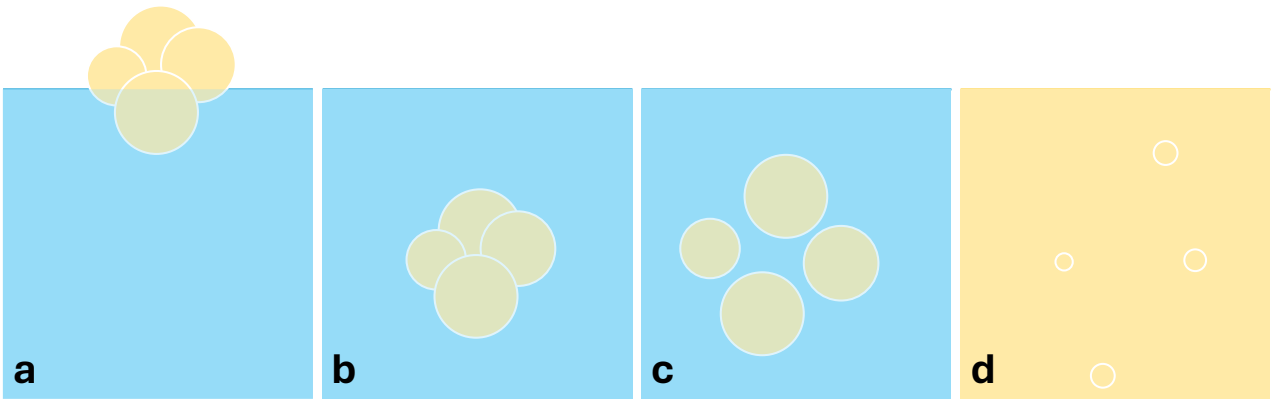

Figure 2-1 Rehydration of powder particles is typically characterised by four stages: a) wetting, b) sinking, c) dispersing, and d) dissolution

Further to the liquid properties (Hardy et al., 2002) and mixing energy (Schober and Fitzpatrick, 2005) mentioned earlier, powder properties themselves play a significant role in the rehydration process (Masum et al., 2020). There is evidence that powder behaviour during the rehydration stages is influenced by physical (structure dependent) and chemical (composition dependent) properties of the powder (Schober and Fitzpatrick, 2005), referred to as physiochemical (also known as physico-chemical/physicochemical) properties (Kelly et al., 2002). There have been several studies investigating how powder production methods can affect powder physicochemical properties (Kelly et al., 2002; Kim et al., 2009; Vignolles et al., 2007), as well as how powder physiochemical properties can impact the rehydration stages (Andersson et al., 2019; Forny et al., 2011; Ji et al., 2016a; Schober and Fitzpatrick, 2005). Some other studies have attempted to directly relate the quality of rehydration with manufacturing parameters (Felfoul et al., 2020; Ji et al., 2016b, 2016a; Nugroho et al., 2021; Rodríguez Arzuaga et al., 2021; Warncke and Kulozik, 2020) or predict the rehydration quality to optimise the powder production quality (Rimpiläinen et al., 2015).

2.1.3. Importance of infant formula powder

As mentioned in the introduction chapter, IF is a manufactured food designed to serve as a nutritional substitute when human breast milk is unavailable or insufficient. With comparable composition and biochemical characteristics to human breast milk, IF is intended to provide adequate nutrition for infants from birth to three years of age (Bakshi et al., 2023; Thompkinson and Kharb, 2007). This particular type of food powder may be the sole source of nutrition for many infants, which makes its significance even greater (National Academies Press, 2004). For this reason, it is strictly regulated by governing bodies (CFR, 2024; Codex, 2023; EUR-Lex, 2016). Additionally, the production rate of IF powder continues to increase. The sector is projected to grow at a compound annual growth rate of over 10% between 2022 and 2030, driven by increases in the number of mothers who work, malnutrition cases, premature birth, middle-class growing incomes, and concerns about infant

nutrition (Bakshi et al., 2023). In 2022, the global IF market reached 68.2 billion USD, with Asia Pacific leading in sales, and is expected to surpass 174.6 billion USD by 2032 (PR, 2023).

2.1.4. Importance of proper rehydration of infant formula powder

An important quality parameter of IF is its solubility in water (cf. Selomulya et al., 2023). Infant nutrition can be significantly impacted by improper rehydration (Fein and Falci, 1999; Gribble et al., 2017; Renfrew et al., 2003; WHO, 2007), potentially causing dehydration (Sunderland and Emery, 1979), adiposity (Altazan et al., 2019; Farrent et al., 2021), or reducing feed concentration and delivery of targeted nutrients (if the dissolved solids in water are less than the intended amount), thus compromising infant growth (FDA, 2024; Fein and Falci, 1999; Renfrew et al., 2003). The mixing guidelines typically instruct shaking or swirling the bottle "gently" until the powder is completely dissolved (MOH, 2022; WHO, 2007), in hot water ≥70°C to reduce the risk of bacterial contamination (Grant et al., 2024; WHO, 2007). While certain agitation styles may be more prevalent in particular geographical regions (O'Shea et al., 2021), it has been shown that different mixing energies and agitation styles may result in varying amounts of powder being dissolved (Mozafari et al., 2024; Schober and Fitzpatrick, 2005).

2.1.5. Undesirable infant formula rehydration attributes

Ideally, the rehydrated IF powder should resemble human milk in both appearance (cf. Pisecky, 2012) and compositional profile of proteins and minerals (Crowley, 2016). In practice, it is almost always possible to observe undesirable rehydration attributes after powder rehydration (Pisecky, 2012); and reducing one may result in increasing another (Mozafari et al., 2024). Figure 2-2 illustrates some of the undesirable rehydration attributes.

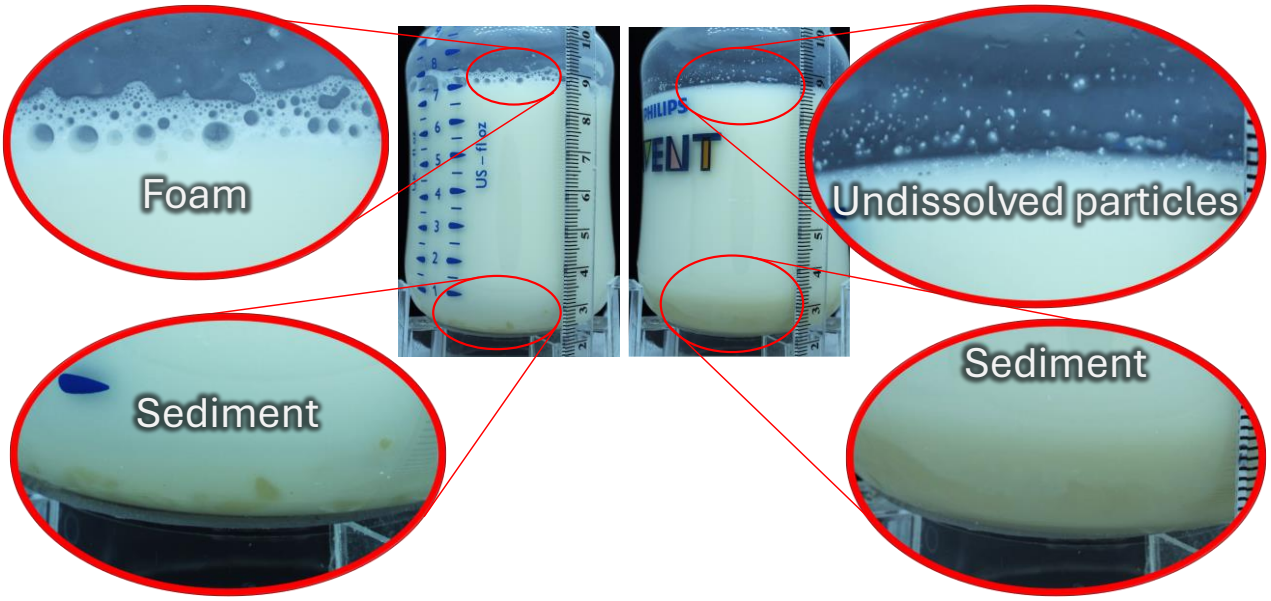

Figure 2-2 Three examples of undesirable rehydration attributes: foam, sediment, and undissolved particles

Any foam or poorly soluble powder in rehydrated IF powder is undesirable (Masum et al., 2020). For example, undissolved particles, including damaged or slowly dissolving particles, may remain after rehydration (Lloyd et al., 2019; Toikkanen et al., 2018). Also, the release of protein into the solution can be limited if the powder forms sediment rather than being homogeneously dispersed and dissolved (Fang et al., 2011). If solubility, which can be considered the most critical stage of rehydration (Selomulya et al., 2023), is poor or insufficient energy is applied during rehydration, sediment may form (Fitzpatrick et al., 2016; Mozafari et al., 2024). Foaming is another undesirable rehydration attribute, as it may lead to aerophagia (Huppertz, 2010), which is deemed to contribute to infantile colic (Daelemans et al., 2018). Even though energetic agitation may help dissolve more solids, it may also result in a greater amount of foam being produced (due to the ingress and trapping of air during agitation) (Mozafari et al., 2024). Thus, powder rehydration should ideally be achieved with the least amount of agitation energy (Richard et al., 2013), emphasising the importance of understanding how powder physicochemical properties affect rehydration.

2.1.6. Scope of the present review

This narrative literature review aims to: i) review the limitations of commonly used manual methods; ii) evaluate robotics as a means of obtaining repeatable sample preparation agitations; iii) discuss the use of computer vision techniques for quantitative evaluation of IF rehydration quality attributes; and iv) explore how human bottle agitation techniques may be transferred to robotic platforms using techniques such as learning from demonstration to obtain realistic rehydration tests based on powder end-user bottle agitation behaviour. The review will finally discuss the major gaps and challenges associated with integrating emerging technologies into IF rehydration analysis.

2.2. Challenges associated with understanding IF powder rehydration

To evaluate the rehydration performance of IF powder, several reference tests are available, either as standards (such as ISO: International Organization for Standardization or IDF: International Dairy Federation (Tamime, 2009)) or in-house methods, sometimes confidential (Pisecky, 2012), developed by manufacturers or research institutions (such as the test described by Lloyd et al. (2019)). However, using these methods, the main rehydration stages are assessed manually by human analysts, prone to subjectivity (Munir et al., 2018; Rimpiläinen et al., 2015) and with limited repeatability (Munir et al., 2017; Pisecky, 2012; Selomulya et al., 2023). Also, when the commonly used rehydration tests are subjective to the analysts who has conducted them (Lloyd et al., 2019; Pisecky, 2012), there is uncertainty finding the source of observed rehydration attributes. Yet, understanding the complex interaction between water and IF powder is necessary to optimise the rehydration process and minimise the variation in the nutritional and functional properties of the resulting mixture (Boiarkina et al., 2018; Hardy et al., 2002; Schuck et al., 2016).

Usually, IF powder is produced by dissolving or dispersing ingredients such as lactose, protein, and oils in water or skim milk, adding minerals, vitamins, and emulsifiers, followed by heat treatment, homogenisation, and spray drying with high hygienic standards (Pisecky, 2012). The formulation

before drying, drying method, powder handling, transportation, and storage can all influence powder physiochemical properties (Masum et al., 2020) and, subsequently, its rehydration quality (Schuck et al., 2016). From the production perspective, both formulations and production parameters of powder can play a role in the physicochemical properties and, as a result, in the rehydration quality of the powder (Rodríguez Arzuaga et al., 2021). Due to the large number of factors involved in powder production, it can be difficult to pinpoint the source of some observed rehydration attributes (Richard et al., 2013). Despite these challenges, the manufacture of high-quality IF powder requires a thorough understanding of the relationship between the starting formulation, processing conditions, and the final powder rehydration properties (Munir et al., 2018). Understanding these relationships can inform manufacturers when to make process adjustments and produce IF powders with consistent rehydration properties (Munir et al., 2017).

The formulations are becoming increasingly complex, as manufacturers strive to tailor their products to meet specific digestion needs and better mimic the protein profile of breast milk (Schuck et al., 2016; Walshe et al., 2021). The produced powder contains macronutrients, e.g., proteins, fats, and carbohydrates, as well as micronutrients, e.g., vitamins (e.g., A, D, E, K) and minerals (e.g., iron, calcium, zinc), and other additives important for brain development (Masum et al., 2020; Thompkinson and Kharb, 2007). The formulation complexity presents challenges for achieving optimal rehydration process (Masum et al., 2020; Schuck et al., 2016). For example, powder surface composition can affect its wetting time (Kim et al., 2002) and solubility (Fang et al., 2008); protein interactions during rehydration or drying process can impact sedimentation (Schuck et al., 2016; Toikkanen et al., 2018) and foam formation (Bals and Kulozik, 2003); and powder particle size distribution and agglomeration can influence its sinkability (Schober and Fitzpatrick, 2005) and dispersibility (Gaiani et al., 2011). Proteins provide essential amino acids required for growth and can be obtained from plant sources (such as soy) or bovine milk (Masum et al., 2020). However, the source of protein can significantly impact the rehydration quality (Le Roux et al., 2020). Although

protein content can directly impact the rehydration process (Ji et al., 2016b), the protein content of various IF powders may vary, mainly due to variations in amino acid compositions and the digestibility of different protein types (Masum et al., 2020). Fat is intended to supply 40-50% of infants' energy needs (Masum et al., 2020), but is inherently insoluble in water. Carbohydrates (mainly lactose) are also a vital source of energy, contributing to gut health by supporting the growth of probiotic bacteria (Masum et al., 2020).

In addition to formulation, several manufacturing parameters can significantly affect IF powder rehydration quality; these include homogenisation pressure, number of passes, heat treatment (temperature and time), spray drying conditions (inlet/outlet temperatures, type of atomiser, and speed), powder handling and packaging methods, storage time, and relative humidity (Sharma et al., 2012; Thompkinson and Kharb, 2007; Toikkanen et al., 2018). The wide variety of processing parameters and formulations can make understanding IF rehydration difficult.

Apart from the physiochemical properties of powders, the tests themselves are labour-intensive, time-consuming, and subjective (Ding, 2021). Typically, human analysts manually perform sample preparation following specific procedures including the amount of powder, the method of mixing, and the duration of mixing or pausing (Pisecky, 2012). Rehydration variables such as power (energy and time) and vortex formation influence the rehydrated sample (Schober and Fitzpatrick, 2005). Consequently, inherent subjectivity and variability across analysts can lead to inconsistency in experimental outcomes (Fang et al., 2008), even in tests evaluating the four main rehydration stages, wettability (Gaiani et al., 2005; Wu et al., 2021), sinkability (Pisecky, 2012), dispersibility (Munir et al., 2018), and solubility (Gaiani et al., 2005; Schuck et al., 2007). In light of the variability of human bottle agitation factors (e.g., agitation time or energy) and the environment (e.g., change in instruments), as well as the limitations of the reference tests (e.g., low discretisation based on only a limited number of classes (e.g., reference images)), standardisation of measurements between

different laboratories and analysts is often difficult (Lloyd et al., 2019; Munir et al., 2017), which limits their application for optimising manufacturing processes (Lloyd et al., 2019).

While the mixing method used in manual experiments can affect the rehydration process (Fitzpatrick et al., 2017; Pisecky, 2012; Schober and Fitzpatrick, 2005; Wu et al., 2021), a wide variety of mixing methods (including stirring (Jeantet et al., 2010), impelling (Schober and Fitzpatrick, 2005), and sonification (McCarthy et al., 2014)) have been employed to explore the impact of mixing on powder rehydration process. While examining powder-water interactions according to the end-user agitation behaviour is necessary (Hardy et al., 2002), and some recent studies have attempted this (Lloyd et al., 2019; O'Shea et al., 2021), no systematic analysis has been conducted to determine whether current mixing methods and human agitation are comparable. Due to the sensitivity of rehydration to the mixing method and the variety of mixing methods, achieving reproducible measurements of rehydration attributes (such as slowly dissolving particles and dispersibility) can be difficult (Boiarkina et al., 2018), especially across laboratories (Lloyd et al., 2019).

2.3. Robotic systems in food sector

Robotics is one of the key technologies for food digitalisation (Lezoche et al., 2020) and Industry 4.0 (Akyazi et al., 2020; Muhuri et al., 2019). It is expected to increase productivity, quality, flexibility, traceability, and consistency, as well as enable the execution of sensitive, harsh, or constrained tasks (Wallin, 1997). The food industry is increasingly demanding robots for analytical automation, provided they can handle complex decision-making and perform challenging pick-and-place operations (Klerkx and Rose, 2020; Wallin, 1997). Klerkx and Rose (2020) identified robotics as a recent trend for enhancing sustainability through the digitalisation of the food industry.

While robotics has existed since the 1950s (Estolatan and Geuna, 2019), its application in the food industry has been relatively limited until the last three decades (Bader and Rahimifard, 2018; Bogue, 2009; Caldwell, 2013; Fernando et al., 2016; Khan et al., 2018; Müller et al., 2014; Wallin, 1997, 1995; Wilson, 2010). Among the main concerns for their adoption are cost and return on

investment, hygiene requirements, and challenges in handling food due to texture (pliable, fragile, and sticky) and size or shape variations of food products, sometimes caused by seasonal changes (Caldwell, 2013). Traditional industrial robots typically lack more advanced sensors and control algorithms and must often be deployed in cages or behind safety barriers (Iqbal et al., 2016). Programming them may require considerable time and expertise (Villani et al., 2018). Collaborative robots (cobots) are designed to alleviate these limitations, featuring relatively lightweight components, more sensitive sensors (e.g., force/torque), and intuitive programming (Bloss, 2016). This is of particular importance to small and medium-sized enterprises (SMEs) (Hentout et al., 2019).

In recent years, robotic systems in food processing have progressed considerably, with applications in fresh produce, meat and poultry, and baked goods. For example, robots and cobots have been used for harvesting, cutting, packaging, and palletising. For handling fluids, soft, or granular materials, robotic end-effectors such as suction cups, jamming grippers, and scoops may allow flexible pick-and-place of irregular shapes (Wang et al., 2022). However, a quantitative measurement of the "engineering" properties of food (e.g., weight and texture) is required for the design of end-effectors, particularly for bin-picking and pick-and-place applications in 3D environment without compromising food quality (Wang et al., 2022). Through sensors and feedback loops, robots can be programmed to consistently dispense liquids and powders in small quantities (Fermier et al., 2003; Wakchaure et al., 2023; Wang et al., 2022) and automate different steps involved in sample preparation, including weighing, mixing, and diluting (Fermier et al., 2003). In comparison with manual methods, they can dispense experiment material with less error (Rodriguez-Gonzalez et al., 2019). The improved repeatability in the experiments can prove especially useful in IF rehydration tests since scooping IF powder manually may involve considerable error (Altazan et al., 2019). More advanced control systems may enable the robot grasping to adapt to food stiffness, shape, weight, fragility, and surface characteristics (Bader and Rahimifard, 2020; Wang et al., 2022). These control systems can monitor and regulate robotic interaction with the environment, such as grasping force

and speed (Caldwell, 2023; Wang et al., 2022). In this way, they may be able to provide a more consistent powder scooping in IF rehydration tests.

2.3.1. Robotics in the measurement of IF rehydration quality

O'Shea et al. (2021) assessed the feasibility of using a cobot to approximate the movements of human agitation while rehydrating IF powder. The cobot simulated four agitation motions: up and down, left to right, swirl, and figure 8. However, the study did not compare the robot's agitation styles to those performed by humans.

Although limited in the dairy industry, other sectors have used robotics for food quality measurements. For example, for evaluation of beer quality, Gonzalez Viejo et al. (2016) developed RoboBEER to minimise the variability associated with manual beer pouring. The robot was integrated with video recording (via a mobile phone) and semi-automated computer vision algorithms in MATLAB to measure foaming properties (maximum foam volume, foam lifetime, drainage, and bubble size). The sensors recorded the beer's colour, alcohol content, temperature, and amount of carbon dioxide released. The results of measurements obtained using RoboBEER were used to classify beers based on their quality and fermentation type.

Despite the challenges, the use of robotics is anticipated to reduce variability in IF rehydration (Duong et al., 2020; Lloyd et al., 2019; O'Shea et al., 2021). In light of the complexity and high subjectivity of some of the current rehydration tests, such as dispersibility (Pisecky, 2012), using a robot that mimics an expert operator may increase the repeatability of the experiments (Misimi et al., 2018).

2.4. Automating the rehydration of IF powder and the assessment of rehydration quality

Despite the importance of understanding the rehydration stages in the food powder industry, it remains difficult to quantify them (Selomulya et al., 2023). Quantitative (Fang et al., 2008), and

digital (Munir et al., 2017) approaches are expected to provide more objective tests and enhance understanding of the rehydration behaviour of new formulations.

Several studies have been conducted on automating rehydration or the measurement of the rehydration quality. Fang et al., (2008) evaluated different methods commonly used in assessing the rehydration properties of food powders, with emphasis on dairy powders. They also discussed several other emerging methods devised to overcome the limitations they identified, such as dynamic wetting measurements and turbidity sensors. However, they stated that many of these technologies still have imperfections (e.g., need for specific experiment conditions and inability to provide complete characterisation alone), and different types of food commodities may require objective quality tests for their specific end use.

To address the lack of repeatability in dispersibility measurements, Boiarkina et al., (2017) used two methods to measure particle size: sieving and laser diffraction, each with its own prerequisite. In sieving, upper and lower limits for fine and coarse particles were used, whereas laser diffraction only incorporated the fine particle limit. They found that the particle sizing technique could predict the dispersibility of in-specification powders with 97% accuracy. However, the method had a high false positive rate of 50% when predicting out-of-specification powder.

In an attempt to reduce the subjectivity of sediment tests, Rimpiläinen et al., (2015) predicted sediment values of milk powder using manufacturing data from an industrial plant. Using traditional offline laboratory analysis, 13 specific plant variables, such as milk flow, total solids, pH, and dryer temperature and pressure were selected as independent predictors. They applied a conditional probability distribution to production data from four subsequent seasons. It was concluded that the trained model could be applied to controlling sediment values in rehydrated milk powder.

Henihan et al. (2019) investigated a fluorescence-based analyser for rapid quantification of soluble proteins. Compared to reference methods, their approach provided faster results. However, the reproducibility was affected by rehydration time, especially for non-agglomerated powders.

Consequently, they recommended developing a standard protocol for rehydrating samples. In a related study, Henihan et al. (2018) suggested that powder fluorescence properties could be used to estimate parameters such as powder storage time, soluble protein content, and surface-free fat.

Lloyd et al., (2019) developed a mixer that mimicked end-user rehydration and an image analysis method to objectively quantify bulk particles in slowly-dissolving particle analysis. The developed method was then evaluated against an in-house laboratory test. While a mixer was used for sample preparation and computer vision was used to count the number of undissolved particles, the image analysis involved manual threshold adjustment. Because of this manual adjustment, there may still be some degree of subjectivity in the measurement process.

There are still several gaps in current infant formula rehydration assessments, including poor reproducibility (Fang et al., 2008; Selomulya et al., 2023), the absence of systematic end-user rehydration characteristics (Hardy et al., 2002; Lloyd et al., 2019), and the failure to fully consider the influence of powder physicochemical properties on the rehydration process (Rimpiläinen et al., 2015). Due to the unreliability of the current tests, several "proxy measurements" (e.g., predicting powder dispersibility solely by its particle size) (Boiarkina et al., 2017) have been developed. However, these approaches also have some limitations, including the underrepresentation of systematic characterisation of end-user rehydration practices (Lloyd et al., 2019) and limited alignment with lab measurement results or false positive rates under certain conditions (Boiarkina et al., 2018; Lloyd et al., 2019). Objective rehydration tests that take into account real-world conditions are still required (Hardy et al., 2002; Lloyd et al., 2019). This can improve the consistency of powder production from batch to batch (Caldwell, 2013).

2.5. Computer vision-based food quality measurement

CV systems have also been increasingly used in objective food quality assessment (Duong et al., 2020) and food safety (Mc Carthy et al., 2018). Until a few decades ago, the high cost of camera sensors restricted the application of CV systems in the food industry (cf. Pedersen, 1991). Since food

exhibits a variety of shapes and colours, using CV methods can be challenging (Patel et al., 2012). However, thanks to recent advances in software and hardware, this approach has become more ubiquitous (Meenu et al., 2021).

There is considerable potential for the use of CV techniques to objectively assess the quality attributes of food and agricultural products (Brosnan and Sun, 2004; Ma et al., 2016; Mery et al., 2013; Patel et al., 2012; Wu and Sun, 2013). Such systems allow for non-destructive, fast, and cost-effective quality assessment solutions that are less subjective than manual visual inspections (Patel et al., 2012). Many food products including fruits, vegetables, meats, bakery products, grains, and dairy products (Brosnan and Sun, 2004; Ma et al., 2016; Patel et al., 2012), have been inspected using image analysis for surface roughness, colour, size, shape, or contaminants (Ma et al., 2016). This method also has been applied to quantify quality attributes of dairy products, such as foam stability in milk (Xiong et al., 2020), counting lumps (Mitchell et al., 2020), unhydrated particles (Lloyd et al., 2019; Mozafari et al., 2022), and foam (Mozafari et al., 2024) after powder rehydration. Also, integrating CV systems with robotics is a promising approach to enhance the automation and objectivity of food quality evaluations (Mozafari et al., 2024).

CV can process colour data at the pixel level, calculate the mean and standard deviation of colour, quantify the area and colour of irregular shapes, identify specific regions of interest, analyse multiple objects, and create colour distribution maps (Wu and Sun, 2013). These systems can analyse various quality attributes such as size, shape, colour, and texture at high speed and with a high degree of accuracy (Brosnan and Sun, 2004; Ma et al., 2016; Wu and Sun, 2013). The classical measurement process using this method comprises image acquisition, image pre-processing, image segmentation, feature extraction and selection, and classification (Mery et al., 2013; Patel et al., 2012). During the preprocessing step, some common problems such as geometric distortions, focus issues, noises, and non-uniform illumination may be corrected (Brosnan and Sun, 2004).

As illustrated in Figure 2-3, a typical CV system for evaluating food quality consists of five main components: lighting, lens, camera, computer hardware, and software (Ma et al., 2016; Patel et al., 2012; Wang and Sun, 2002).

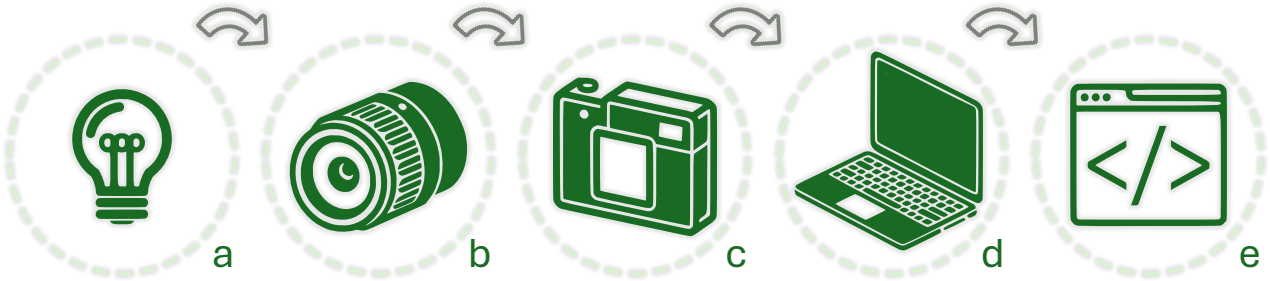

Figure 2-3 Components of computer vision systems: (a) light source, (b) lens, (c) camera, (d) hardware, and (e) software

Selecting the camera, lens, and lighting, is influenced by the specific food inspection problem and affects the system's performance (Brosnan and Sun, 2004; Ma et al., 2016; Mery et al., 2013; Patel et al., 2012; Wu and Sun, 2013). For example, the camera resolution can have a significant impact on the quality of the image and the visibility of the defect being inspected (Cubero et al., 2011). Also, the illumination should be designed carefully as it directly relates to the image quality and accuracy of the entire system (Brosnan and Sun, 2004; Patel et al., 2012). Some of the factors in illumination design include type of light (incandescent, fluorescent, LED), the lighting configuration (backlighting, front lighting, side lighting) and the lighting model (point lighting, diffuse lighting) (Patel et al., 2012). For example, front lighting is used to measure surface features (e.g., apple defects), while backlighting is used to measure sub-subsurface or edge features (e.g., the size of chicken pieces) (Brosnan and Sun, 2004).

The software algorithms for CV are mainly divided into classical and Machine Learning (ML) approaches (O'Mahony et al., 2019). Generally, classical approaches require less data for software development and have a lower computational cost during algorithm development. However, they may also be subject to the effects of the surrounding environment, including lighting and camera settings. ML techniques, on the other hand, require more training images to learn how to identify patterns within pixels. However, since these techniques statistically "learn" the patterns based on real

examples, they can be expected to provide greater performance flexibility. A possible issue is that some machine learning approaches are not easily interpretable, which can make it difficult to identify the cause of the weak algorithm performance.

Both monochrome and colour cameras have been applied in several areas in the food industry (e.g., colour cameras for the detection of specific fruits or meat quality inspection and monochrome cameras for the detection of their defects) (Brosnan and Sun, 2004). Other imaging techniques that have been applied to milk powder or other food quality assessment include hyperspectral (Khan et al., 2020), ultrasound, infrared, CT (computed tomography), MRI (magnetic resonance imaging) (Ma et al., 2016), and X-ray imaging (Caldwell, 2023). High-resolution array cameras and CV systems, along with advanced signal processing devices such as FPGA chips, are used for real-time quality measurements, product sorting, and hygiene inspection (Wakchaure et al., 2023) from receipt of raw materials to the final packaged products (Caldwell, 2023).

2.5.1. CV based sensing of powder or rehydration attributes

The quality of IF powder has been quantified using various image analysis approaches. For instance, Munir et al. (2018) used hyperspectral imaging (HSI) for real-time monitoring of milk powder quality. Based on the HSI results, it was possible to classify powder functional characteristics and the factory they originated from. The authors pre-processed hyperspectral data and identified/removed artefacts from the images. The data was normalised using a standard normal variate and cleaned using a grey-level co-occurrence matrix. Using Principal Component Analysis (PCA) and partial least squares regression, the HSI data successfully discriminated between different samples. The partial least squares regression method was successful in predicting moderate levels of accuracy for dispersibility, which is a fundamental functional property. However, according to the authors, HSI has certain limitations in the analysis of milk powder samples. For example, compared to other food powders, milk powder has a consistent texture and subtle colour variations that are difficult to distinguish.

Ding et al., (2020) used image analysis to quantify the effects of particle shape on dispersibility. They tested four brands of Instant Whole Milk Powder (IWMP) and sieved the powders into three size categories (< 180 μm, 180-355 μm, and > 355 μm). The images were captured using light microscopy, and the geometric descriptors were determined by MATLAB image processing. The dispersibility was determined using the New Zealand Dairy Board method (Pisecky, 2012). PCA, partial least squares regression, and artificial neural networks were used to measure the correlation between shape factor and dispersibility. It was observed that circularity and convexity influenced particle dispersibility differently depending on the particle size category. However, the study only evaluated four powder brands, which may not be sufficient to generalise the findings.

2.5.2. CV based food quality assessment challenges

In contrast to human evaluations, imaging-based techniques can provide objective quantitative measurements of several quality attributes simultaneously in a non-destructive manner (Mozafari et al., 2024). However, since they can be sensitive to ambient conditions, some applications may require consistent and constrained viewpoints and specialised lighting to achieve satisfactory results (Ding, 2021; Mozafari et al., 2024). Thus, CV systems are associated with several challenges, including designing and selecting the appropriate illumination system and hardware components (Brosnan and Sun, 2004; Patel et al., 2012) as illustrated in Figure 2-3. Moreover, food products may not be homogeneous, and the variations in shape and size can pose challenges in image analysis (Brosnan and Sun, 2004; Wu and Sun, 2013). The challenge arises because generalising any new observation (e.g., size, colour, lighting, texture) requires an increase in number of observations during algorithm development, which can be resource-intensive (Wu and Sun, 2013). Despite these challenges, the use of CV in the food industry has continued to grow because it offers potential for improved quality control and process optimisation (Brosnan and Sun, 2004; Ma et al., 2016; Mery et al., 2013; Patel et al., 2012; Wu and Sun, 2013). The ability of this technology to provide quick, accurate, and non-

invasive quality assessments makes it an attractive tool for meeting consumer demands for high-quality food products in the agri-food industry (Ma et al., 2016).

2.6. Potential gap between automated and end-user agitation

In many industries (such as pharmaceutical, cosmetic, and food), understanding and mimicking the mixing behaviour of consumers is necessary to ensure that powders of high quality are produced (Hardy et al., 2002; Lloyd et al., 2019; Quadro, 2015; TP, 2016). However, there have been a limited number of studies systematically mimicking end-user powder-liquid mixing behaviour (Lloyd et al., 2019; O'Shea et al., 2021). In standard laboratory methods, different mixers are used, which may not reflect how end-users rehydrate powders at home. In the case of IF powder, infants' susceptibility to nutritional deficiencies during critical stages of physical growth and neurological development (Prado and Dewey, 2014), combined with the fact that IF may be the only source of nutrition for some infants (National Academies Press, 2004), can make complete rehydration and release of intended nutrients in the water particularly important. More research is required into ways to make the mixing procedure for rehydration tests more realistically representative of the agitation behaviour applied to powder and water by the end users (while maintaining test objectivity). A study of this kind may also be useful in other research fields, such as the dissolution of pharmaceutical powders in liquids (Kumar et al., 2018).

2.7. Mimicking human bottle agitation

The methods used to "mimic" human arm movements by robots should ideally be developed systematically (Ravichandar et al., 2020). This systematic approach is required to take into account the possibility of other similar movements performed by humans, which can enhance the generalisability of the learned movements. However, some studies have attempted to simulate the mixing of powder and liquid subjectively (Lloyd et al., 2019; O'Shea et al., 2021). Lloyd et al. (2019) conducted market research by asking consumers to rehydrate various milk powders. The mechanical

mixer was then modified to achieve residue left after rehydration similar to those observed in consumers' samples. This resulted in a mixing procedure involving rotating the mixer paddle 13 times clockwise and 13 times counterclockwise within eight seconds. However, the study provides limited information regarding the market research conducted to characterise the domestic rehydration methods. Additionally, the comparison of the agitations is not described in detail, such as the number of participants and milk powders, or the methods for analysing consumer rehydration. Conducting a subjective approach for mimicking the agitations is perhaps due to the difficulty of developing more objective methods for robots to mimic human movements (Ravichandar et al., 2020). For example, while the robot's degrees of freedom (DoF) should be high enough to mimic a demonstration, dealing with increased DoF can be challenging (Ravichandar et al., 2020). Robots' motors may also be less agile than human muscles (Hong et al., 2023). Because of differences in physical embodiment, robots and humans often behave differently to achieve the same results (Billard and Grollman, 2013).

Machine learning techniques can also be applied to other relatively large data processing problems in the food industry, such as robotic food handling (Misimi et al., 2018). It is common to use machine learning techniques to increase the flexibility of the data processing and obtain more generalised insights (Zhou et al., 2019). By using these techniques, researchers have explored the application of learning from demonstrations (LfD) to optimise robotic movement tasks (Ravichandar et al., 2020). LfD is a strategy in robotics that allows an intuitive method of teaching a robot new skills through demonstration. This approach, if its implementation challenges are addressed, is intended to reduce the time and cost of automation, especially for Small and Medium-sized Enterprises (SMEs) with high product variability and low volumes (Ko et al., 2015; Zhu and Hu, 2018).

CV combined with LfD has also shown promising results for inferring tasks from demonstration videos (Liu et al., 2018). For example, based on LfD techniques combined with visual RGB-D and tactile feedback, Misimi et al. (2018) transferred the skill of handling food material to a robot. Their

learning approach based on SVM enabled a six DoF robot to learn how to handle fragile food items through around five hundred teleoperated demonstrations of random lettuce placements. For automated measurement of IF rehydration quality, a possible approach is to record videos of humans preparing the formula and, then, train models to identify key patterns related to the rehydration process (cf. Brito et al., 2020). Among these patterns are agitation motions, including trajectories, amplitudes, and frequencies (Kulak, 2021), which can yield the most frequent rehydration patterns according to human demonstrators (cf. Z. Liu et al., 2022). LfD is particularly of interest when the desired robotic motion is not well known and cannot be easily defined or scripted (Ravichandar et al., 2020).

Meanwhile, cobots have been employed to reproduce demonstration movements in industrial settings (e.g., Zaatari et al., 2021) with repeatability that is difficult for humans to achieve (L. Liu et al., 2022). Unlike traditional robotic motion programming, LfD techniques provide the opportunity to bridge human expertise with robotic precision. This may produce agitations that are both natural (as the motions are learned from human demonstrators) and reproducible (as the learned motions are performed by a robot). However, as LfD typically relies on human demonstrations, variability in these demonstrations may pose algorithmic challenges in the acquisition and articulation of agitation parameters (Ravichandar et al., 2020). This can be problematic, particularly considering high-speed agitations and the need to encode or learn a mapping that transfers the learned skills from human demonstrations to motions executable by robots (Ravichandar et al., 2020).

LfD can encompass both high-level learning, which involves understanding the sequence of actions required for a task, and low-level learning, which focuses on recognising the precise trajectory of a task (Kyrarini et al., 2019). Because humans and robots interact with their surroundings in fundamentally different ways (Billard and Grollman, 2013), certain demonstration methods may require remapping the demonstrated task for the robot, known as a “correspondence problem”. According to Figure 2-4, the demonstration methods can be categorised into three groups: (i)

Kinesthetic Teaching: this method involves the operator physically moving the robot to demonstrate the required task. It is commonly used in teaching manipulation tasks while the robot records the joint angles. In this approach, there is no "correspondence problem", and the teacher does not require much technical training to demonstrate the task (Zhu and Hu, 2018); (ii) Teleoperation: in this method, the robot is controlled remotely by an operator using tools such as joysticks or haptic devices. It is useful for teaching complex trajectories, repetitive tasks that require accuracy, or manipulating a robot in hazardous conditions (Ravichandar et al., 2020); and (iii) Passive Observation: in this method, the robot mimics teachers based on movement data obtained from sensors (usually CV-based).

Figure 2-4 Three main demonstration methods: (a) Kinesthetic Teaching, which involves demonstration of the task through touching the robot arm, (b) Teleoperation, which involves the use of a remote controller (e.g., a joystick) to demonstrate the task, and (c) Passive Observation, which involves collecting data from the demonstration using sensors or computer vision systems

The observed action sequences are then mapped to robot capabilities, including solving the "correspondence problem" between human and robot actions (Ravichandar et al., 2020). The Passive Observation method seems to be most appropriate for IF bottle agitation since it obtains the agitation data by observing the bottle in hand, rather than from haptic devices or robotic arm sensors. Directly observing bottle movements is expected to result in observation of more realistic agitation movements (e.g., the influence of fluid dynamics on bottle movement, or the effect of how the bottle feels in the participant's hand on their perceptions and bottle agitation behaviours). Kinesthetic Teaching may not capture realistic agitation frequencies, due to the weight and inertia of the robot arm. Similarly, the use of a tool such as a haptic in the Teleoperation method may not accurately represent the natural agitation of the bottle.

To learn from the observations, a wide variety of algorithms have been used. Some of the commonly used techniques include: (i) Gaussian Mixture Models (GMM): these models encode the variability of demonstrations and enable robots to generalise observed movements (Kyrarini et al., 2019); (ii) Hidden Markov Models (HMM): these models provide robots with the ability to learn different sequences of actions by encoding sequential patterns in the observed task (Kyrarini et al., 2019); (iii) Dynamic Movement Primitives (DMP): this method provides reliable control over learned motions by storing motor skills in a format that can be modified for use in other settings (Ravichandar et al., 2020). There are advantages and disadvantages to each method, depending on the particular learning task. For example, a GMM approach alone may not be able to learn the temporal dependency and frequency of IF bottle agitation (cf. Vogt et al., 2017). Additionally, since HMM approaches are designed to learn sequences, they may have difficulty performing an entire smooth agitation cycle. Since phase-based methods such as DMP can learn both smooth paths and timing, they seem to be more suitable for learning rhythmic tasks (Ernesti et al., 2012; Kulak et al., 2020) such as IF bottle agitation movements. However, it has been common in recent years to develop hybrid approaches that incorporate the advantages of each approach (Kulak et al., 2020; Vogt et al., 2017).

Although LfD has demonstrated some promise in addressing food handling challenges, Ko et al. (2015) highlighted some difficulties LfD may encounter in industrial applications, such as high accuracy requirements, repeatability, adaptability, system complexity, and production speed. To overcome these issues, they proposed a learning architecture to achieve flexibility along with accuracy and speed needed in industrial applications. Recent research has focused on developing techniques for detecting and eliminating inconsistent demonstrations, predicting the intended actions of teachers, and enabling robots to perform learned tasks in new environments without additional training data (Kyrarini et al., 2019; Misimi et al., 2018).

2.8. Integration of emerging technologies and their synergies

The food processing and agricultural automation industries are currently undergoing transformation driven by emerging technologies (Derossi et al., 2023; Kadalagere Sampath et al., 2023; Sane and Sane, 2021). Integration of these technologies has the potential to enable automated and standardised manipulation of food objects. Robotics, advanced sensing systems (such as force sensors and high resolution cameras), and machine learning have provided solutions to some previously unsolved challenges associated with characterising food properties and quality, crop harvesting, and food handling (Derossi et al., 2023; Sane and Sane, 2021).

Numerous studies have integrated emerging technologies to address existing automation challenges in the food industry. Lillienskiold et al. (2022) used robotic systems with haptic feedback, image analysis, and machine learning to develop food grasping strategies. Tai et al. (2023) replicated scooping food by using robotic process automation combined with "active perception". Robotic systems equipped with soft grippers and 3D vision are now available for better handling of food products (Derossi et al., 2023). Multi-finger robotic hands, CV, tactile sensing, and techniques for interacting with deformable and soft objects can be integrated to solve food handling problems (Kadalagere Sampath et al., 2023). In the agriculture sector, robots, image analysis, and deep learning have been applied to automate crop harvesting (Sane and Sane, 2021). Rajendran et al. (2023) presented a fruit harvesting system that includes robotic arms, end effectors, a CV system for fruit identification, and a method for motion planning.

However, in practice, developing manipulation strategies for objects with different shapes and sizes (Kadalagere Sampath et al., 2023) or heterogeneous objects (Derossi et al., 2023) remains a challenging process. The challenges associated with robot handling of food products have resulted in many tasks in the food industry still being performed manually, which are both labour-intensive and subject to large variations (Misimi et al., 2018). Particularly in the food industry, some experiments require complex operations to be performed by experts. This complexity exacerbates the difficulty of

maintaining consistency (Misimi et al., 2018). To address the challenges associated with handling food and agricultural products, integrated modular solutions both in terms of hardware (Derossi et al., 2023) and software (Sane and Sane, 2021; Tai et al., 2023) can be beneficial. Modular architectures can be flexible, precise, and fast simultaneously, aligning with the demands of the food industry. For example, the integrated platform for food scooping tasks (Tai et al., 2023) consists of modules that encode interaction data, capture state information, and implicitly represent food properties to guide real-time robotic scooping actions. Modular solutions based on emerging technologies can lead to improved product quality, reduced waste, and increased productivity (Derossi et al., 2023; Sane and Sane, 2021). Moreover, although the use of robots and the CV systems may increase productivity and minimise the costs of the quality inspection process, there may be difficulties in establishing communication between the automated systems (Leidenkrantz and Westbrandt, 2019), or the integration of sensors into the robot to handle food products (Misimi et al., 2018).

2.9. Conclusion

A review of current methods for evaluating IF rehydration properties identified several shortcomings, including subjectivity, poor reproducibility, and lack of standardisation. Despite the potential of emerging technologies such as robotics and CV to provide solutions, practical implementation challenges exist relating to module design and the architecture of the entire automated system. However, to ensure consistent product quality control based on end-user needs, more objective and representative rehydration quality tests are required. Also, developing automated analytical tools could provide a more objective understanding of the effects of formulation and processing parameters on IF powder rehydration.

If the robot has the necessary electromechanical capabilities and the control system is properly designed, robots can be programmed to mimic human movements during bottle agitations using systematically characterised agitations. This would reduce the variations resulting from human

analysis. Further research is necessary to characterise human bottle agitation and to validate robotic agitations against common human agitations. The process of mapping human motions to robots and the variability between demonstrations pose implementation challenges. Likewise, for other automation modules such as CV systems, it is crucial to compare automated measures with reference methods for validation.

Computer vision is considered an objective and non-destructive method to provide quantitative measurements of quality attributes. There are some challenges in designing and selecting the CV system components. Also, the variations in the studied quality attribute in the dairy or other food products (e.g., shape and size of the defect) pose challenges in image analysis. Furthermore, the possibility of new observations (e.g., size, colour, and texture) may require an increase in the number of observations during algorithm development, which can be resource intensive. Despite these challenges, the use of computer vision in the food industry has continued to grow because it offers the potential for objective quality control and improving process optimisation.

Transforming manual bottle agitation styles into automated protocols requires interdisciplinary research e.g., process engineering, sensors, control systems, and data analysis. Because powder rehydration preferences may vary according to culture and geographic location, it may be difficult to develop a universal solution. However, one potential for a robotics rehydration platform is to use LfD techniques and learn agitations based on demonstrations from different geographical locations. The platform could therefore mimic specific powder rehydration styles regardless of the laboratory's location. In addition, identical rehydration assessments could be guaranteed if manufacturers or researchers use the same robot and program.

Chapter 3 (Platform development): An Automated Platform for Assessing Infant Formula Rehydration

Parts of this chapter have been published in:

- *Mozafari, B., O'Shea, N., Fenelon, M., Li, R., Daly, D.F. and Villing, R., 2024. An automated platform for measuring infant formula powder rehydration quality using a collaborative robot integrated with computer vision. Journal of Food Engineering, 383, p.112229. https://doi.org/10.1016/j.jfoodeng.2024.112229*
- *Mozafari, B., O'Shea, N., Fenelon, M. and Villing, R., 2022, June. Towards Image Processing-based Quantification of White Particles in Reconstituted Infant Formula. In 2022 33rd Irish Signals and Systems Conference (ISSC) (pp. 1-6). IEEE. https://www.doi.org/10.1109/ISSC55427.2022.9826210*

3.1. Introduction

The purpose of this chapter is to describe the development of an automated platform for evaluating the rehydration quality of IF powder. The automated platform integrates a collaborative robot with a computer vision system developed in-house. The cobot was used for preparing the IF mixture in a standardised manner. In this chapter, the cobot bottle agitation movements were identical to those used in another study outside the scope of the thesis (O'Shea et al., 2021). However, the cobot program was enhanced to handle the bottle for automated imaging and visualisation of the unhydrated particles in the bottle's blank headspace (e.g., the red dashed line in Figure 3-4). The computer vision system was used to assess the quality of the prepared mixture and quantify three rehydration properties that may be undesirable in a rehydrated IF powder.

After describing how the platform was developed, the chapter describes a preliminary assessment of the platform by comparing its estimates of three rehydration properties with those of

people using a random subset of the same automated-captured images. Chapter Four describes a subsequent evaluation of the platform in comparison to commonly used laboratory tests.

The findings of the present chapter provide a foundation for the remainder of the experiments in this thesis. Therefore, although benchmarking of the platform based on laboratory tests common in food and dairy science was not conducted for this chapter, some basic laboratory measurements were performed to ensure that platform measurements have meaningful relationships with basic laboratory tests (such as particle size and dissolved solids measurements).

3.2. Related works

As described in Chapter Two, the rehydration attributes of IF powders are often associated with product quality and end user acceptance. Ideally, IF powders should completely and rapidly dissolve in water and resemble milk in appearance after rehydration. However, in reality, they may demonstrate some undesirable rehydration attributes such as foam, sediment, and undissolved particles (Masum et al., 2020; Sharma et al., 2012). Therefore, IF powder manufacturers perform quality tests to determine how well the powders dissolve in water, commonly referred to as "instant properties" (Pisecky, 2012). For example, wettability and dispersibility tests have been frequently used to assess the different stages of rehydration in water in a certain amount of time (Sharma et al., 2012).

Currently, powder rehydration assessment methods are subjective (Munir et al., 2017), depending on the amount of agitation energy used by a human in the preparation of the mixture (Lloyd et al., 2019; O'Shea et al., 2021) and an individual's interpretation of the mixture quality (Lloyd et al., 2019). An objective method is required to better understand powder rehydration behaviour (Munir et al., 2017). Emerging technologies, such as computer vision (CV), are expected to improve the objectivity, reproducibility, and accuracy of testing (Fang et al., 2008). The primary reason why human evaluations are still widely used for rehydration quality instead of digital methods is that digital data collection is challenging (Munir et al., 2017). Furthermore, appropriate software,

hardware, and data management systems are required for real-time data analysis, and companies need to justify their investments when implementing digital systems, as they can create additional expenses and require interdisciplinary expertise (Munir et al., 2017).

Recently, some studies have sought to address the lack of objective rehydration quality measurements. Lloyd et al. (2019) developed a CV algorithm to measure the number of undissolved "bulk particles" and a mixer that mimicked the end user agitation movements to ensure consistency during powder rehydration. To count the number of particles, they used a 5 Megapixels camera and a flow cell with a dark background to increase contrast and reduce the impact of ambient factors (e.g., lighting). Their image processing methodology involved normalizing the image background, creating a binary image using a manually selected threshold, and performing a connected components analysis with a threshold on particle area. A recent study conducted by the author of this thesis examined undissolved "surface-floating particles" (Mozafari et al., 2022). The study developed a preliminary version of "digitally-generated" reference images based on particle size and particle size distribution measurements obtained from a confocal microscope and laser scattering instrument. A computer vision algorithm for counting particles was developed and then evaluated by manually scoring the images based on the reference images. Other rehydration attributes associated with the rehydration of IF powders, such as foaming and sedimentation, do not appear to have been adequately assessed using a CV approach in the literature to date.

Despite the limited number of such studies conducted for rehydrated dairy powders, several other studies have applied the image analysis approach to assess the quality of various drinks. The methods include manual assessment of images (Crumpton et al., 2018; Novak et al., 2015) with the aid of computer applications such as ImageJ (Schneider et al., 2012), Artificial Neural Networks (ANNs) (Gonzalez Viejo et al., 2018; Morelle et al., 2021; Panckow et al., 2021), and classical methods. While ANNs can be more flexible than classical approaches, they may require more lab experiments to obtain the necessary data for training (Huang et al., 2007). Classical approaches have

been applied to measure: (i) foam height in beer (Cimini et al., 2016; Nyarko et al., 2021), wine (Condé et al., 2017), milk (Ewert et al., 2016; Münchow et al., 2015); (ii) particle shape of milk powder (Ding et al., 2021); and (iii) curdling and sediment in soy milk (Brown et al., 2019).

The classical methods used to measure rehydration attributes may differ. For example, the study conducted by Condé et al. (2017) employed the circle Hough transform to determine the size of the foam bubbles in wine. The algorithm computed the likelihood of circular shapes occurring within the image. However, it is possible for foam to have a noncircular shape (Walstra, 1989).

In another study on the foaming properties of liquid milk, Münchow et al. (2015) used a threshold pixel intensity approach to measure the foam height and its stability in milk containing different fat or protein content. They collected images every second for 10 minutes to determine the stability of foam from different steam-frothed milk samples. It was reported that image processing decreased the dependency of measurements on human interpretations, which offered a reliable means for understanding the impact of different milk ingredients on foam height and stability. Backlighting was used before thresholding to increase the contrast between milk and foam. This technique cannot be used to detect some other rehydration attributes, such as sediment, in a mixture. For example, when Brown et al. (2019) assessed the curdling of soy milk in coffee, they applied thresholding on the Fourier transform rather than enhanced-contrast images obtained from backlighting. They analysed the images using Fourier transform to evaluate the phase separation and sedimentation processes. However, their report does not provide details regarding the algorithm used for image analysis or whether the images were captured or analysed automatically.

3.3. Aims of the present study

The present study aimed to develop and evaluate an automated platform for quantifying three visible indicators of rehydration quality in a non-destructive and objective manner. Since some powder rehydration quality tests are categorized into distinct levels and rely on subjective assessments, automating them is a challenge for the dairy powder industry (Munir et al., 2017). To our knowledge,

this is the first time an automated platform has been developed to quantify three visible rehydration attributes using the same rehydrated powder sample. The platform consisted of a CV system using three classical vision approaches and a collaborative robot (cobot). Our study focused on measuring: (i) foam height; (ii) sediment height; and (iii) the number of undissolved particles (referred to as "white particles" in this document). The research involved: (i) rehydrating IF powders using a cobot; (ii) automatically capturing images of the rehydrated powder from six different viewpoints in five imaging rounds using an industrial camera integrated with the cobot; (iii) applying three developed CV algorithms to quantify the three rehydration attributes; and (iv) evaluating CV estimates of all three visible rehydration attributes in comparison to those of eight participants presented with a random selection of the same cobot-captured images.

3.4. Automated platform development

3.4.1. Platform overview

The platform consisted of a dual-arm YuMi collaborative robot (cobot) (ABB corporation, Switzerland) with seven degrees of freedom on each arm and an in-house developed vision system (Figure 3-1). The cobot was used to ensure that the same agitation energy, time, and motions were used during the preparation of the mixtures. Using the touch screen, the operator could select the style and duration of bottle agitation and the number of scoops of powder to be added to the bottle. The process of heating and adding water to the empty bottle was carried out manually (it was not part of the automated platform).

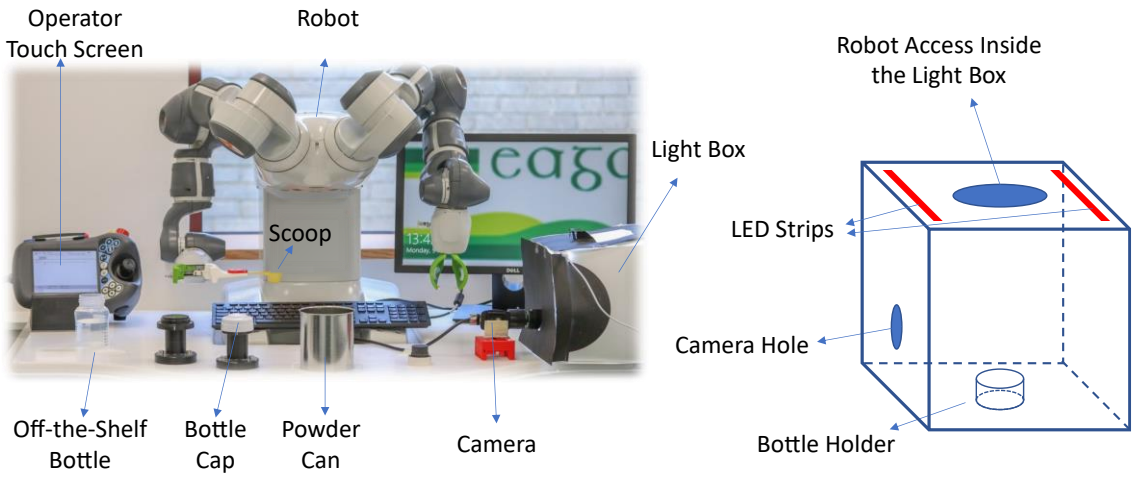

Figure 3-1 Platform architecture for preparing mixtures and capturing bottle images

As mentioned in Chapter One and the overview of the present chapter, the robot agitations described in this chapter were previously developed outside the scope of this thesis. However, the robot program was enhanced by adding an automatic imaging module as will be described in section 3.4.2.

3.4.2. Integrated computer vision system

Although the YuMi robot used in this study was equipped with SmartGrippers having 1.3 Megapixel cameras on each arm and Cognex image processing software (ABB, 2021a), preliminary trials indicated that the resolution of the cameras was not sufficient to evaluate the rehydration attributes (Figure 3-2).

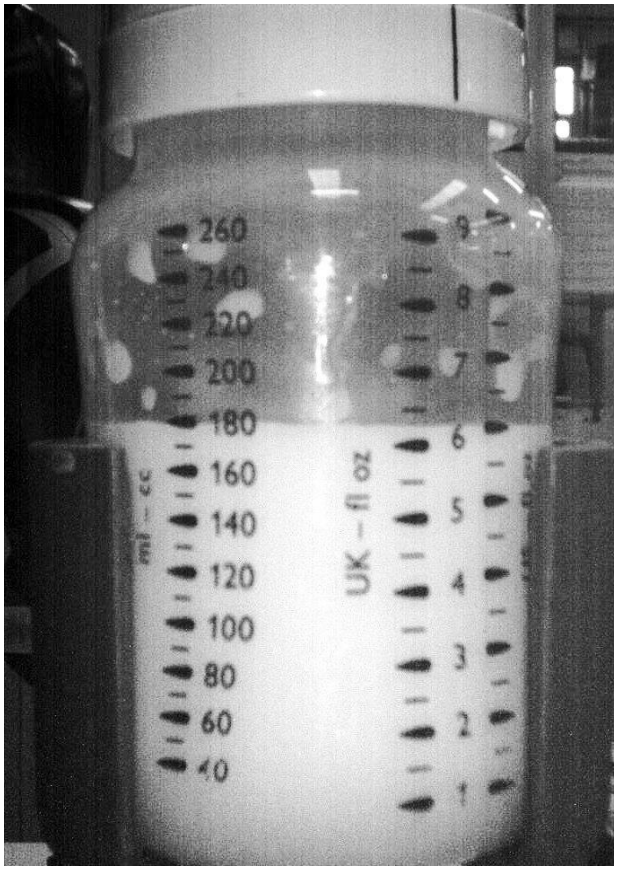

Figure 3-2 Images automatically taken by YuMi's Cognex AE3 camera with internal illumination were not of sufficient quality to be used in this study

Additionally, the camera was monochrome, limiting image segmentation capabilities. It was therefore necessary to incorporate an external high-resolution vision system into the platform design. The visibility of rehydration attributes, specifically particles, was evaluated first using a Canon EOS 80D camera (Canon Inc., Tokyo, Japan) with two lenses of 50 mm f/1.4 and 18-135 mm f/3.5-5.6. As a result of this evaluation, it was possible to estimate the characteristics of an appropriate industrial camera and lens that could be incorporated into the platform. During the selection process for the camera, the size and resolution of the image sensor were given a high priority. The use of a larger image sensor (and pixel size) was preferred to obtain adequate image illumination without increasing signal gain (which can result in noise in images and adversely impact the performance of image analysis algorithms, particularly for particle detection). During lens selection, several factors were taken into consideration, including high resolution (usually measured as line pairs per mm, and determined by the quality of its glass material, which affects the price), a small minimum focusing

distance (because the vision system has to fit on the robot table and capture the sample images from a close distance), an adequate field of view (to ensure that it can capture the entire bottle in the minimum focusing distance), and a greater depth of field (to ensure rehydration attributes are visible despite the curvature of the bottle).

The vision system included a 5536 × 3692 pixels (21 Megapixels) industrial camera (U3-3800CP Rev.2.2, iDS Imaging, Germany) with a pixel size of 2.4 µm, a 1:1.8/16 mm lens (CF16ZA-1S, Fujinon, Fuji Photo Film Co., Japan), and a cubic lightbox (23 cm × 23 cm × 23 cm) with two LED strips (2 × 550 LM) secured on top (inside the lightbox, front and back) to provide uniform lighting. The camera communicated with the cobot using socket messages transmitted using USB3 and TCP/IP over Ethernet (Figure 3-3) to capture the images automatically.

The vision system evaluated the rehydration quality of the IF mixtures in a commercial 260 ml baby bottle (Philips Avent, Glemsford, England). The purpose of using a commercial bottle was to ensure that the conditions in which the mixtures are prepared are as close as possible to those applied by the end user. Two specific objectives were pursued by preparing the mixtures in a commercial bottle: i) ensuring a realistic fluid dynamic inside the bottle; and ii) evaluating the rehydration quality of the mixture in the same bottle without further disturbing the mixture (which may result in foam displacement and sediment re-dispersion into the mixture). Consequently, computer vision algorithms were required to handle the presence of commercial marks on the bottle. Following this approach, a preliminary evaluation of the platform quality assessment based on the measurements from participants was possible.

The overall platform architecture is shown in Figure 3-1. A hole of 40 mm diameter was made in the lightbox for positioning the lens to capture the bottle, which had a size of 10 cm × 7 cm. The distance between the lens and the bottle was 9 cm, and the f-number of the lens was fixed at 8 to create a larger depth of field compared to the lens's maximum aperture of f1.8. To reduce reflections

from the glossy bottle, the inner sidewalls of the lightbox were covered with white matte paper, except for the black background behind the bottle.

The bottle holder (inside the lightbox) was constructed from a transparent acrylic plate to reduce shadows at the bottom of the bottle and improve the visibility of any possible sediment. A ruler was attached to the bottle holder to evaluate foam and sediment height (described in sections 3.5.5.1 and 3.5.5.2).

3.4.3. Image acquisition

After agitation, the cobot placed the bottle on the transparent holder inside the lightbox (Figure 3-1) and waited 10 s for the mixture to stabilize. It then communicated a command to a laptop (Core i7-6700HQ) over the socket to capture an image using the camera. The camera exposure time was 250 ms, and the signal was not amplified to minimise noise in the images. Each high-resolution captured image was cropped three times, once for each rehydration attribute (rather than capturing three separate images) to minimise possible changes in rehydration attributes due to time passing or fluid disruption during the imaging process. After capturing the first image, the cobot "gently" rotated the bottle around the Z (vertical) axis by 60° and captured another image, repeating this rotate-and-capture process until six images from equally spaced viewpoints of the bottle were captured. These six images constituted a single imaging round. It took 20 s to perform the "gentle" bottle rotation to reduce the disturbance of the mixture. All images were saved and processed on the laptop. For CV ratings, the images were converted from BMP to PNG format. The platform communication schematic is presented in Figure 3-3.

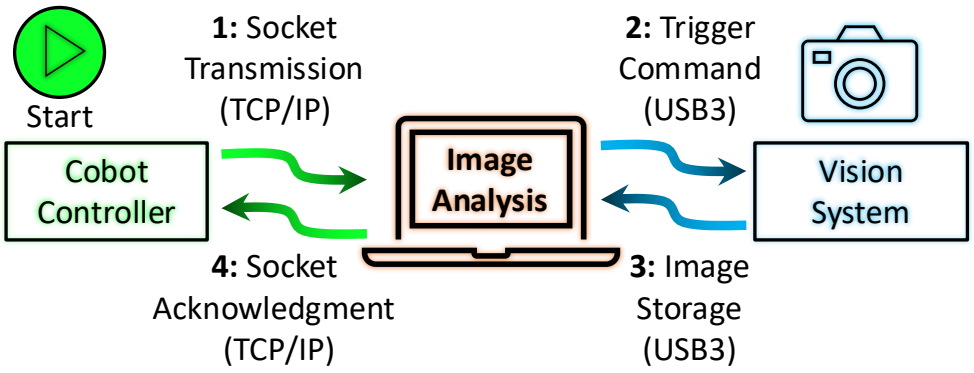

Figure 3-3 Platform communication schematic

To ensure data integrity and maintain electronic records as recommended by FDA regulation CFR 21 Part 11 (Winter and Huber, 2000), every cobot-captured image was saved in a unique folder with the exact time and date in the format of yy-mm-dd-hh-mm-ss. Throughout the project, a private internal network was used to back up images to ensure that the original data would remain unchanged. A text file was also provided as metadata explaining the structure of the stored data (such as imaging round, expected visible defects in images, and folder naming) for data users.

The entire imaging procedure for each cobot-prepared mixture involved **five** imaging rounds (each comprising of six images from different viewpoints around the bottle). The **first four** rounds were used to monitor the change in foam and sediment height. The **fifth** (and last) round was used to count white particles. Before the fifth round, the cobot removed the bottle from the lightbox, then inclined and rotated it for visualisation of white particles in the bottle's blank headspace, if present. The **first three** rounds of imaging were followed by a 3-min rest period to allow foam height change. The same viewpoints were used to capture images of the bottle during all imaging rounds.

3.4.4. Computer vision algorithms

Python and the OpenCV library (Bradski, 2000) were used to calibrate the camera and develop the image-processing software. The calibration was performed by photographing a 9×6 OpenCV chessboard pattern printed on approximately A6-sized paper using the same camera settings and distance as when imaging the samples. For the development of vision algorithms, five powders (P1,

P2, C1, C2, and C3) were randomly selected. The rehydration attributes subjectively observed in these mixtures can be found in Table 3-1.

Table 3-1 The mixtures used for developing the algorithms and corresponding rehydration attributes

Mixture	Foam	Sediment	White Particles
C1	High	Low	Low
C2	Medium	Medium	Low
C3	Medium	Medium	Medium
P1	Low	High	Medium
P2	Low	High	High

Algorithms were developed for estimating each of the three rehydration properties and these are described in sections 3.4.4.1 to 3.4.4.3. The six cobot-captured images obtained during an imaging round and the Region of Interest (ROI) (i.e., the cropped images) for each of the three algorithms are illustrated in Figure 3-4.

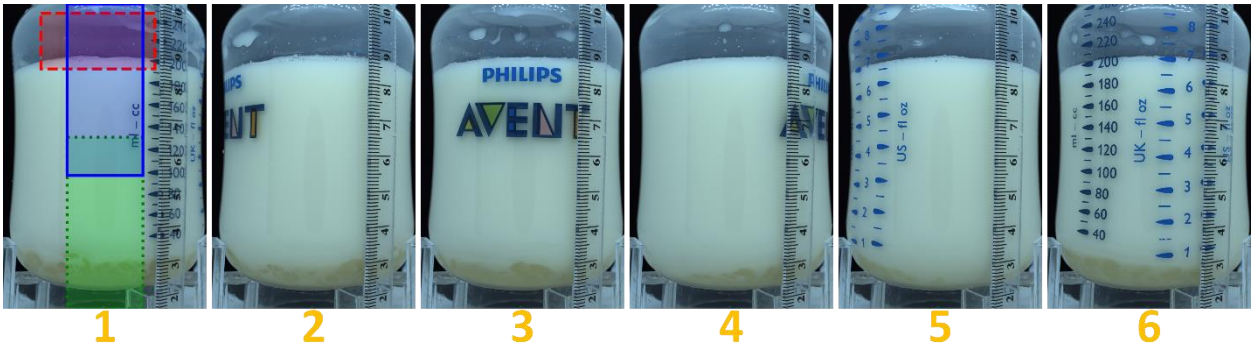

Figure 3-4 Six different bottle viewpoints in an imaging round. The ROI of Foam Height, Sediment Height, and Number of White Particles algorithms are illustrated in Image 1 (left) in Blue (solid line), Green (dotted line), and Red (dashed line)

The three image processing algorithms began rating the rehydration properties as soon as the images were captured. The results of the image analysis were available within approximately five seconds. While the algorithms were analysing the image, the robot rotated the bottle (which took twenty seconds plus ten seconds of rest time, as described in section 3.4.3) to obtain the next image. Therefore. the software used for the image analysis on this platform was quicker than its "physical counterpart" and can be considered "real-time" (Bélanger et al., 2010). The software was designed with a parallel architecture, which enabled the robot to operate without waiting for the images to be

analysed, preventing the image analysis software from becoming a bottleneck during the cobot imaging of the samples. Moreover, since the original images and timestamps have been stored, they can be processed using any other techniques or algorithms later. To enhance the traceability of experiments, it is beneficial to have data stored and timestamped from samples (which can be done through food digitalisation (Serazetdinova et al., 2019)).

3.4.4.1. Foam Height Estimation Algorithm

During a preliminary evaluation prior to developing the algorithm, some large bubbles were observed to be elliptical rather than circular, while some mixtures contained small bubbles (Figure 3-5). According to the literature, foam bubbles can have a variety of sizes and shapes (Walstra, 1989).

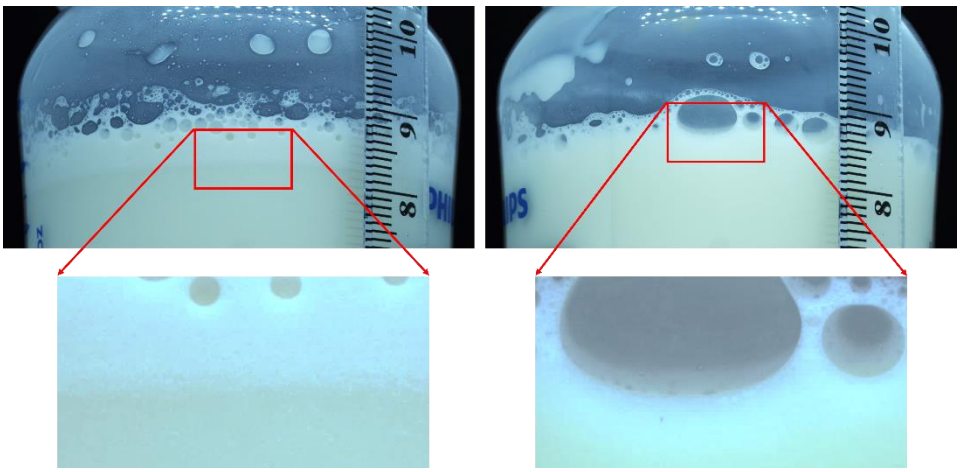

Figure 3-5 Bubble size and foam-mixture boundary in different mixtures (left: mixture C1 with small bubbles, right: mixture P1 with elliptical bubbles) – mixtures were prepared and photographed automatically using the platform

Therefore, a derivative filter convolution was used to calculate the image gradient to detect foam regardless of the shape and size of the bubble. The foam algorithm pipeline is illustrated in Figure 3-6. The purpose of this algorithm was to determine the height of foam, not to interpret its shape.

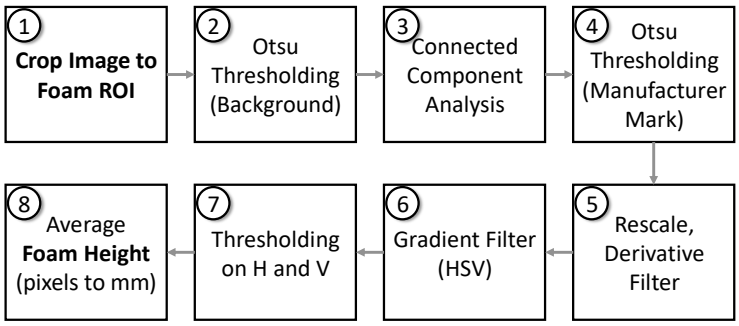

Figure 3-6 Foam height estimation algorithm

The steps of the foam algorithm are as follows.

1. The image was cropped according to foam ROI illustrated in Figure 3-4.
2. The black background visible through the transparent bottle was removed using Otsu thresholding.
3. Using connected component analysis, the small droplets or pieces of foam were isolated from the main body of the mixture including foam (the largest component in the binary image) and removed as they were not of interest for foam detection. Accordingly, the upper boundary of the foam was detected as the highest pixel in the largest component. To ensure successful thresholding (step 2), it was checked that the largest component accounted for 10%–90% of the ROI.
4. Otsu thresholding was used again to remove the manufacturer's label and bottle marks (their colours were different from the main body of the mixture). Since the bottle marks cast shadows on the mixture, the entire image columns were removed if they contained a bottle mark.
5. Before lower foam boundary detection, the image was scaled down to 20% to reduce calculation costs and to minimise the possibility of highlighting smaller features such as noise.
6. The liquid-foam boundary was detected by convolving a filter size of 11 pixels (equivalent to 0.5 mm on the scaled image which is approximately the smallest bubble diameter visible in the images) from four different directions (due to the circular edges of bubbles).

7. A fixed threshold was manually set for segments H and V (H > 60 & V > 100) to determine boundaries in the processed image.
8. After detecting the boundary between the liquid and foam mediums, the foam boundaries were fully detected. The foam height was then calculated in pixels and converted to millimetres.

3.4.4.2. Sediment height estimation algorithm

The sediment algorithm pipeline is illustrated in Figure 3-7.

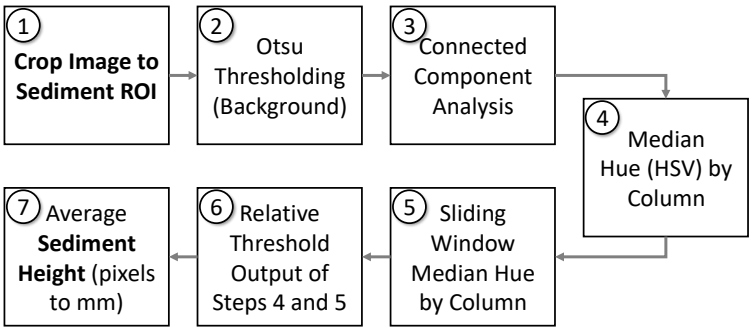

Figure 3-7 Sediment height estimation algorithm

The steps of the sediment algorithm are as follows.

1. The image was cropped according to sediment ROI illustrated in Figure 3-4.
2. The black background visible through the transparent holder under the bottle was removed using Otsu thresholding.
3. Connected component analysis was performed to ensure that the lower sediment boundary was detected without any remaining noise in the base region using the same function as the foam algorithm. The lower pixel of the largest component, which was the main body of the mixture and possible sediment, was then selected as the lower boundary of the sediment.
4. The median Hue level of each image column in the entire ROI was calculated in the HSV colour space.
5. A sliding window of 1 mm with a 0.5 mm overlap was used to scan each column of the ROI and calculate the Hue median.

6. Whenever the median Hue of a sliding window and its subsequent windows in a column exceeded that of the column, the window was considered as the upper boundary of the sediment in that column (as sediment is thicker and less diluted than the rest of the mixture on top, it was assumed to have a higher Hue). This method was applied to all image columns within the ROI.
7. The sediment height was then calculated in pixels and converted to millimetres.

3.4.4.3. Number of White Particles algorithm

The detection of white particles was based on image sharpness and mean shift algorithms as reported in Mozafari et al. (2022). The algorithm pipeline is illustrated in Figure 3-8.

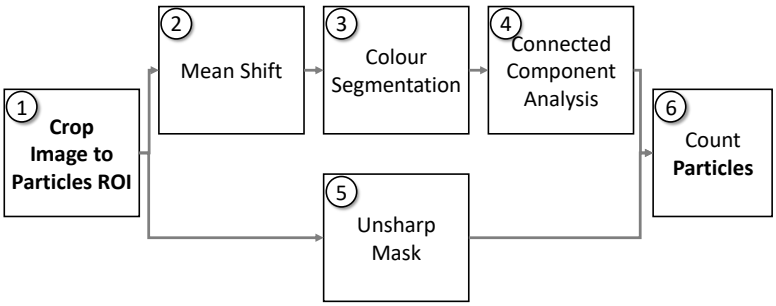

Figure 3-8 Number of white particles detection algorithm

The steps of the white particles algorithm are as follows.

1. The image was cropped according to particles ROI illustrated in Figure 3-4.
2. Mean shift was used to classify the colours and emphasise the particles margin. The window was approximately 100 μm in size, which was in the expected range of these particles (Toikkanen et al., 2018).
3. The pixels that fell inside a manually selected colour range ($75 < H < 115$, $25 < S < 105$, $175 < V < 255$), were segmented (choosing the colour range was accomplished by manually examining the particles' colours in the development dataset).

4. A connected component analysis was applied to ensure that only particles with a width and height of 100 µm to 1 mm and a surface area greater than one-third of their width × height are retained.
5. Unsharp masking with a kernel size of approximately 500 µm was applied to find the sharp regions in the image. It was expected that the sharp regions may contain particles.
6. The logical conjunction between steps 4 and 5 was detected as particles.

In this algorithm, particles were counted. However, in order to allow for better comparison with participant ratings, the assigned numbers by CV were also categorized as scores using a logarithmic scale as described in Mozafari et al. (2022).

3.5. Platform evaluation based on visible rehydration attributes

This section presents the methods for evaluating platform performance. To validate the effectiveness of CV for visually estimating foam height, sediment height, and white particles, we examined whether people and CV algorithms would produce similar estimates when presented with the same cobot-captured images. The agreement between the CV and human estimates was assessed using the method described in section 3.5.6. Section 3.4.3 describes how images were captured.

3.5.1. Participants (demographics)

Eight participants were recruited to rate images that had been captured by the platform and used by the CV algorithms. All participants were researchers in dairy-related fields. They gave their informed consent to participate (Appendix 2 contains the relevant ethical approval).

3.5.2. Infant formula powders

Twenty-nine stage-1 IF powders were used, of which 14 were off-the-shelf powders available in Ireland or the Netherlands, and 15 were pilot plant powders produced by Moorepark Technology Ltd.,

Fermoy, Co. Cork, Ireland. Throughout this document, the commercial powders are referred to as C1 to C14, and the pilot plant powders as P1 to P15.

3.5.3. Rehydration process using robotic agitations

The cobot prepared two mixtures for each powder using two different agitation styles: Swirl and Shake (the latter is referred to as "up and down" in O'Shea et al. (2021)). The procedure was conducted as follows.

1. On the cobot pendant, an operator (the author) entered the agitation style, the desired number of scoops of a powder, and the agitation duration, which was 15 s for all the samples in this study.
2. 180 ml of water (38°C) was manually added to the bottle and placed in front of the cobot and the start button on the cobot pendant was pressed.

The platform performed the rest of the experiment automatically. It included: (i) rehydration of the powder, (ii) imaging of the bottle, and (iii) rating of the captured images using the developed CV algorithms. The Shake agitation was more energetic than the Swirl agitation according to a preliminary analysis of data collected from the robot controller (data is presented in Chapter 5). The robotic scooping, levelling of powder in scoops, and agitation movements used in this study were designed to approximate those of humans during bottle preparation. Formal evaluation of the robot movements in comparison to human movement is described in Chapter 5.

3.5.4. Infant formula powder and mixture properties

The following properties of these powders and the corresponding prepared mixtures were determined.

Powder Particle Size Distribution (PSD): The PSD of each powder was measured using the Mastersizer™ 3000 laser diffraction machine (Malvern Instruments Ltd., Malvern, England). Measurements were performed in triplicate by the machine with the obscuration limits set between 1% and 5%, refractive index 1.45, absorption index 0.1, and air pressure 0.5 barg.

Liquid Particle Size Distribution: The PSD of each mixture was measured using a Mastersizer™ 3000 (Malvern Instruments Ltd., Malvern, England). Measurements were performed in triplicate by the machine with the obscuration limits set between 3% and 10%, refractive index 1.45 (1.333 for water as dispersant), absorption index 0.01, and stirrer speed 1750 RPM.

Target Total Solids: To calculate the target total solids (TTS) in triplicate, the cobot scoop was manually filled with powder, levelled with a blade, and weighed. The average weight was multiplied by the number of scoops recommended by the manufacturer for preparing each mixture to determine the TTS.

Dissolved Solids: A single dissolved solids (DS) measurement of each mixture was conducted using a SmartTrac™ (CEM Corporation, NC, USA). The sample was collected approximately from the centre of geometry for each mixture.

Transferring the prepared mixtures for measurements (e.g., to determine the DS) was done by hand rather than by trolley to minimise the introduction of additional vibrations. It was observed that the introduction of vibration into the prepared mixture can compromise the accuracy of measurements, particularly when measuring small quantities (i.e. the difference between the TTS and DS). Vibrations can cause sediment to re-disperse in the mixture, making it difficult to obtain a consistent mixture for measurements.

3.5.5. Participant instructions and supports

To reduce the number of images and make the rating process feasible for participants, one of the first four imaging rounds in each mixture (which aimed to monitor the foam and sediment height) was selected randomly and cropped at the top and bottom to show only foam or sediment regions. From the fifth imaging round (which aimed to count the number of white particles), no random selection was performed so all images were cropped to be rated by participants. In total, 288 cropped images per rehydration attribute were shuffled and distributed randomly to the eight participants such that each participant rated 36 images per rehydration attribute. Participants rated images in accordance

with a Standard Operating Procedure (SOP) developed for the experiment (Appendix 1). For each of the three rehydration attributes, the SOP included an image showing the rehydration attribute and expectations for the outcome. By using Python and the OpenCV library, the contrast of all images was increased to enhance the visibility of rehydration attributes.

3.5.5.1. Foam height

A ruler visible in the images was used by participants to measure the foam height. It was possible for participants to zoom into the images to count the number of millimetre grades on the ruler and report foam height in the region "as close to the ruler as possible". Participants could report measurements with a resolution of 0.5 mm in case they detected foam height between the two ruler grades.

3.5.5.2. Sediment height

As with the foam height measurement, participants were asked to rate the sediment height with a resolution of 0.5 mm and "as close to the ruler as possible". Participants had the option of zooming into images.

3.5.5.3. Identification and rating of white particles

Figure 3-9 illustrates six digitally generated reference images used by participants to rate the presence of white particles. Compared with our previous study (Mozafari et al., 2022) that used Mastersizer™ and microscope data for developing the reference images, the reference images in this study were improved to show particles with a similar shape to actual particles.

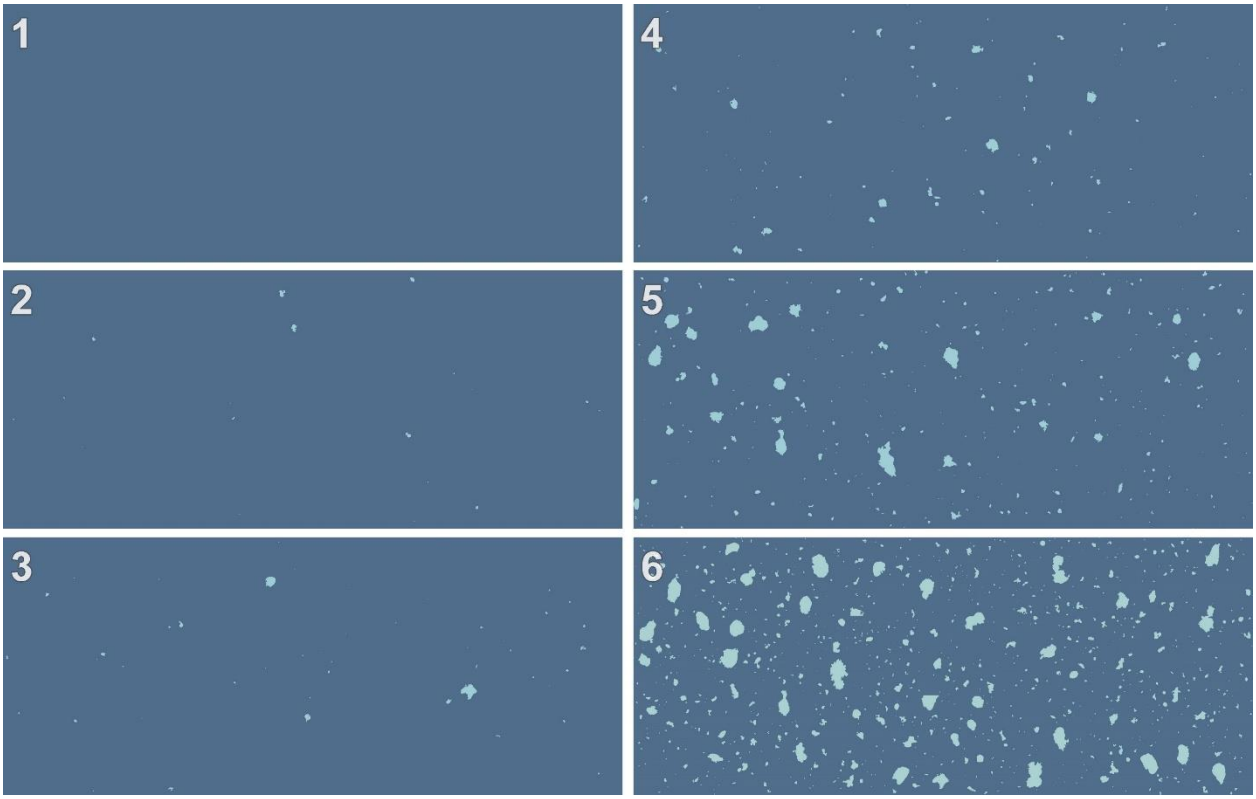

Figure 3-9 The digitally generated reference images provided for participant ratings

The six reference images were generated using the ImageJ computer application (Schneider et al., 2012) and Python. First, from the entire dataset of sample images, five samples' images with the highest level of white particles were selected subjectively by the author and labelled as samples with an "extreme" number of white particles. Then ImageJ was used to detect particles in the selected "extreme" images. The ImageJ outputs were imported into Python as binary images, and the particles visible in the images were separated and placed in an unordered collection known as a bag. To create each of the reference images, a uniform random selection was made from the bag of particles. The number of particles in reference image six was determined by averaging the number of particles in the selected "extreme" images. The number of particles in each of the other reference images was chosen in a logarithmic manner as described in Mozafari et al. (2022).

As illustrated by Figure 3-10, to distribute the particles in the reference images: (i) an empty image was generated in the same size as the cropped images in ImageJ, (ii) the randomly selected particles were sorted by size from large to small, and (iii) for each particle, a random (x, y) was

selected as the position of the particle in the image; if the particle (with known width and height) did not overlap the previously placed particles or image boundaries, it was placed in the image; otherwise, another random (x, y) was selected until the criteria was met.

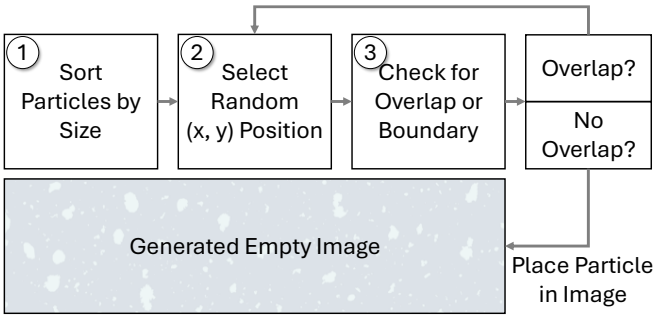

Figure 3-10 The Algorithm for digitally generating a reference image

A webpage was developed for participants to display the sample images to be evaluated alongside the reference images. The purpose of this was to ensure that reference images and mixture images had consistent relative scaling for all participants. Participants could scroll through the reference images up and down on the page and compare them with the static sample images (which were slidable left and right) to score the presence of white particles in the mixtures.

3.5.6. Data analysis

Data was analysed using R (R Core Team, 2020) and visualised using the ggplot library (Wickham, 2016). Pearson correlation coefficients and their significance (p-values) were calculated to quantify the possible linear relationships between the rehydration attribute estimates of participants and CV. While correlation assesses the strength and direction of the linear relationship between two variables, it does not evaluate the degree of concordance between the two methods (participants' and CV estimates). Thus, Bland-Altman plots were generated for all measurements, as well as Krippendorff's Alpha for white particle ratings, to analyse the degree of agreement between CV and participants' estimates. Student's t-test was used to evaluate if differences in rehydration attributes arising from each agitation style were significant.

3.6. Results and discussion

The results of the powders and prepared sample measurements are discussed in section 3.6.1. Additionally, this section discusses the possible impact of robotic agitation on particle size and dissolved solids in mixtures. Sections 3.6.2 to 3.6.4 compare the estimations of rehydration attributes between CV algorithms and participants. Sections 3.6.2 to 3.6.4 also discusses the impact of agitation style on the rehydration attributes estimated by CV, and the relationships between CV sediment height estimations, powder particle size, and dissolved solids.

3.6.1. Powder and mixture properties

According to PSD in Table 3-2, the D90 of commercial powders was greater in minimum (252 > 202 [µm]), maximum (478 > 397 [µm]), and average (357 > 310 [µm]) than that of pilot plant powders. Similarly, D[4, 3] of commercial powders showed a larger minimum (142 > 102 [µm]), maximum (286 > 205 [µm]), and average (202 > 173 [µm]) than that of pilot plant powders. Therefore, the particles of commercial powders in this study were often larger than those of the pilot plant powders, possibly due to a larger primary particle size or better agglomeration.

Table 3-2 Physical properties of the powders

Powder	**C4**	**C5**	**C6**	**C7**	**C8**	**C9**	**C10**	**C11**	**C12**	**C13**	**C14**	**P3**
$D[4, 3]_{Powder}$ (µm)	153	286	169	142	190	244	182	173	254	177	255	194
$D90_{Powder}$ (µm)	282	478	306	252	316	426	308	317	468	318	451	361
Target Total Sol. (%)	16.7	16.33	15.67	16.33	14	14.78	15.56	16	13.67	16	14.67	13.7
Powder	**P4**	**P5**	**P6**	**P7**	**P8**	**P9**	**P10**	**P11**	**P12**	**P13**	**P14**	**P15**
$D[4, 3]_{Powder}$ (µm)	205	170	119	102	146	192	191	178	204	192	180	173
$D90_{Powder}$ (µm)	397	323	237	202	290	330	327	305	346	313	306	296
Target Total Sol. (%)	14.33	12.5	13.67	13.67	12.78	12.78	12.78	12.5	11.67	13.31	12.58	12.64

Ji et al. (2016) reported that the PSD of a powder plays an important role in determining its rehydration attributes. This can be a measure of how much surface area is available for water absorption. Therefore, it can affect the rate of water absorption, which affects the rate of rehydration.

For example, agglomeration can increase the size, void spaces, and porosity of particles and allow more water to be absorbed in a shorter period of time, which results in a faster rehydration process (Ji et al., 2016b). Due to the fact that the cobot prepared all of the mixtures in a standard time of 15 seconds and identical agitations (for either swirl or shake style) in this study, the CV was expected to show the possible relationship between PSD and the measured rehydration quality (section 3.6.3 explains this further).

According to Table 3-2, TTS ranged from 11.7% to 16.7%, with an average of 14.1%, due to variations in powders (e.g., particle size) used in the study, particularly in the case of pilot plant powders. The TTS indicates the percentage of solids that ideally should be present in the prepared sample. Rehydration requirements, both in terms of time and energy, can also be influenced by the TTS (Fitzpatrick et al., 2016; Walshe et al., 2021).

Table 3-3 gives the PSD and DS for the rehydrated powders obtained using Shake and Swirl agitations.

Table 3-3 Physical properties of the mixtures prepared using Swirl and Shake robotic agitations

Mixture	**C4**	**C5**	**C6**	**C7**	**C8**	**C9**	**C10**	**C11**	**C12**	**C13**	**C14**	**P3**
$D[4,3]_{Mixture\_Swirl}$ (µm)	0.58	42.2	0.74	4.17	2.33	2.42	27.4	1.1	4.85	49.4	1.79	2.72
$D90_{Mixture\_Swirl}$ (µm)	0.89	167	1.25	0.93	6.86	7.47	130	1.29	0.75	169	4.66	5.92
$D[4,3]_{Mixture\_Shake}$ (µm)	0.54	23.5	0.73	1.03	2.36	2.31	23.8	1.1	0.55	24.9	1.84	2.37
$D90_{Mixture\_Shake}$ (µm)	0.86	129	1.24	0.88	7.09	7.11	123	1.27	0.71	116	5.06	4.92
Dissolved $Sol._{Swirl}$ (%)	9.26	8.49	11.25	11.30	12.28	12.23	12.41	12.90	12	11.98	10.87	14.14
Dissolved $Sol._{Shake}$ (%)	13.24	13.62	14.28	14.03	13.33	13.4	14.11	14.48	13.22	13.09	13.84	14.85
Mixture	**P4**	**P5**	**P6**	**P7**	**P8**	**P9**	**P10**	**P11**	**P12**	**P13**	**P14**	**P15**
$D[4,3]_{Mixture\_Swirl}$ (µm)	2.1	2.73	2.19	2.56	2.53	68.1	68.1	1.08	1.52	1.55	4.35	1.59
$D90_{Mixture\_Swirl}$ (µm)	3.92	5.78	6.19	6.95	5.31	203	203	1.75	3.35	2.98	3.26	2.87
$D[4,3]_{Mixture\_Shake}$ (µm)	2.39	1.28	1.48	1.97	2.19	22.9	22.9	0.9	1.49	1.6	1.29	1.4
$D90_{Mixture\_Shake}$ (µm)	5.01	2.38	3.73	5.24	4.54	124	124	1.68	3.29	2.97	2.43	2.67
Dissolved $Sol._{Swirl}$ (%)	11.53	10.02	8.73	7.43	11.37	7.27	7.74	7.25	7.93	10.37	10.38	8.88
Dissolved $Sol._{Shake}$ (%)	15.36	12.14	14.26	13.55	13.27	11.62	8.35	9.57	10.83	11.86	12.33	11.75

There have already been studies using the DS to assess the "solubilisation ability" and the change in mixture PSD to assess dispersion (Fitzpatrick et al., 2016; Mimouni et al., 2009). In the current study, the difference between TTS and DS was observed to be related to sediment as explained in section 3.6.3. If the DS is less than the TTS, it can be argued that some parts of the solids have not dissolved and have therefore settled (or floated). It was observed that on average, Shake agitation resulted in higher DS than Swirl agitation, as a result of the fact that Shake agitation was more energetic than Swirl agitation. The DS in mixtures P3, P4, and P6 prepared using Shake agitation are higher than the TTS. Perhaps this is due to the high compressibility of powder and the fact that the TTS was measured manually. When powder is scooped with greater force it may be packed more tightly in the scoop, resulting in a higher powder weight in the scoop, and a higher TTS (cf. Altazan et al., 2019; Crowley et al., 2014). As part of the Chapter 4, the cobot will be used to measure the TTS to ensure greater consistency.

PSD D90 values of the mixtures prepared by Shake and Swirl agitations ranged from 0.71 to 129 (μm) and 0.75 to 203 (μm), respectively. The results indicate that there was a wide range of particle sizes in the mixtures. In addition, mixtures prepared by the Shake agitation often displayed smaller particle sizes than those prepared by the Swirl agitation (considering D[4, 3] or D90 of Shake versus Swirl agitation in Table 3-3). According to Table 3-3 the D90 in mixtures obtained using the Shake agitation had a lower median ($4.1 < 5$ [μm]) and average ($28.3 < 39.3$ [μm]) than the mixtures prepared with the Swirl agitation. This may be due to the more energetic agitations associated with the Shake agitation, which could result in more rehydration of powder particles due to the breakage of the solid bonds between particles (Bock et al., 2007). However. further studies are needed to explore the effects of the powder PSD on rehydration (Benkovic and Bauman, 2009).

3.6.2. Comparison between the foam height estimates of computer vision and participants

For evaluation purposes, the foam height estimates corresponding to a single random imaging round (six images from different viewpoints) of each mixture were averaged separately for participants and CV. This was done because the foam height estimates from any single viewpoint of a mixture can be expected to slightly vary, and the objective was to get a foam height estimate for the mixture rather than from a single image. The CV estimates for all mixtures, independent of the agitation method, exhibited a Pearson correlation of 0.82 ($p < 0.001$) with participant estimates. When the agitation method was considered, this correlation was 0.69 ($p < 0.001$) for Swirl agitation and 0.86 ($p < 0.001$) for Shake agitation as shown in Figure 3-11.

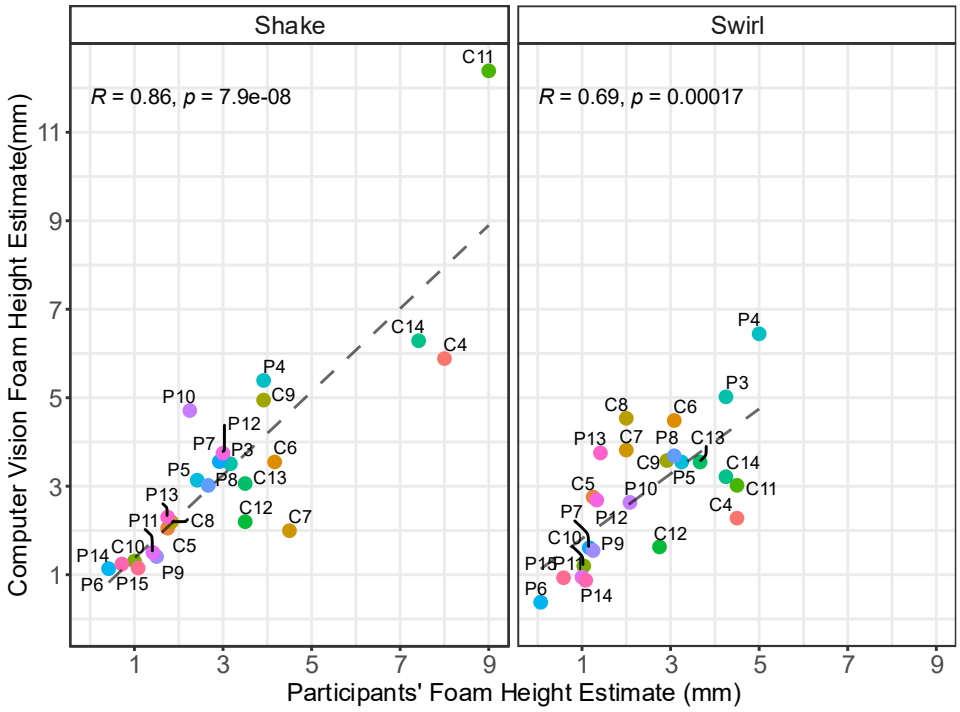

Figure 3-11 Comparison of computer vision and participant foam height estimates on cobot-captured images for mixtures prepared using the Shake (left) and Swirl (right) agitation. Each dot represents the average foam height of a single random imaging round of a single mixture estimated by participants and computer vision.

The CV foam height estimates are more closely correlated with the participants' estimates for samples prepared using the Shake agitation. This behaviour can be explained by the fact that mixtures prepared

using Swirl agitation were on average found to have less foam (and therefore more difficult to measure) than those prepared using Shake agitation, both according to CV and participants. Also, considering the results for the foam height estimates of the Swirl samples were smaller, the correlation becomes more sensitive to the accuracy of the measurements, while the theoretical resolution of the participants' ratings in this study was limited to 0.5 mm. Furthermore, in a small number of cases (some viewpoints of some mixtures), the CV algorithms provided estimates that were obviously not correct; this was observed in mixtures C4 and P10 in the Shake agitation and mixtures C4 and C8 in the Swirl agitation. There could be a number of factors responsible for this, including lighting conditions, bottle marks, and the colour of the mixture.

As explained in section 3.5.5, Figure 3-11 only shows one randomly selected imaging round for each mixture that was evaluated by participants. While the platform monitored the foam and sediment height over time (during the first four imaging rounds), two mixtures, C8 and C14, exhibited a relatively high increase in foam height at two consecutive time points (Figure 3-12).

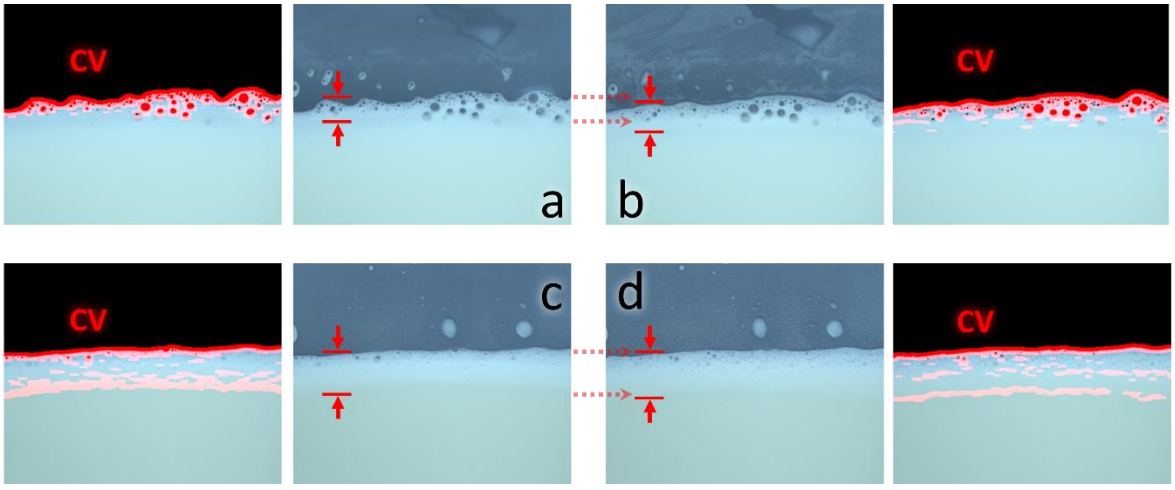

Figure 3-12 Manual validation of increased foam height over time in samples C14 (from time 0 (a) to 5 (b) minutes) and sample C8 (from time 5 (c) to 10 (d) minutes) illustrated alongside their corresponding CV estimations. The end of horizontal dotted arrows (marked manually) subjectively shows how the lower and upper foam boundaries change over time.

It is in agreement with the phenomenon of foam drainage described by Huppertz (2010) which refers to the process of liquid separation and migration within a foam structure over time.

Figure 3-13 shows Bland Altman graphs assessing the agreement between participants and CV for foam height estimates.

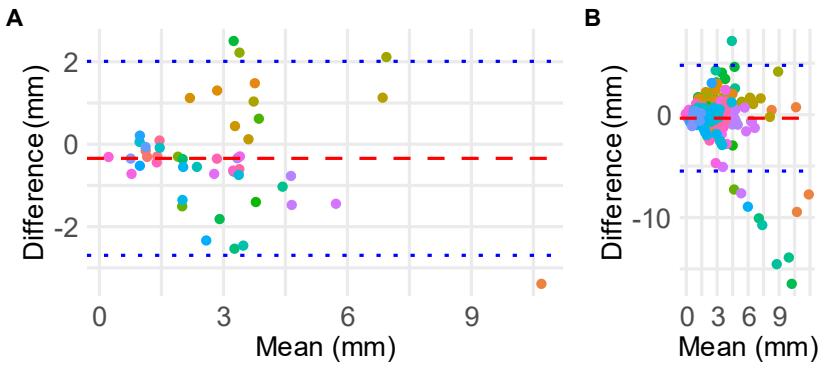

Figure 3-13 Bland Altman graph for foam height estimated by participants and CV. A: average of each imaging round; B: all individual images (without averaging).

When the foam height estimates were averaged across the six viewpoints of an imaging round, the 95% confidence interval (CI) between the foam height estimates was 2.1 mm, indicating good agreement between participants and CV. When considering individual images, the CI was 5.1 mm. The larger CI (and hence lesser agreement) on individual images was expected since the participants and CV made estimations from slightly different parts of the foam (with participants focusing on the area near the ruler only). However, when the foam estimates were averaged across six viewpoints around the bottle, much of that difference disappeared (i.e., reduced from 5.1 mm to 2.1 mm). It is worth noting that, in Figure 3-13, the apparent diagonal structure of points on the results for individual images is a side effect of the participant foam height estimates having a resolution of 0.5 mm. It also suggests that the difference between measurements increases as the mean value increases. In some bottle viewpoints, the participant may rate sediment/foam as large while the CV system rates it as small (e.g., because the participant only measures sediment/foam close to the ruler, while CV performs averaging across the entire ROI, or when CV/participant makes an error).

3.6.3. Comparison between the sediment height estimates of computer vision and participants

Similar to the foam height estimate, the sediment height estimate corresponding to a single imaging round (six images from different viewpoints) for each mixture was averaged separately for participants and CV. The CV sediment height estimates exhibited a correlation of 0.77 ($p < 0.001$) with participant estimates when the agitation method was not considered. When separated by agitation method, Figure 3-14 shows that the correlation was 0.78 ($p < 0.001$) for Swirl and -0.16 ($p = 0.45$) for Shake.

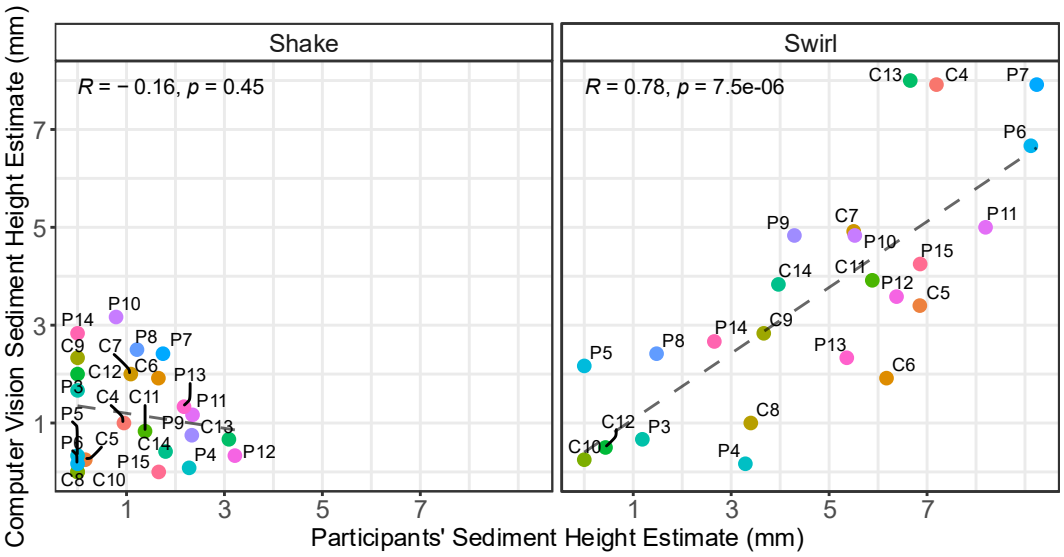

Figure 3-14 Comparison of computer vision and participant sediment height estimates on cobot-captured images for mixtures prepared using the Shake (left) and Swirl (right) agitation. Each dot represents the average sediment height of a single random imaging round of a single mixture estimated by participants and the computer vision.

It appears that the detection of sediment height may be more challenging in mixtures prepared using the Shake agitation. The reason for this may be the more energetic agitations involved in Shake style, which results in less sediment being detected in the mixtures. Similar to the foam height estimate, participant sediment estimates were limited to 0.5 mm resolution, which may explain the weaker correlation when small amounts of sediment are present.

In most powders, sediment decreased when a more energetic agitation was applied during rehydration (i.e., Shake agitation). Generally, both CV and participants estimated lower sediment levels for mixtures prepared with Shake agitation compared to Swirl agitation. This finding is supported by the fact that the DS measurements reported in Table 3-3 are higher for Shake agitation. Considering all mixtures, it was found that the difference between the TTS and the DS (i.e., solids introduced but not dissolved) was correlated with the sediment height estimated by CV ($r = 0.75$, $p < 0.001$) and participants ($r = 0.70$, $p < 0.001$). This relationship might be explained according to the law of conservation of mass, if the added powder has not been sufficiently rehydrated, the mixtures should show sediment (or lumps). For example, Fitzpatrick et al. (2016) observed that milk protein isolate with high sediment content had low solubilisation percentages after comparing the mass of dissolved solids (using an oven) with the initial powder mass. The current study also found weak but significant correlations between the powder particle size D90 and sediment estimates for the Swirl agitation, both according to CV ($r = -0.44$, $p = 0.03$) and participants ($r = -0.48$, $p = 0.02$). In the case of Shake agitation, neither CV estimates ($r = -0.13$, $p > 0.5$) nor participant estimates ($r = -0.14$, $p > 0.5$) demonstrated a significant correlation. This suggests that smaller powder particles may contribute to higher sediment levels if a sufficiently energetic agitation is not performed during rehydration. This behaviour could be explained by the fact that smaller particles have a smaller air gap between (or within) them, making water penetration difficult (Ji et al., 2016b).

Figure 3-15 shows Bland Altman graphs assessing the agreement between participants and CV for sediment height estimates.

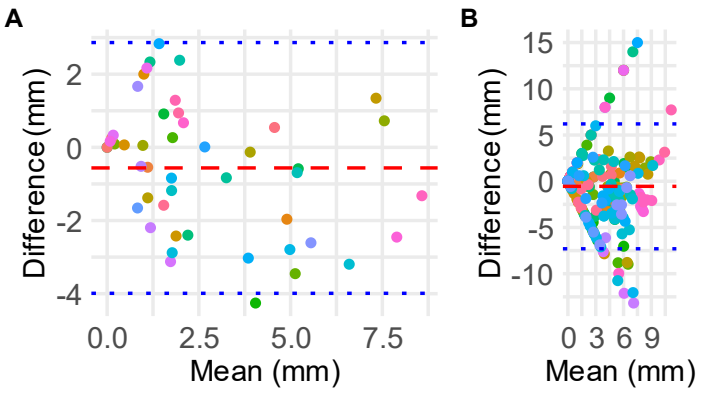

Figure 3-15 Bland Altman graph for sediment height estimated by participants and CV. A: average of each imaging round; B: all individual images (without averaging).

When averaged across an imaging round as normal, the 95% CI for sediment estimates was 3.4 mm. Assessing images individually results in a CI of 6.9 mm. Similar to foam height estimates, the larger CI is expected since participants and CV measure the sediment in slightly different places in the image. In some mixture images, the sediment height varies across the image and the difference between participants and CV can be rather large in these cases. Additionally, the apparent diagonal structure results can be explained similarly to section 3.6.2.

3.6.4. Comparison between the white particle ratings of computer vision and participants

White particles were counted by CV but counting individual particles is impractical for participants. Hence white particles were categorically rated (1–6) by participants (by matching them to the reference images described in section 3.5.5.3). Similar to the foam and sediment estimates, CV counts and participant ratings of white particles corresponding to a single imaging round for each mixture were averaged separately. Therefore, the average participant rating for an imaging round often falls between existing categorical values and is treated as a continuous valued variable for analysis. As illustrated in Figure 3-16, the correlations between the CV number of particles and participants' ratings were 0.6 ($p = 0.0019$) for Shake and 0.56 ($p = 0.0045$) for Swirl agitation.

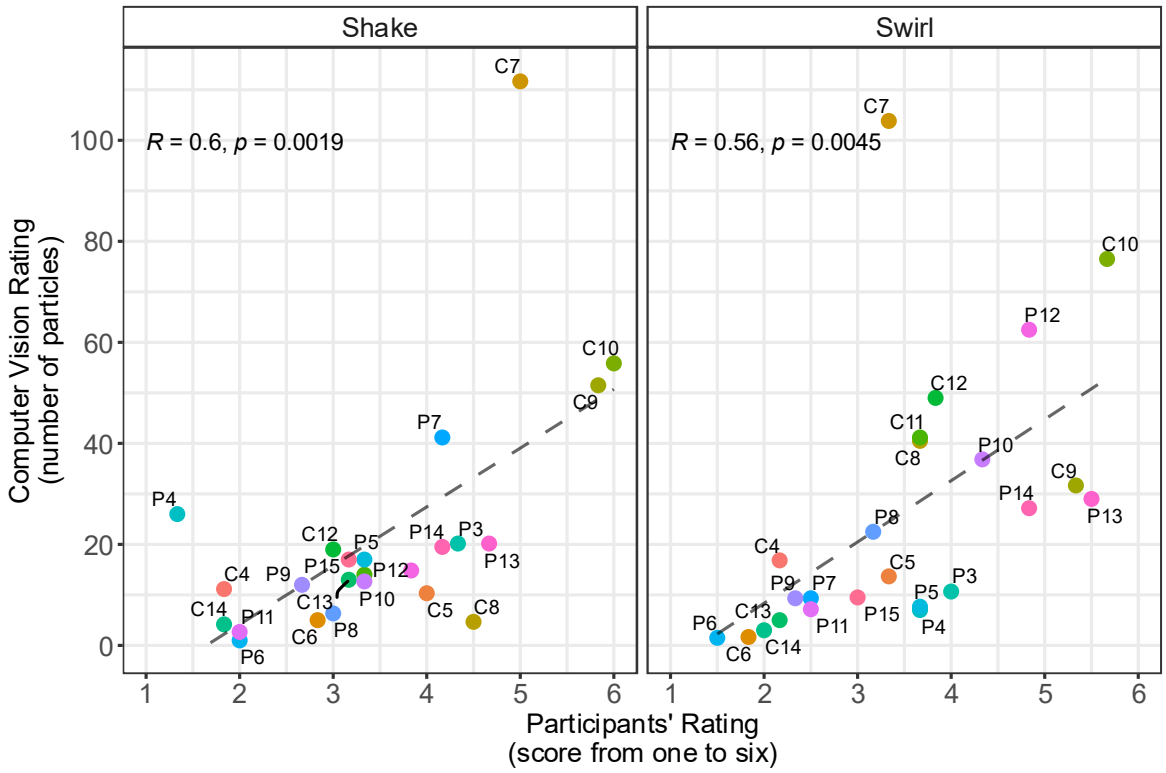

Figure 3-16 Comparison of white particles counted by computer vision and categorically rated by participants (in average of each imaging round)

According to Weber-Fechner's hypothesis, human perception functions on a logarithmic basis (Fechner et al., 1966). Therefore, the results of the CV detected number of particles were categorized in a logarithmic manner in six scores (the approach was the same as described in Mozafari et al. (2022)). According to Figure 3-17, using this approach, the correlations between CV and participants' ratings increased to 0.67 ($p < 0.001$) for Shake and 0.72 ($p < 0.001$) for Swirl agitation. Independent of the agitation method, the CV and participants' ratings were correlated by 0.68 ($p < 0.001$).

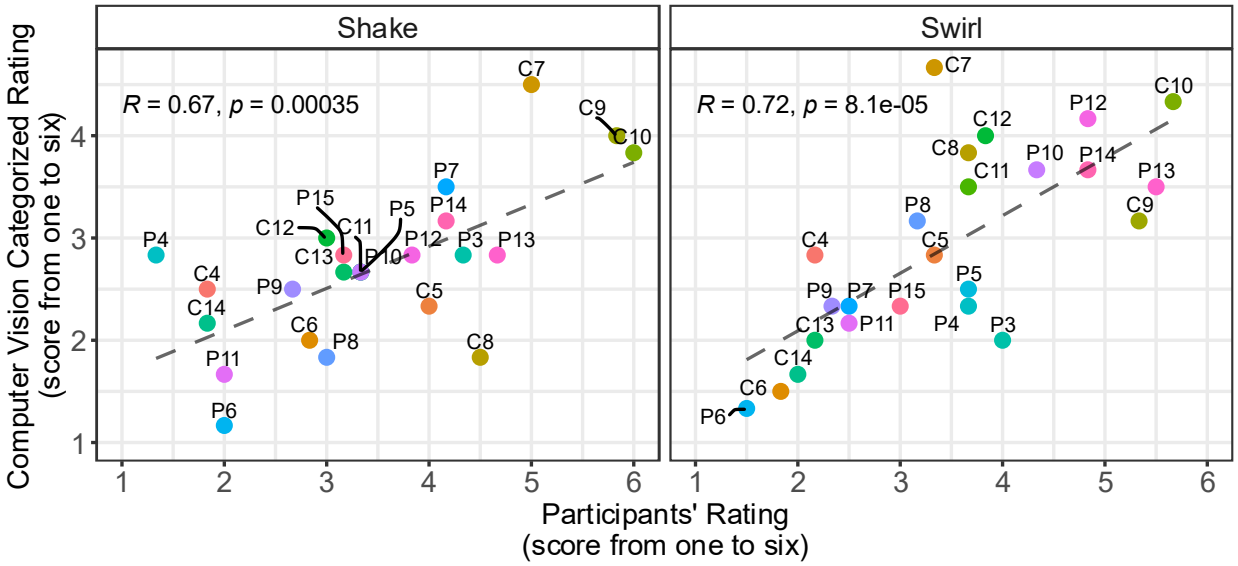

Figure 3-17 Categorized computer vision ratings of white particles compared to the participants' ratings

Although agitation style appears to affect CV sediment ($p < 0.001$) and foam height estimates ($p = 0.018$) (in the first imaging round, i.e., before further changes in foam or sediment heights occur), CV ratings of white particles, both in terms of their numbers ($p = 0.52$) and score ($p = 0.40$), do not appear to be significantly affected. It is possible that the 15 s of agitation by the cobot was insufficient to dissolve white particles since they are inherently difficult to dissolve (Lloyd et al., 2019; Toikkanen et al., 2018).

Figure 3-18 illustrates a Bland Altman graph based on the average of the imaging rounds (since this is an ordinal rating). The magnitude of 95% CI for CV ratings is 1.7 score.

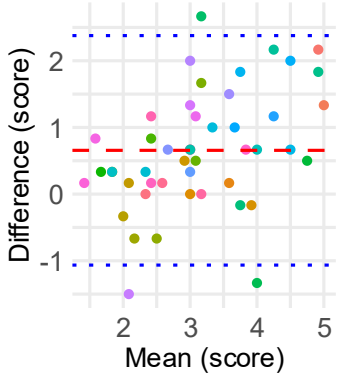

Figure 3-18 Bland Altman graph for an average of white particles in each imaging round rated by participants and CV

For individual images, Krippendorff's Alpha was 0.31 between CV and participants' ratings. This number was 0.54 if the average of the imaging rounds was considered instead. The averaging was expected to reduce the variation of ratings and increase the agreement, especially when in each imaging round different participants rated the six viewpoints of the bottle randomly. While this increase suggests that there is a higher agreement between the CV and participants' particles rating when a complete imaging round is considered rather than individual images, the Krippendorff's Alpha still falls below the threshold for reliable agreement. Without taking into account CV ratings, Krippendorff's Alpha for the participant ratings (which, as explained in section 3.5.5, were from different viewpoints of the same sample), was 0.39. This suggests that the agreement between different participants rating the same sample from different viewpoints is similar to the agreement between the automated and participants' ratings.

3.7. Conclusion

This thesis chapter aimed to provide an automated powder rehydration testing platform that can be incorporated into a laboratory or manufacturing plant environment. The platform was used to: (i) rehydrate IF in a commercial bottle, in a manner that is similar to how the end user would rehydrate it at home, and (ii) objectively and nondestructively quantify three visible powder rehydration attributes. As far as the author is aware, the concept of automated rehydration characterisation has not been explored in the literature to date, and this platform is the first of its kind developed for gaining objective insights into powder rehydration.

The CV foam height estimates, sediment height estimates, and white particles ratings were compared with those of participants on the same cobot-captured images used in the CV system. The correlations were 0.82, 0.77, and 0.68, respectively. Furthermore, the difference between the Target Total Solids and Dissolved Solids of the mixtures was correlated to the CV ($r = 0.75$) and participants' ($r = 0.70$) sediment height estimates. These correlations suggest that incomplete rehydration contributes to sediment formation. Additionally, for Swirl (less energetic) agitation, powder particle

size D90 showed weak but significant negative correlations with sediment height estimates of CV (r = -0.44) and participants (r = -0.48). It suggests that powders with smaller particles may not be able to rehydrate without a sufficiently energetic agitation, therefore, resulting in an increasing sediment height. The results of both participants' and CV measurements indicate that agitating the mixtures more energetically (i.e., Shake agitation) increased foaming and reduced sedimentation but did not affect the number of white particles significantly.

Even though the algorithms performed satisfactorily for this study, they may be improved, particularly for the foam and white particles algorithms by considering shape-related factors. Also, the flexibility of CV ratings may be improved by applying machine learning techniques. For example, the same "digitally generated" particles used in the current study may be useful for training a network for the detection of white particles.

The results of the current chapter show that the platform has the potential to automatically rehydrate IF powders and objectively estimate the visual manifestation of three rehydration attributes. Moreover, except in the case of sediment resulting from Shake agitation, the platform CV estimates both correlate and agree well with those of human raters. Chapter four will discuss the relationship between CV estimates and commonly used laboratory methods, including sediment weights and slowly dissolving particles. Moreover, even though the cobot's scooping and agitation movements in this study were designed to approximate the movements performed by end users, chapter five intends to characterise the arm movements of ten people to fine-tune the robotic bottle agitation movements.

Chapter 4 (Platform evaluation): Exploring the impact of infant formula powder properties on rehydration quality using an automated platform

A manuscript based on this chapter is being prepared for submission to Innovative Food Science & Emerging Technologies as:

- *Mozafari, B., Villing, R., Fenelon, M., Li, R., Daly, D.F. and O'Shea, N., Exploring the Impact of Infant Formula Powder Properties on Rehydration Quality Using an Automated Platform.*

4.1. Introduction

This chapter aimed to answer two research questions and provide a deeper understanding of the platform performance and the insights it may provide.

First, continuing from Chapter Three, the present chapter further examined whether there are any relationships between automatically quantified rehydration attributes and twenty commonly used laboratory tests on powders and the corresponding rehydrated powders (such as sediment weight, dispersibility, and particle size of powder and the corresponding rehydrated powder). It was expected that analysing the relationship between automated measurements and traditional measurements would provide new insights into platform performance and rehydration process. As for the dissolved solids and particle size measurements which were also conducted in Chapter Three, similar findings were expected in the present chapter.

Secondly, based on the relatively extensive (a comparable number of experiments and IF powder samples have not been reported in the literature) data collected from the commonly used laboratory tests, this chapter also investigated the possibility of predicting the results of the manual laboratory tests, specifically dispersibility, which is a time-consuming and subjective test (Boiarkina

et al., 2017), based exclusively on the automated estimates of the rehydration attributes (foam height, sediment height, number of white particles, and mixture colour) generated by the platform. Predictions based on measured mixture properties (such as particle size and optical scattering methods) have already been reported in the literature as a more rapid (Chen and Lloyd, 1994) and accurate (Galet et al., 2004) method. However, such a prediction has not been reported previously using visual manifestations of rehydration attributes. Since this approach can also estimate other rehydration attributes simultaneously, such as sediment height, foam height, and the number of unhydrated particles (Mozafari et al., 2024), it may be advantageous.

As mentioned in Chapter Two, IF powder rehydration quality is critical as poor rehydration can adversely impact the nutritional value, safety, and visual appeal of the rehydrated IF powder (Martin et al., 2016; Masum et al., 2020; Renfrew et al., 2003; Sharma et al., 2012). The rehydration properties of IF powders are strongly influenced by formulation, manufacturing parameters (Crowley, 2016; Munir et al., 2017), and the agitation energy used by the end-user during rehydration (Fitzpatrick et al., 2017; O'Shea et al., 2021). Both the initial formulation and the manufacturing parameters used to transform the liquid concentrate into powder interact in a complex manner and significantly impact the final physicochemical characteristics of the powder, which, in turn, impacts rehydration properties (Schuck et al., 2016). However, as mentioned in Chapter One, quantitative and objective approaches are required to better correlate powder physicochemical attributes with rehydration properties (Ding et al., 2020b; Munir et al., 2017).

As illustrated in Figure 4-1, the ideal rehydration of infant formula powder in water involves rapid and complete progression through the following steps: (i) wetting of particle surfaces upon contact with water; (ii) sinking of wetted particles throughout the water; (iii) breakdown of agglomerates into discrete primary particles (dispersion); and (iv) dissolution of individual particles into water (solubilisation) (Fang et al., 2008; Schober and Fitzpatrick, 2005). Occasionally, however, wettability, sinkability, dispersibility, and solubility issues can adversely affect the rehydration

process, resulting in undesirable rehydration attributes such as sedimentation, lump formation, and flecking or slowly dissolving particles (Masum et al., 2020; Sharma et al., 2012; Toikkanen et al., 2018).

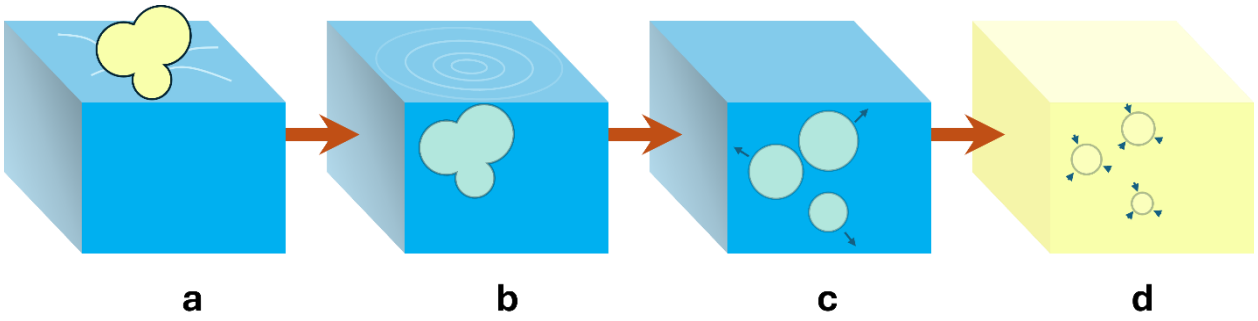

Figure 4-1 Four rehydration stages of dairy powders; (a) wetting, (b) sinking, (c) dispersion, and (d) solubilisation

There are several physical and compositional attributes of particles that can determine their rehydration, including:

***Particle size*:** Smaller particles possess a greater specific surface area (surface per unit of mass). However, smaller particles can increase cohesive forces between particles (Fang et al., 2008; O'Donoghue et al., 2019). They also result in smaller spaces between particles that can make water penetration difficult. An optimal particle size is reported to be ~150-250μm, depending on the powder type (Gaiani et al., 2011; Sharma et al., 2012).

Particle density: Higher particle density is reported to accelerate sinking rate upon wetting (Fitzpatrick et al., 2017; Freudig et al., 1999; Murphy et al., 2020). On the other hand, better wetting is associated with higher agglomeration, resulting in a lower particle density (Freudig et al., 1999).

Particle morphology: Irregular particle shapes and internal void spaces created by pockets of trapped air during drying can improve wettability (Gaiani et al., 2011; Han et al., 2022; Tamime, 2009). However, irregularity can result in a less free-flowing powder (Fu et al., 2012).

Surface composition: Hydrophilic compounds (e.g., lactose) on particle surfaces accelerate water interactions during the wetting stage, while hydrophobic components (e.g., fat) result in poor wettability (Kim et al., 2002). Increased fat lowers wettability, and surface fat coverage is more detrimental than bulk fat (Fitzpatrick et al., 2017).

Protein content/type: Higher total protein, especially casein, is reported to reduce solubility. Although whey proteins disperse easier, their wettability is poor (Ji et al., 2016b). However, some studies have not observed this behaviour (Walshe et al., 2021).

To assess dairy powder rehydration properties, a variety of qualitative and quantitative laboratory techniques are employed (Pisecky, 2012). In some tests, the powder rehydration properties are inspected visually. Among these tests are wettability, slowly dissolving particles, foam formation, and some sediment measurement tests, which are highly dependent on a technician's perception of the degree of observed rehydration properties (Pisecky, 2012) and suffer from low discretisation and a high degree of subjectivity (Crowley et al., 2016; Lloyd et al., 2019). With these methods, it is difficult to detect small differences between powders' rehydration properties (Lloyd et al., 2019). Also, measurement of some parameters, such as foam dissipation rate, may be time-consuming for a technician since the sample must be monitored for a specified duration of time. Therefore, current methods have limitations, including insufficient automation, subjectivity, poor repeatability and reproducibility, laborious, time consuming, and difficulty providing insight into rehydration kinetics (Fang et al., 2008; Munir et al., 2017). Moreover, many of the traditional tests focus on only one stage of rehydration and do not closely replicate the actual rehydration procedure used by end users (Hardy et al., 2002; Pisecky, 2012). When a powder does not perform well during a particular stage of rehydration, that does not necessarily mean that it cannot perform well during the overall rehydration process (McSweeney et al., 2021). Manufacturers may obtain more consistent products for consumers if they have a better understanding of the rehydration process (Pisecky, 2012), particularly based on the procedure used by the end user (Hardy et al., 2002; Lloyd et al., 2019).

As discussed in Chapter Two, and illustrated in Chapter Three, developing an integrated rehydration platform requires specialised expertise across several fields, including robotics, image processing, computer programming, statistics, and, dairy science and technology, which prevents widespread adoption of these platforms in the IF or dairy processing industry (Munir et al., 2017;

Serazetdinova et al., 2019). Due to the challenges associated with digital data collection (e.g., system integration, requirement of additional skills and resources, and management of software, hardware, and data), only a limited number of automated tools have been reported for quantitatively assessing the rehydration of dairy powders (Munir et al., 2017).

Recently, some rehydration properties have been quantified using computer vision (CV) techniques. Lloyd et al., (2019) developed a method for identifying bulk slowly dissolving particles that combined machine-assisted reconstruction, flow cell imaging, and a custom image processing algorithm. Authors of the present study developed a fully automated rehydration quality measurement platform, incorporating a cobot integrated with a camera, which rehydrated IF powders and estimated foam and sediment height, and the number of undissolved particles (referred to as white particles) in the mixtures (Mozafari et al., 2024). Eight participants evaluated the foam and sediment height estimate algorithms using a ruler visible in the cobot-captured images. Additionally, six reference images were digitally generated, and the participants separately rated the presence of white particles in the cobot-captured images. To maintain the scale between reference images and rehydrated sample images, a webpage was developed for participants. The CV algorithm for estimating the number of white particles, and a preliminary version of the digitally generated reference images had been developed in a previous study by the authors (Mozafari et al., 2022). The purpose of these studies was to reduce the subjectivity associated with the way humans prepare mixtures and perceive rehydration properties. Ding et al., (2020) developed a model to predict powder dispersibility and slow-dissolving particles using particle morphological features extracted from image analysis. They found that particle shape metrics were a key indicator of dispersibility.

Despite the challenges, it is imperative to develop automated platforms to fully exploit the benefits of Process Analytical Technologies (PAT). These platforms provide real-time quantitative data while reducing subjective human evaluation (Munir et al., 2017). In addition, the combination of robotics and CV may enable more reproducible measurements and the generation (and storage) of

experimental datasets that are more likely to allow improved traceability (Serazetdinova et al., 2019). In this way, well-recorded data and quantitative attributes related to powder rehydration could be obtained, something that conventional methods are not able to provide. Also, predictive models can be developed that may be useful in better understanding the water transfer processes during rehydration (Schuck et al., 2016) and guiding powder production so that poor-quality powder can be detected earlier (Munir et al., 2018), saving resources.

In response to the first research question mentioned at the beginning of this chapter, the current study aimed to: (i) validate the performance and repeatability of the platform's CV algorithms in estimating sediment height and the number of white particles in comparison to standard reference methods commonly used in the laboratory; and (ii) identify potential relationships between powder physicochemical properties (obtained using the standard reference methods) and rehydration properties quantified by the automated platform. Regarding the second research question of the present chapter, the study proposed and evaluate a multivariate model to predict the outcome of the dispersibility reference method based solely on properties estimated by the automated platform, as a rapid screening method. Measuring dispersibility using the standard method is a highly subjective process, as it requires adherence to using a specific spatula, stirring method, and stirring duration (GEA, 2005a). Several studies have already attempted to predict this test as "proxy measurements" (Boiarkina et al., 2017; Ding et al., 2020a).

4.2. Materials and Methods

4.2.1. Infant Formula Powders

Twenty-three stage-1 IF powders were analysed, including sixteen commercial (C4-C19) and seven pilot plant (P9-P15) powders. Three types of measurements were conducted on these powders: (i) commonly used lab measurements (i.e., reference methods) according to Table 4-1, (ii) modified reference methods according to Table 4-2, and (iii) automated platform estimates. After completing

the measurements, first, a comparison was made between the results from the modified reference methods and the output from the CV system on the automated platform to evaluate the platform estimates. Secondly, a model to predict measurements of commonly used lab methods and modified methods solely based on the automated platform estimates was developed and evaluated. To prevent interhuman variation, each measurement was to be conducted by the same individual (however, this was not achieved for insolubility and particle density measurements).

4.2.2. Commonly Used Lab Measurements (Reference Methods)

Table 4-1 lists the eighteen physicochemical powder properties and their corresponding mixture properties that were measured.

As a measure of the presence of undissolved material in the mixture based on Table 4-1, the difference between TTS and DS was used. Solids introduced into a solution but not completely dissolved should manifest as undissolved material, such as clumps or sediment (Mozafari et al., 2024). However, for the DS measurement, it is important to collect samples from the body of the mixture rather than from any region near sediment at the bottom or clumps at the top of the mixture, where the mixture may be thicker and exhibit a higher DS as a result. Therefore, the samples for the DS measurements were collected from the bottle's centre of geometry, and the pipettes were placed in the rehydrated samples at an identical depth (aligning the pipette grades with the top edge of the bottle). Moreover, to avoid disturbing possible sediment or clumps in the mixtures, the samples were collected gently (the pipette vacuuming process took approximately five to ten seconds).

The span parameter, which is used for characterising powder particle size distribution (Bhandari et al., 2013), was calculated According to Equation (4.1) to examine a possible relationship of the powder particle size distribution with the rehydration attributes.

$$span = \frac{D90 - D10}{D50} \tag{4.1}$$

Table 4-1 List of the commonly used laboratory measurements (reference methods) conducted in the present study on powders and their corresponding prepared mixtures

number	Measurement Method
1	Powder moisture was measured in duplicate using the GEA "Powder moisture – accurate standard method" (GEA, 2006a).
2	Particle density was determined in duplicate using a helium pycnometer (AccuPyc™ II 1340, Micromeritics Inc., USA) according to the GEA method (GEA, 2006b).
3	Bulk volume measurements were made in duplicate using the GEA reference method (GEA, 2006c).
4	Powder insolubility was measured in duplicate using the GEA method (GEA, 2006d).
5	Powder flow index was determined in duplicate using a flow tester (Brookfield Engineering Laboratories Inc., MA, USA).
6	Protein content of powders was quantified in triplicate using the Dumas combustion method via the LECO machine (LECO Inc., USA) with a protein conversion factor of 6.3800.
7	The measurements of wettability were conducted in duplicate using the GEA method with 100 ml of 40°C water, but the powder was dropped using a plate and cylinder instead of a funnel and pestle (GEA, 2009).
8	A duplicate measurement of dispersibility was conducted using the IDF method (GEA, 2005a).
9	Target Total Solids (TTS) for each powder was measured in triplicate by filling an empty bottle with the powder using the robot. A TTS was determined by dividing the weight of the powder by the weight of the water and the powder.
10	A duplicate comparison was made between the volume of commercial scoops, provided in the manufacture's cans, and that of the robot scoop. Using the calculated volume ratio, the robot added the powder to the bottle, to prepare the samples as closely as possible to the manufacturer's recommendations on the packaging. For volume comparisons, the scoops were weighed based on the maximum amount of water they could hold.
11	The percentage of Dissolved Solids (DS) in rehydrated powders was determined in duplicate using a SmartTrac™ (CEM Corporation, NC, USA) that utilises a microwave to evaporate sample moisture and determine weight differences.
12	The Dumas combustion method via the LECO machine (LECO Inc., USA) was used to measure the protein content in the sediment once (protein conversion factor = 6.3800). Samples of sediment were collected in aluminium foils and dried in an oven at 102°C for two or three days, depending on the amount of sediment in each sample. A pestle and mortar were used to grind the dried sediment, and the powdered sediment was fed into the machine for protein measurement.
13	The particle size distribution of powders was measured by laser diffraction (Mastersizer 3000™, Malvern Instruments, UK) in duplicate. The obscuration levels were from one to five percent, with refractive index of 1.45, absorption index of 0.1, and air pressure of 0.5 barg. In the current study D90 is primarily discussed as a descriptor of powder particle size.
14	The particle size distribution of reconstituted mixtures was measured by laser diffraction (Mastersizer 3000™, Malvern Instruments, UK) in duplicate. The stirrer speed was 1750 RPM, with an obscuration level of three to ten percent, refractive index of 1.45 (1.333 for water as dispersant), and absorption index of 0.01. In the current study D90 is primarily discussed as a powder particle size.
15	Powder particles morphology parameters were measured once using Malvern morphology machine. The current study focused on circularity, convexity, and elongation.
16	Lactose content was measured in duplicate by a technician using the HPLC method described by Pirisino, (1983).
17	The powder surface free fat was measured in duplicate by a technician using the GEA method (GEA, 2005b) which uses petroleum ether as the solvent.
18	Powder colour was measured in duplicate using a Konica Minolta CR-400 Chroma Meter (Chiyoda, Tokyo, Japan) after calibration with its white tile.

4.2.3. Modified Reference Methods

For sediment measurement, current methods use relatively large pore size sieves that cannot catch finer fractions of sediment, and they do not take into account possible sediment left in the beaker after filtration (e.g., the "sludge" test (Pisecky, 2012)). Current methods for analysing undissolved particles also have repeatability issues (Lloyd et al., 2019). Therefore, these methods cannot provide a reliable benchmark for assessing the performance of our automated platform without modification. Consequently, these methods were modified as shown in Table 4-2 to increase sensitivity (for sediment) and repeatability (for white particles). The modified methods aimed to provide a benchmark for the mixtures evaluated using the automated platform.

Table 4-2 List of modified reference methods

Methods Available in the Literature	**Modified Methods (based on the methods from literature)**
	Before performing the tests: 1. The robot prepared the samples in the same manner as for the vision system 4.2.4.1), but without performing any imaging. 2. There was a three-minute rest period for the sample. During this time, any potential clumps on the surface of the mixture was scooped out and discarded.
Slowly Dissolving Particles (SDP) (Lloyd et al., 2019) ** Highlighted modification: The glass tube was emptied from bottom rather than top.	Presence of White Particles (WP) test: 1. Within one minute, the mixture surface was scooped into the pipe section of a glass funnel closed at the bottom with a stopper. The remainder of the mixture was used for the SW test. 2. After three minutes, the stopper was removed to pour the sample into the sink (discarded). 3. Five minutes later, the presence of white particles sticking to the glass pipe was compared against the pictures in the reference method (SDP test) and a score from one to five was assigned.
Sludge Test (Pisecky, 2012) ** Highlighted modification: A Whatman filter grade 4 and a vacuum pump were used rather than a 600 µm sieve.	Sediment Weight (SW) test: 1. After sample collection for the WP test, two-thirds of the mixture (from the top to the 60 ml mark on the bottle) was gently (around 30 seconds duration) vacuumed from the top of the mixture into the sink. This was done to prevent the filter from becoming clogged with potential bulk particles. 2. A vacuum pump and Watman filter grade 4 (25µm) were used to filter the remainder of the mixture (60 ml). 3. The weight of sediment remaining in the bottle was added to the weight of the sediment on the filter (minus the weight of the empty bottle/filter).

Some standard tests recommend that when a sample falls between two scores, it should be assigned the highest score (GEA, 2006e, 2005c). Thus, to maintain the ordinality of the results of the WP test, the results were rounded to the higher integer after averaging the duplicated measurements.

Unlike the modified reference methods for WP and SW tests described in Table 4-2, the original methods do not require the samples to be prepared in a commercial bottle. In this study, the mixtures were prepared in a baby bottle to ensure that the experimental process could be as representative of that used by end users as possible.

For benchmarking purposes, samples for these tests were prepared using the same automated platform and baby bottle described in section 4.2.4.1. According to the reference for the WP test (Lloyd et al., 2019), liquid samples should be collected in glass tubes (not funnels) and then inverted into a sink. In the original form of the test, it is expected that surface white particles (if any) will adhere to the glass surface. However, the author observed that obtaining repeatable scores may be challenging using this test, likely due to a substantial particle count being discarded immediately after inverting the tube, since they tend to float on the liquid surface. Therefore, in our modified method, a glass pipe (funnel) was used instead of a glass tube, and the mixture was drained from the bottom of the pipe by removing a stopper.

The reference method for the SW test step 2 specifies the use of a sieve with a pore size of 600 μm (Pisecky, 2012). Additionally, in the SW test step 3, only the sediment weight in the sieve is reported (the remaining sediment in the beaker or bottle is not considered). However, the sieve with a size of 600 μm was too large for our application and could not capture the more diluted fraction of the sediment that had smaller particles. Also, ignoring the remaining sediment in the bottle after filtering the mixture could compromise the accuracy of the comparison of the platform's CV estimate with the reference method, as CV measured all visible sediment from the intact bottle non-destructively without neglecting anything. Therefore, a Whatman filter grade 4 (which has a 25 μm pore size) and a vacuum pump were used for sediment filtering. Filtration was not time-limited (as

the filtration rate of different samples can differ due to several reasons such as the presence of undissolved crystals or protein), and it continued until all liquid was removed at least from the filter edges when feasible. However, for most samples, the filtration usually took about 30 seconds. It should be noted that a "sediment disc" was also used for sediment filtration during the development of the SW test. However, a preliminary evaluation with seven pilot powders (data not shown here) showed that the Whatman filter could considerably increase the sensitivity of sediment weight measurements. Sediment weight using the Whatman filter demonstrated a correlation of 0.92 with sediment height in the bottle (measured manually using the ruler as a reference), which was more promising compared to a negative correlation of -0.67 for the sediment disc.

4.2.4. Automated Measurements by Rehydration Platform

4.2.4.1. Robotic Platform

The current study used the same automated rehydration characterisation platform described in Chapter Three. The mixture preparation and image capture methods were also the same.

4.2.4.2. Computer Vision Methods

The detailed information on the CV algorithms used are provided in Chapter Three. A logarithmic classification was used to assign an ordinal score to the presence of white particles in addition to particle counts (Mozafari et al., 2022). In the current study, the particle counts were classified into five categories to match the one-to-five scoring in the manual WP test (Table 4-2). The current study did not aim to evaluate the performance of the foam height algorithm. A further component of the current study was colour measurement of the rehydrated powders based on the cobot-captured images. To accomplish this, a horizontal strip of 3000 by 1000 pixels was cropped from the middle of the images, under the trademark on the bottle, and the colour median was calculated in the same software environment (and the same L*a*b* colour space) described in Chapter Three.

4.2.5. Data analysis

Python was used to analyse the results statistically. Pearson correlation analysis was used to identify relationships between the results of the modified reference tests and CV estimates as well as possible relationships between powder physicochemical parameters and rehydration properties. Due to the ordinal nature of the WP test, the Spearman correlation was preferred over the Pearson correlation (Hauke and Kossowski, 2011). P-values were used to assess the significance of the correlations. The significance of the difference between the rehydration properties of different agitation styles was tested using Student's t-test. To evaluate the repeatability of measurements, Root Mean Square Error (RMSE) and Normalised Root Mean Square Error (NRMSE) were used. NRMSE was determined by dividing the RMSE by the standard deviation of the observed values in each method (Otto, 2019).

4.2.6. Multivariate Model Development

A multivariate predictive model based on random forest was developed in Python using the Scikit-learn library (Pedregosa et al., 2011). A random forest consists of several decision trees generated from random selections of observations (i.e., our rehydrated samples) and their features (e.g., foam, sediment, etc.). The reason for choosing a random forest was to first avail of the power of decision trees in identifying feature interactions (as required in the rehydration problem, which has complex interactions between the rehydration attributes), and secondly to account for the diversity of observations in the training set (as rehydration behaviour can be considerably different from powder to powder). A total of 40 estimators (decision trees) with a maximum depth of ten were trained on the 23 rehydrated samples. To prevent overfitting, each of these estimators was trained with a minimum leaf and split of four and two, respectively. Validation of the model was performed using Leave-One-Out Cross-Validation (LOOCV) with 23 folds to account for all 23 powders. RMSE and Pearson correlation was used to evaluate the performance of the model. A Student's t-test was used to

determine whether there were significant differences between rehydration attributes in each agitation style.

4.3. Results and discussion

4.3.1. Evaluation of the Platform Measurements and Their Repeatability

Using the automated platform, sediment height, foam height, and the number of white particles were quantitatively characterised. For the evaluation of the algorithms, CV estimates of sediment height were compared with SW reference test, and CV ratings of white particles were compared with WP reference test (Table 4-2).

4.3.1.1. Sediment height estimates

The sediment height estimated by the platform's CV (with values ranging from 0-10.1 mm in the last imaging round when the sediment has settled) was positively correlated with the SW test (with values ranging from 1.1-20.5 g). The correlations were 0.75 for swirl, 0.89 for shake, and 0.79 independent of the agitation style ($p < 0.001$).

Table 4-3 presents the correlations, the RMSE, and the coefficients of variation for duplicated measurements for both the CV and reference methods.

Table 4-3 Relationship between duplicate measurements of sediment using the computer vision and modified reference methods for sediment weight

	Correlations between duplicate measurements		RMSE, NRMSE between duplicate measurements		Coefficients of variation for duplicate measurements	
	Swirl	Shake	Swirl	Shake	Swirl	Shake
CV	0.92	0.93	1.22mm, 0.49	0.98mm, 0.45	0.41, 0.35	0.51, 0.59
SW test	0.95	0.91	2.52g, 0.42	0.89g, 0.46	0.59, 0.63	0.57, 0.60

Even though the platform estimated sediment height, and the SW test measured sediment weight, the similarity of the coefficients of variation (which is independent of the measurement unit) between the duplicated measurements for both CV estimates and SW test suggests that the variability in the two

methods is comparable. Furthermore, the repeatability of the coefficient of variation in CV was comparable to that of the SW test. These findings provide confidence in the repeatability of the sediment image analysis algorithm.

A limitation of the current CV based sediment quantification method is that sediment height estimates from two-dimensional images may not accurately reflect the complex 3D sediment topology.

4.3.1.2. Presence of White Particles

The CV counts were logarithmically classified into five classes, averaged between the six bottle viewpoints, and rounded to the nearest integer to be comparable to human ratings based on the WP test (which has ordinal results based on five reference images). The correlations between the categorised CV particle counts and the manual WP test were 0.57 for swirl, 0.53 for shake, and 0.55 independent of the agitation style. The weak correlation may result from several factors. First, the CV ratings were categorised logarithmically as described in section 4.2.4.2 . The WP test, however, does not include any systematic evaluation of the reference pictures, such as the particle count in each picture. In addition, the reference method determines the presence of particles by comparing the reference images to the glass pipe from any arbitrary viewpoint (and particle distribution may not be uniform on the surface of the pipe). The platform, however, rates white particles from specific viewpoints. These differences make it difficult to compare the two approaches and interpret the results. There may also be other reasons for the weak correlation such as an algorithmic failure to detect particles larger than expected (the expectation was derived based on the literature and the observation of the training dataset when developing the algorithm) or inherent differences between the two approaches. For example, the platform and the WP test used different methods for visualisation of white particles, as well as different materials and diameters in the plastic bottle and glass funnel, which may explain the differences in particle adhesion patterns. It has been reported that particle “adhesion” and “trapping” behaviour are influenced by several factors including surface

material and suspension flow rate (Uno and Tanaka, 1972, 1970). As a means of "trapping" the particles in the present study, as part of the WP test, the liquid in the glass pipe was released quickly into the sink via removing the stopper, whereas the robot tiled and rotated the plastic bottle gently. The "trapping" of particles on the surface may be impacted by the drainage rate and inner diameter of the bottle or the pipe (which impacts the speed of the liquid flowing over the surface) and the surface material (e.g., glass or plastic). For example, sample C17 showed a low particle count in the bottle's blank headspace despite receiving a score of 5 on the WP test (i.e., perceived by the author to have the highest level of particles present) (Figure 4-2).

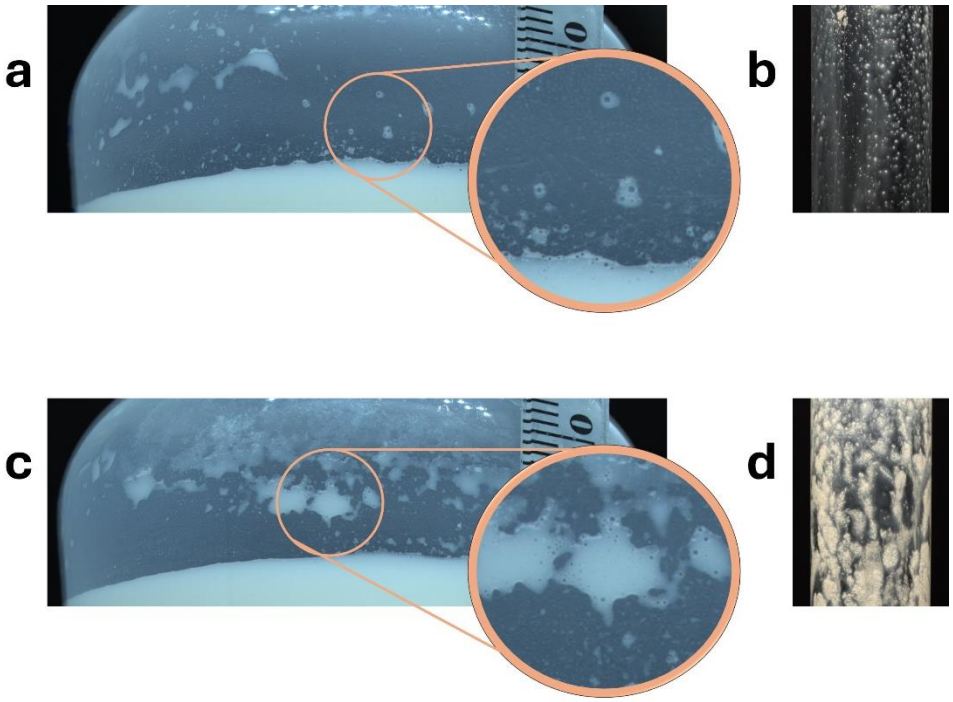

Figure 4-2 White particles in sample C17. The plastic bottle's blank headspace appears relatively clear in samples prepared using shake (a) and swirl (c) agitations. There are small particles visible in the glass funnel for shake (b) and swirl (d) samples.

Table 4-4 presents the correlations, the RMSE, and the coefficients of variation for duplicated measurements for both the CV and WP reference methods. To compare the repeatability of CV ratings with the WP reference method, CV ratings for different viewpoints of a sample were averaged and logarithmically classified to produce ordinal scores from one to five. This was done for each of the duplicate measurements separately. The CV repeatability correlations (between the two sets of ordinal scores) decreased to 0.71 (swirl) and 0.66 (shake) due to the reduced discretisation in the scoring

format (from counting the particles to classifying them as scores). Using the CV approach to count the particles resulted in a relatively a relatively high RMSE due to the fact that the scale for the number of particles reported in this approach is much larger than the scoring range of 1-5 in the reference method. Despite this, its normalised RMSE is lower than that of the reference method.

Table 4-4 Relationship between duplicate measurements of white particles using computer vision and modified reference methods for white particles

	Correlations between duplicate measurements		RMSE, NRMSE between duplicate measurements		Coefficients of variation for duplicate measurements	
	Swirl	Shake	Swirl	Shake	Swirl	Shake
CV particle count	0.93	0.87	19.7, 0.51	8.2, 0.59	1.23, 1.69	0.98, 1.30
CV classified scores	0.71	0.66	0.84, 1.02	0.54, 0.83	0.39, 0.55	0.40, 0.39
WP test	0.73	0.75	1.02, 0.72	0.83, 0.71	0.37, 0.36	0.31, 0.30

In the current study, the presence of particles was rated by one of the authors. However, the perception of particles may differ from person to person, which can increase the variation between measurements taken by different people (Lloyd et al., 2019) and impact the human-platform comparison. Also, increasing the scoring scale (e.g., to 1-6 as in Chapter Three) may help better capture the underlying relationship between the platform and human ratings as the higher scale can provide a higher level of discretisation for the scoring of particles by humans. In comparison with the subjective 1-5 scoring scale, the numerical particle counts of the platform allow for a more nuanced differentiation between samples (Lloyd et al., 2019). By providing reproducible quantitative particle counts, the platform reduces subjectivity. Despite these findings, the discrepancy observed in sample C17 and the algorithm failure in the detection of aggregated particles indicate that further work is needed to determine how particles adhere to one another and to the surfaces of different materials. The current CV algorithm may sometimes count other non-particle components in images as white particles (e.g., foam or droplets). This may contribute to the lower correlation between the duplicated measurements

in shake agitation (which generates more foam) for CV scoring. It should be noted, however, that human raters in the reference test also had difficulty distinguishing between foam or droplets, and particles in some samples. Improved algorithms based on machine learning may provide greater flexibility in particle detection in future iterations. However, the automated counting of white particles provides numerical results that are more discrete than the 1-5 grading scale used in the reference test. Further validation studies would be beneficial to fully characterise the platform's performance.

4.3.2. Relationships Between Powder Properties and Platform Estimated Rehydration Metrics

As a secondary objective, the automated platform was used to examine relationships between powder physicochemical properties and rehydration behaviour.

4.3.2.1. Relationships with Platform's Sediment Estimates

Compared to swirl agitation, shaking agitation resulted in lower sediment heights and sediment weights ($p < 0.001$). For swirl and shake agitation, CV estimates of sediment height were correlated with the difference between target total solids and dissolved solids (unhydrated powder) by 0.71 and 0.80, respectively. This finding is consistent with literature (Fitzpatrick et al., 2016), and our previous study (Mozafari et al., 2024). It is possible to explain this connection by considering the law of conservation of mass. Powder, when added to a mixture but not dissolved, must manifest as clumps, sediments, or other undissolved forms. As long as this undissolved powder is completely sedimented, it is expected to be detected by the CV. However, it may appear in the mixture as clumps on the top or as any other unhydrated material that has not yet settled. When CV estimates were replaced by modified reference method measurements, the correlations increased to 0.94 and 0.85, respectively. The lower correlations for the CV estimates may be attributed to the inherent differences in the measurements (filtration catches any undissolved materials even in the liquid portion of the mixture

whereas CV only detects settled material), algorithm performance, and the fact that the current vision method is unable to perceive the complete 3D topography of sediment inside the bottle. However, the repeatability results (Table 4-3) indicate that the platform can provide rapid, non-destructive, and objective estimation of sediment and monitor its change over time.

According to Figure 4-3, in swirl motion, sediment height increased over time for 21 samples (average: 1.16 mm, min: 0.04 mm, max: 3.56 mm) and decreased for two samples (average: 0.06 mm, min: 0.01 mm, max: 0.12 mm).

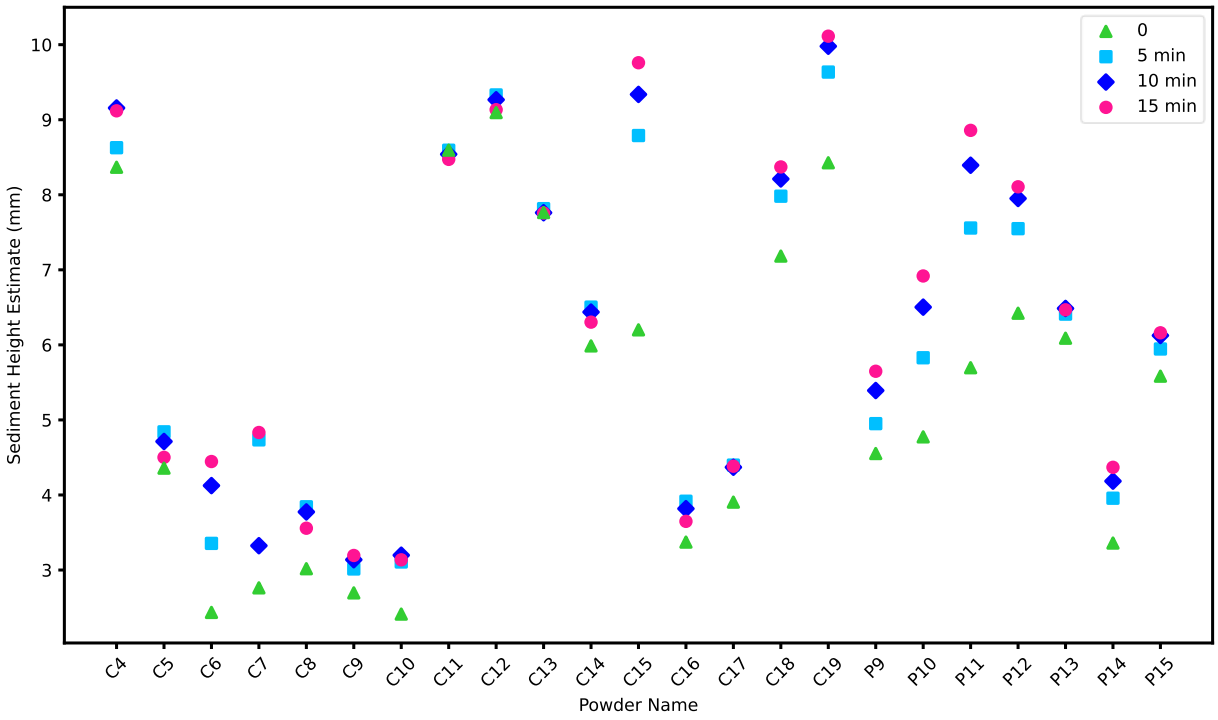

Figure 4-3 Sediment changes over time for swirl samples monitored by the computer vision algorithm

Figure 4-4 illustrates normalised sediment height (i.e., sediment height at each time step divided by sediment height at time zero) in samples prepared using swirl agitation to provide clearer comparison of sediment height changes.

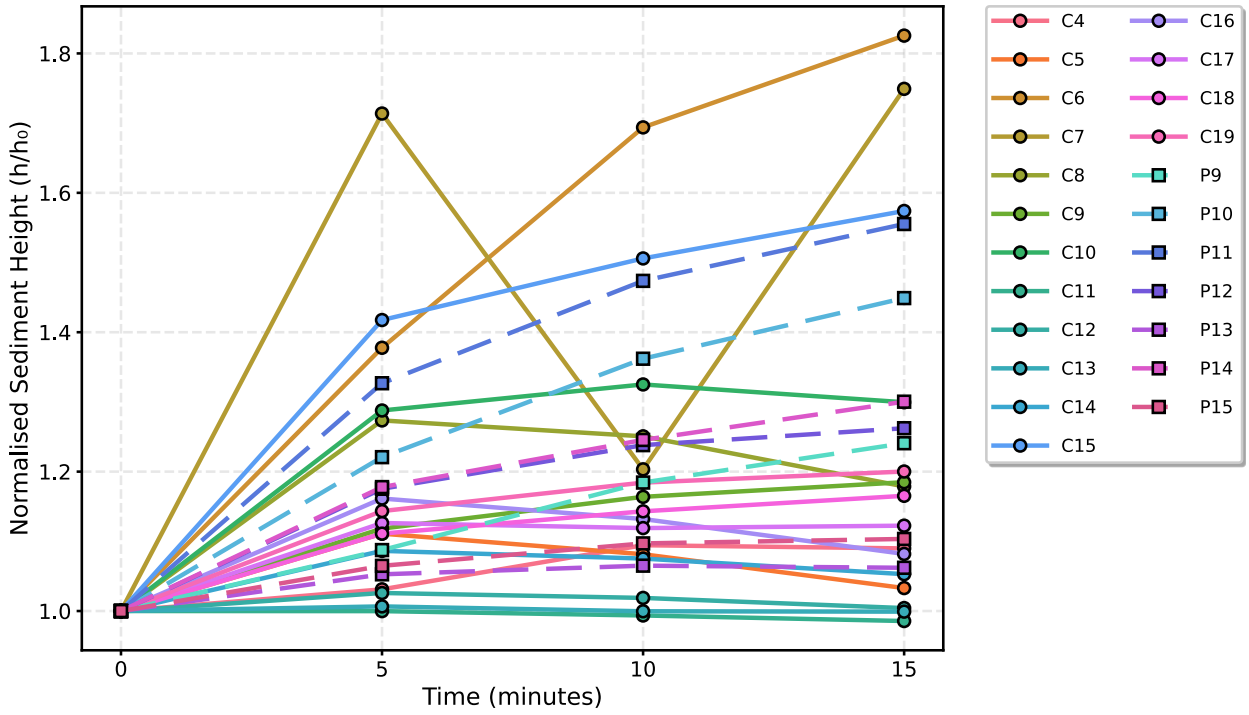

Figure 4-4 Normalised sediment height (h/h_0) over time for swirl samples monitored by the computer vision algorithm. In two samples, the final sediment height was smaller than the initial height.

The unusual pattern in sample C7 can be explained by the fact that this sample has relatively small sediment heights. When the numbers are smaller, a small change in the measured sediment height for any reason (which is explained later in the current section) can have a large impact on the sediment height ratio.

As illustrated in Figure 4-5, in shake motion, sediment increased for 16 samples (average: 2.05 mm, min: 0.03 mm, max: 5.12 mm) and decreased for seven samples (average: 0.34 mm, min: 0.11 mm, max: 0.80 mm). Figure 4-6 shows the normalised sediment height for samples prepared using shake agitation.

The duplicated sediment height estimates from time 0 to 15 min correlated ($p < 0.001$) by 0.92 (swirl) and 0.85 (shake). It appears that the trends observed by CV are reproduced in the duplicate measurements, which suggests that they are not the result of chance.

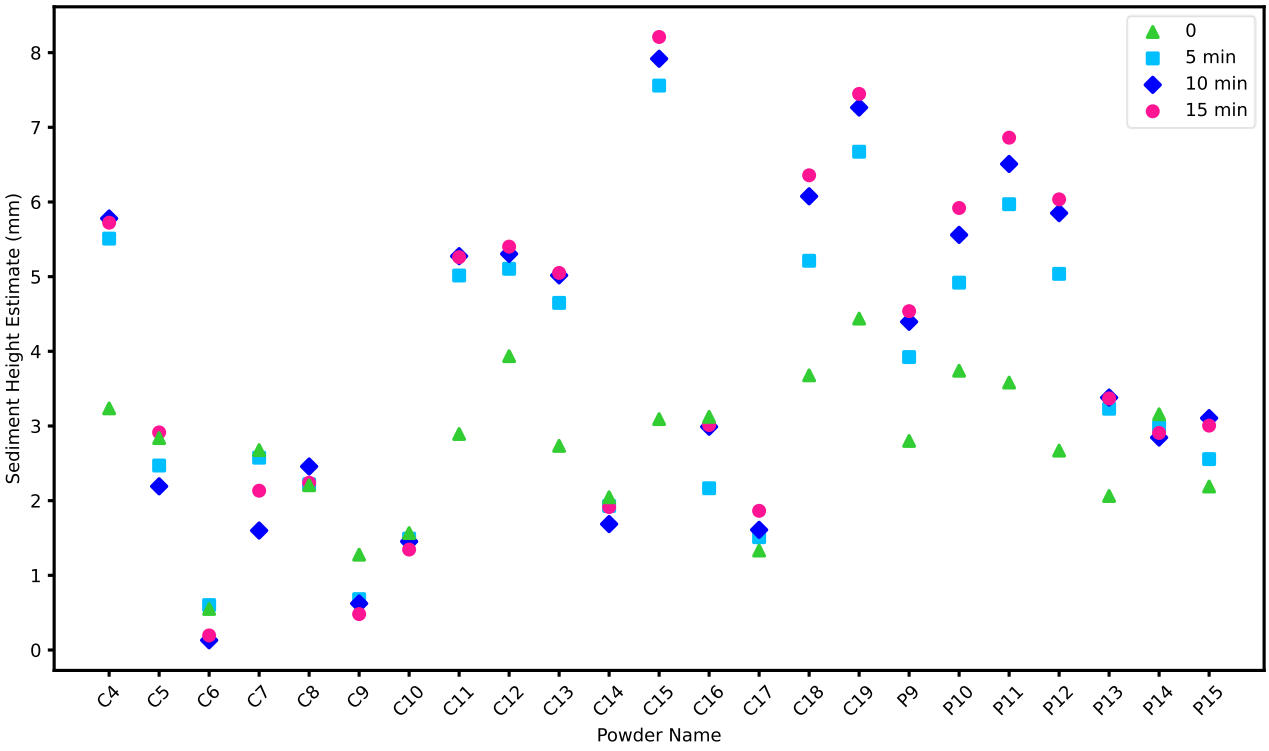

Figure 4-5 Sediment changes over time for shake samples monitored by the computer vision algorithm

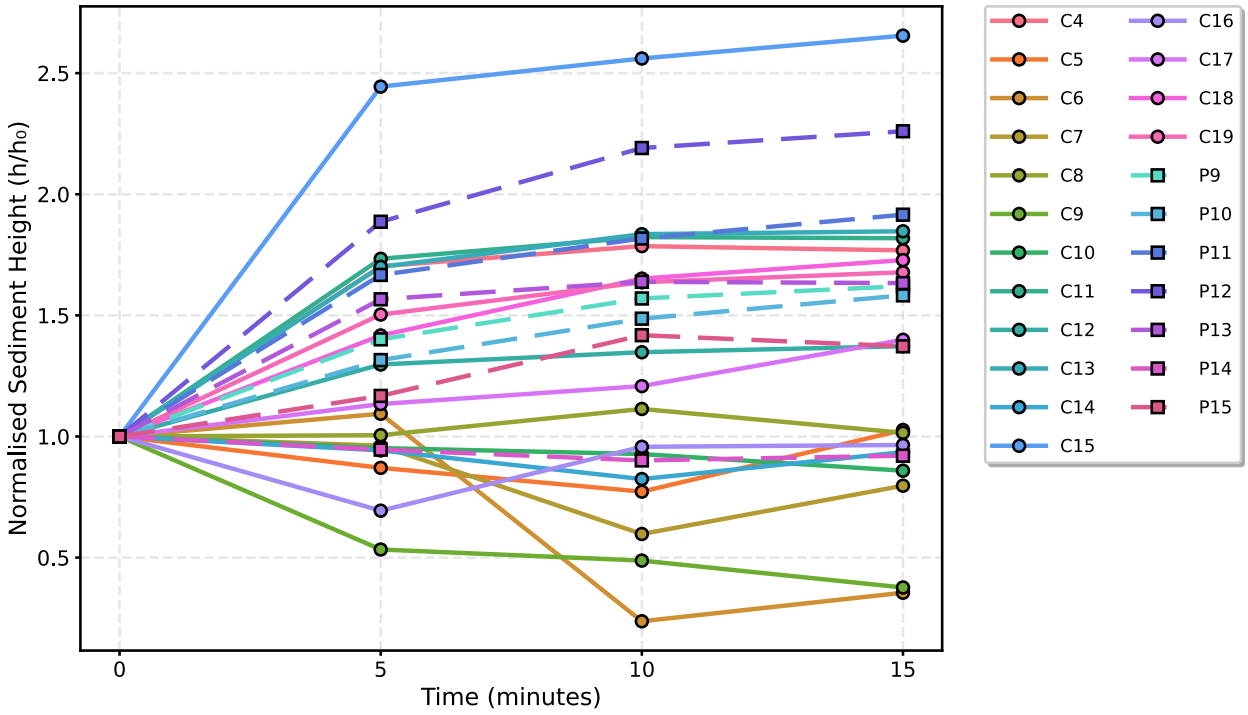

Figure 4-6 Normalised sediment height (h/h₀) over time for shake samples monitored by the computer vision algorithm. In seven samples, the final sediment height was smaller than the initial height.

The increasing or decreasing behaviour of sediment height may be related to the presence of undissolved powders, such as visible clumps. Although clumps were not quantified in the current study, it was observed that almost all samples with a high level of sedimentation had visible clumps on their surface. In support of this hypothesis, the change in sediment height from imaging rounds one to four in samples prepared with swirl agitation showed negative correlation of -0.65 with DS in samples prepared with the shake agitation. This may indicate that more energetic agitation can result in a higher level of dissolved solids because of disruption of clump structures (Fitzpatrick et al., 2017), or any smaller undissolved powder structures present in the mixture body that are not visible on the surface (Ji et al., 2016a). This is further supported by the fact that the correlations between DS and TTS in swirl and shake motions were 0.07 and 0.75, respectively, suggesting that shake agitation is more effective at dissolving particles intended to be dissolved (including sediments and clumps). The presence of more dissolved solids can also increase the viscosity of the solvent liquid (mixture, i.e., powder being mixed with water) (Walshe et al., 2021), decrease wettability (Ji et al., 2016a), and increase the likelihood of clump formation (Kim et al., 2002).

When performing the modified sediment reference tests, during the “rest period” mentioned in Table 4-2, some clumps were observed to sink into the mixture and disappear from the surface, whereas other clumps were observed to rise to the surface and become visible (possibly detached from the sediment at the bottom). An explanation for this phenomenon may be found by illustrating the shape of the observed sediment and clumps. As shown in Figure 4-7, some clumps still appear to resemble the shape of the powder scoop that had been added to the water at the beginning of rehydration. The added powder remained in a “ball” shape (Figure 4-7 , a) after being separated from the scoop and had not spread properly across the water surface.

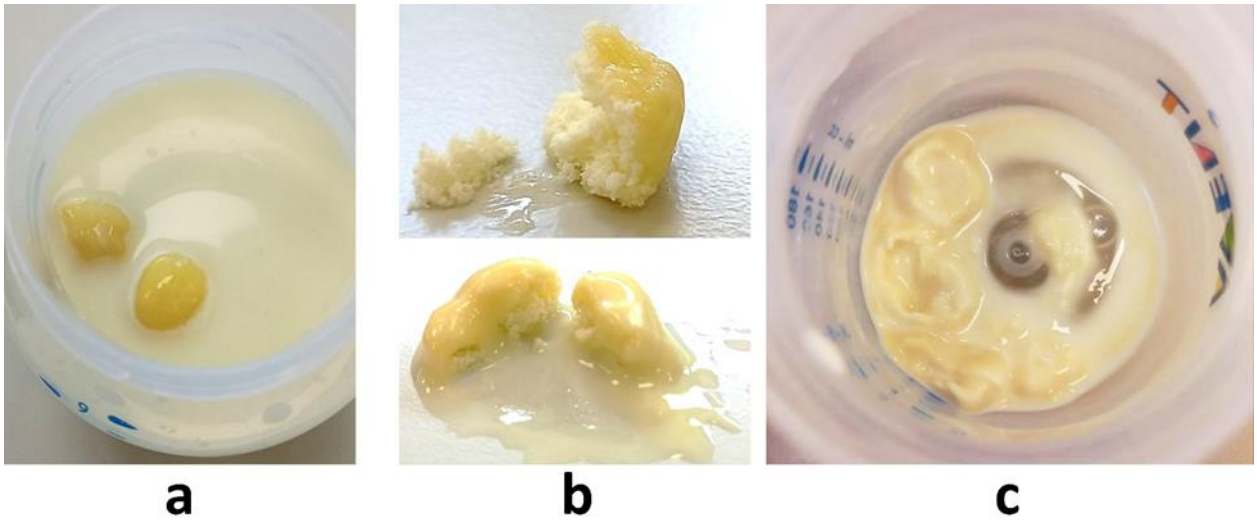

Figure 4-7 Sample P11 prepared by the cobot using the Swirl motion. Unwetted powder scoops formed clumps; (a) illustrates two clumps on the surface after robotic rehydration, (b) illustrates the clumps cut with a knife, and (c) illustrates sunken clumps after surface clumps were discarded using a scoop and the mixture was vacuumed (the modified reference method (test b) described in Table 4-2).

As illustrated in Figure 4-8, in addition to particle physiochemical characteristics, flowability also seems to be an important factor in rehydration, along with the four commonly known stages shown in Figure 4-1. Powders that spread easily over the water surface can increase the powder-water contact area and are more likely to become wet (i.e., the first stage in Figure 4-1).

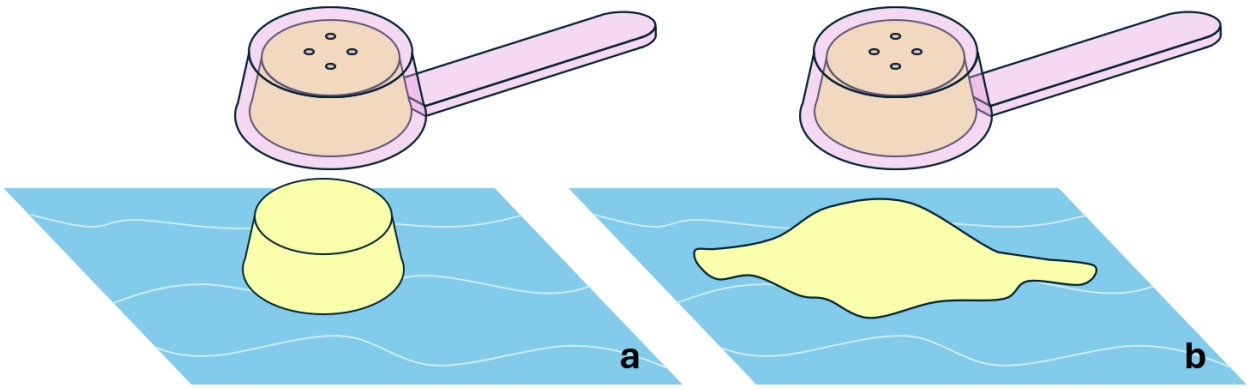

Figure 4-8 Powder flowability appears to be a critical factor in increasing the powder contact area with water. The powder-water interaction of (a) low flowability and (b) high flowability powders is illustrated.

Consequently, a scoop of added powder may become wet from the outside while still containing dry powder inside (Mitchell et al., 2015). It appears that some sediments have shapes similar to scoop-shaped clumps (Figure 4-7, c), suggesting that a clump may sink and form sediment if enough water penetrates it and makes it heavier than the solvent liquid. A similar observation was made by Mitchell et al., (2015) as well, who reported two types of clumps, floating clumps near the surface, and

sedimented clumps, which they termed “flake-like aggregates”. Clumps are typically surrounded by a viscous shell (Fitzpatrick et al., 2017). The reported flake-shaped clump may be the same viscous shell of a clump that has lost its dry powder content due to dissolution after water penetration (e.g., due to more energetic agitation that has broken the viscous shell). Even when a clump has sedimented, this does not necessarily indicate that there is no dry powder within it (but the current study did not explore this aspect further).

Dilution of the viscous layer in the clump shell may explain the sediment’s tendency to decrease over time in some samples. The viscous shell of clumps may adhere to one another when several scoops of powder with a poor flowability are added, as shown in Figure 4-7a and Figure 4-8a. A heavy clump (denser than the solvent liquid) may be attached to a lightweight clump causing them to sediment together. Over time, if the bond between the viscose layers of the clumps is weakened for some reason (e.g., dilution, vibration, etc.), the lighter clump may float to the surface. This can result in a decrease in visible sediment height at the bottom of the bottle. It has already been reported that clumps may separate from sediment and rise to the surface (Mitchell et al., 2015). Also, in the present study, it was observed that most samples that experienced a decrease in sediment height (two out of two for swirl and four out of seven for shake) had been prepared using the four powders with the worst dispersibility. Dispersibility was correlated with absolute value of decreased sediment heights in the seven shaken samples (Figure 4-6) by 0.93 ($p = 0.002$). This relationship was also observed for the two swirled samples (Figure 4-4). Therefore, in powders with poor dispersibility, the small disturbance introduced by rotation of the bottle by the cobot for imaging may have a greater chance to re-disperse “initial sediment” (Ji et al., 2016a) in the suspension. The “initial sediment” may be composed of powder particles that are slightly denser than the mixture but have not dispersed and dissolved during agitation. Consequently, they settle over time, but they may re-disperse with a small disturbance (e.g., robotic bottle rotation). It has been reported that poor dispersibility can contribute to both the formation of sediments and clumps (Pisecky, 2012).

Sediment height was weakly and negatively, but significantly, correlated with the flow index (swirl: $r = -0.38$, $p = 0.009$, shake: $r = -0.51$, $p < 0.001$) as well as the surface free fat level (swirl: $r = -0.33$, $p = 0.027$, shake: $r = -0.46$, $p = 0.001$). The result suggests that powders with better flow properties may rehydrate more efficiently (as reported in pharmaceutical applications (Kim et al., 2022)), but additional work outside the scope of the current study would be required to investigate this further. It has been suggested that poor flowability may contribute to the formation of clumps during the rehydration of dairy powders (Hazlett et al., 2021). It has also been reported that powders with poor rehydration properties may form either clumps or sediments after rehydration (Pisecky, 2012).

The observed relationship between flowability and sediment formation can demonstrate the importance of flowability in the rehydration process, and may further explain why agglomeration and increased porosity do not invariably improve rehydration (Crowley et al., 2016). Furthermore, surface free fat may not necessarily be a limiting parameter in rehydration, for instance when the solvent is warmer than the melting point of fat. Contrary to some reports in the literature (Kim et al., 2005), surface free fat showed a significant positive correlation of 0.60 ($p = 0.002$) with the flow index. The stickiness of particles cannot be directly related to the surface free fat alone, as it is also dependent on the total fat content (Nijdam and Langrish, 2006) and particle size (Nugroho et al., 2021). Therefore, surface free fat does not appear to negatively impact the flowability of powders with relatively less fat content, such as skim milk powder (Kim et al., 2005) or IF. In the present study, the flow index was primarily affected by physical parameters. It showed a negative correlation of -0.61 ($p = 0.002$) with interstitial air (bulk volume change after tapped 100 times (GEA, 2006b)) and a 0.53 ($p = 0.009$) correlation with particle morphology elongation. It did not show a significant relationship with lactose content ($r = 0.30$, $p = 0.17$).

In general, the platform ability to monitor changes in sediment height over time seems to provide useful information regarding the stability of the mixture and the presence of undissolved

powder structures such as clumps or inadequately dispersed powder in the mixture. The platform's high reproducibility and ability to distinguish subtle differences in sedimentation kinetics (e.g., sediment height change over time), which is missed by traditional methods, may assist in identifying new rehydration characteristics.

There was a weak but significant correlation of -0.31 ($p = 0.03$) between powder particle size D90 and CV sediment height in swirl agitation. This correlation was not significant for Shake agitation ($r = -0.25$, $p = 0.09$). One interpretation is that, in the absence of energetic rehydration, smaller powder particles may contribute to higher sediment formation (Fitzpatrick et al., 2016). While a small powder particle size is reported to decrease wettability (Fitzpatrick et al., 2016; Freudig et al., 1999) and increase lump formation (Fitzpatrick et al., 2017; Mitchell et al., 2015), agitation energy appears to be influential on the wetting of smaller particles (Wu et al., 2021) and disruption of clumps (Fitzpatrick et al., 2017).

4.3.2.2. Relationships with Platform's Foam Estimates

The foam height in the first imaging round (when foam had not yet dissipated) was higher following shake agitation compared to swirl agitation ($p = 0.023$). However, this p-value was below the threshold for being highly significant ($p < 0.001$).

In shaken samples, CV foam height estimations showed the strongest correlation with powder distribution span index (ranged from 1.30 to 1.83) at 0.65 and powder brightness (L) at 0.61. The span index represents the relative width of the particle size distribution, which is influenced by several factors, including powder manufacturing parameters, and impacts powder colour (Pugliese et al., 2017). For example, homogenisation before drying is one of the manufacturing parameters that can influence the concentrate span index (Mercan et al., 2018), and the D90 of rehydrated powders and fat globule size in concentrate (Zacaron et al., 2023), which may increase the amount of foam (Huppertz, 2010; Xiong et al., 2020) and sediment (Zacaron et al., 2023). Accordingly, foam height in shaken samples correlated with sediment height in swirled ($r = 0.61$, $p = 0.002$) and shaken ($r =$

0.52, p = 0.01) samples, and D90 of swirled (r = 0.53, p = 0.009) and shaken (r = 0.50, p = 0.02) samples. Specifically, fat globules have a greater impact on foaming at temperatures below their melting point around 40°C (Huppertz, 2010; Xiong et al., 2020), including the mixtures in the current study. Therefore, according to the correlations, samples that produce sediment, are also likely to produce foam under more energetic agitation. The foam height in shaken samples also showed a negative correlation with protein content (r = -0.57, p = 0.004). Although protein is reported to contribute to foam stability (Xiong et al., 2020), foam formation may not be directly related to protein content. Foamability is also affected by the molecular weight and structure of proteins, which should be considered when comparing studies (Ho et al., 2021). At higher protein concentrations, the viscosity increases (Walshe et al., 2021), which may inhibit air diffusion into the liquid during mixing and account for the negative correlation between foaming and protein content in our study.

4.3.2.3. Relationships with Platform's White Particles Ratings

White particle ratings were not significantly influenced by agitation style both according to CV counting the particles (p = 0.26) and the WP test (p = 0.9). This was also observed in our previous study (Mozafari et al., 2024) and was expected since these particles are inherently difficult to dissolve (Toikkanen et al., 2018).

For swirl agitation, the number of white particles rated by CV correlated by -0.40 (p = 0.006) with the difference between TTS and DS. This correlation was not significant for shake agitation (r = -0.25, p = 0.09). Accordingly, powders that dissolved better using a less energetic agitation are likely to have more white particles visible on the surface, possibly due to protein denaturation during ineffective agglomeration. Although the agglomeration process is expected to improve rehydration and reduce sediment, if inefficient, it can overheat the particles and cause protein denaturation (Schmidmeier et al., 2019). Also, when CV ratings are replaced with the modified white particles reference method ratings, the correlations remain similar at -0.52 (swirl) and -0.41 (shake) with sediment weight in Swirl motion, and -0.57 (swirl) and -0.47 (shake) with the difference between

TTS and DS. Based on the same reasoning, the dispersibility of samples correlated by -0.37 ($p = 0.01$) and -0.40 ($p = 0.006$) with the CV white particle numbers for swirl and shake agitations, respectively.

In the manufacture of fat-filled milk powders, different thermal treatment methods can significantly impact powder colour, surface free fat, and flecking levels, with surface free fat contributing to fleck formation (Finnegan et al., 2021). However, the current study did not find a significant correlation between surface free fat and white particle ratings, whether viewed from the perspective of the CV (swirl: $r = 0.18$, $p = 0.4$; shake: $r = 0.33$, $p = 0.1$) or the WP test (swirl: $r = 0.30$, $p = 0.2$; shake: $r = 0.34$, $p = 0.1$).

4.3.2.4. Other Powder-Rehydration Properties Relationships

As discussed earlier in the introduction, powder properties play a complex role in rehydration. Figure 4-9 illustrates some of the significant relationships as well as our findings regarding the flowability and sediment in green arrows. Table 4-5 lists the references for relationships shown in Figure 4-9.

Table 4-5 Detail of the references in Figure 4-9

[1]: (Freudig et al., 1999)	[2]: (Kim et al., 2002)	[3]: (Schober and Fitzpatrick, 2005)	[4]: (Gaiani et al., 2007)	[5]: (Fang et al., 2008)	[6]: (Tamime, 2009)	[7]: (Gaiani et al., 2011)
[8]: (Sharma et al., 2012)	[9]: (Mitchell et al., 2015)	[10]: (Ji et al., 2016a)	[11]: (Ji et al., 2016b)	[12]: (Fitzpatrick et al., 2016)	[13]: (Fitzpatrick et al., 2017)	[14]: (Toikkanen et al., 2018)
[15]: (Schmidmeier et al., 2019)	[16]: (O'Donoghue et al., 2019)	[17]: (Murphy et al., 2020)	[18]: (Han et al., 2021)	[19]: (Walshe et al., 2021)	[20]: (Wu et al., 2021)	[21]: (Han et al., 2022)

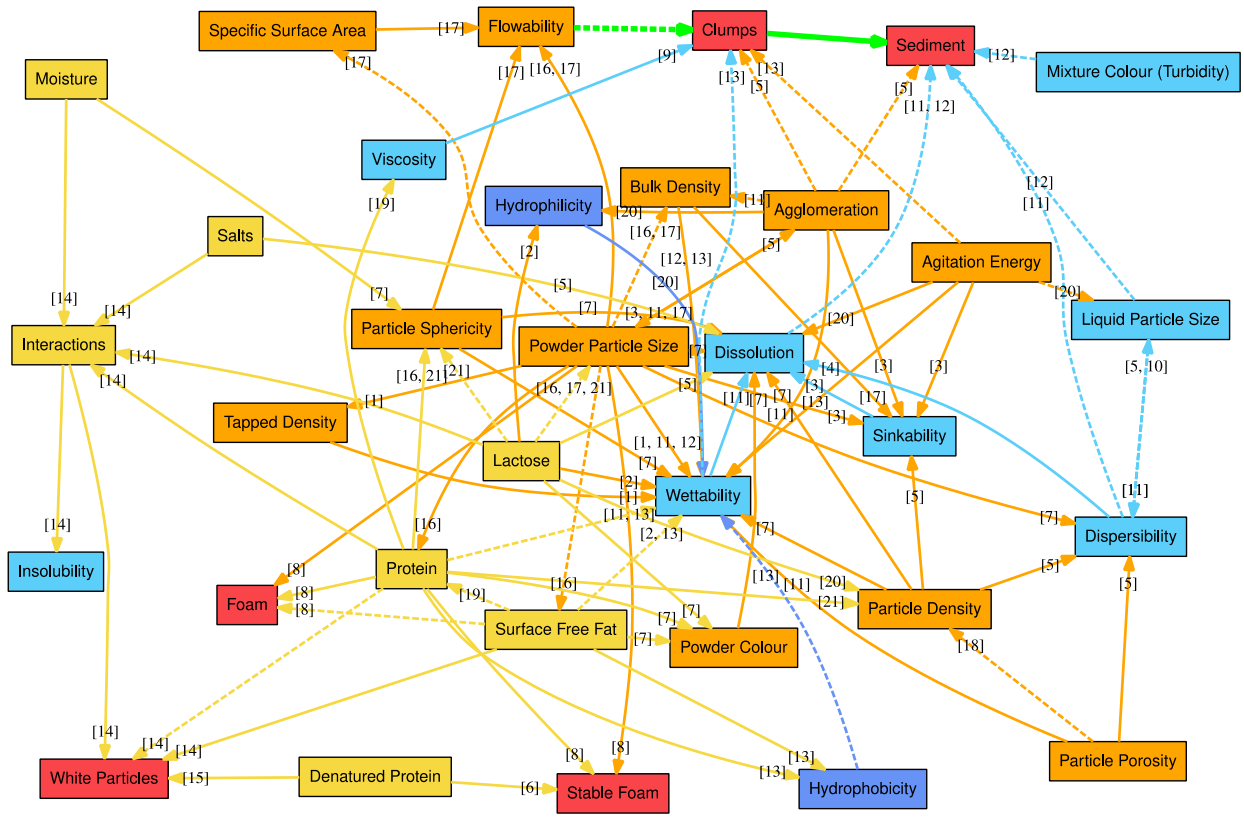

Figure 4-9 The literature already reports some relationships between powder chemical properties (yellow), powder physical properties (orange), powder-water interaction (blue and purple), and rehydration properties of the prepared mixture (red). Green arrows indicate our findings that are not well considered in literature. The solid and dotted arrows indicate direct and reverse relationships, respectively. The references are mentioned in brackets near arrowheads with details provided in Table 4-5.

In the present study, insolubility index showed correlations of -0.33 (swirl) and -0.23 (shake) with sediment weight (i.e., negative relationships, unexpectedly), -0.32 (both swirl and shake) with the difference between target total solids and dissolved solids, and -0.26 (swirl) and 0.11 (shake) with CV sediment height estimates. According to these observations, contrary to some opinions (Fang et al., 2008), the insolubility index does not appear to have a meaningful relationship with sedimentation, clump formation, or dissolution of other "soluble" particles (referred to as "solubilisation ability" by Fitzpatrick et al., (2016) and Mimouni et al., (2009)). It appears that insoluble particles are only a fraction of the total amount of powder, while other particles may be soluble (Pugliese et al., 2017). The presence of insoluble particles in a powder sample may not necessarily indicate the powder's solubility behaviour as a whole (Schmidmeier et al., 2019). Inefficient agglomeration, for example, can increase the overall heat load and cause protein denaturation, which can result in insoluble particles being formed (Schmidmeier et al., 2019). Despite

the presence of insoluble particles, the agglomerated powder sample may generally show acceptable rehydration behaviour.

Insolubility can be influenced by several factors, including the interaction between proteins, salts, lactose, and humidity (Fang et al., 2008; Toikkanen et al., 2018), heat treatment, the presence of lactic acid or addition of heat stabilising agents before drying, type of spray dryer, level of salt ions in the protein (Sharma et al., 2012), mineral contents, and solvent rehydration temperature (Mimouni et al., 2009).

4.3.3. Prediction of Reference Method Results

As a final step, a multivariate model was developed to investigate the prediction of the results of the dispersibility test based solely on the rehydration properties quantified by the automated platform.

4.3.3.1. Dispersibility Prediction

Based on platform metrics, a random forest model (Figure 4-10) was developed to predict dispersibility determined by the standard IDF method (GEA, 2005a). The model inputs were the automated platform measurements for change in sediment height estimates during the first two imaging rounds (time 0 to 5 minutes) and mixture colour (using the CV system) in the shaken samples. While the model predicted dispersibility with an RMSE of 3.53%, the RMSE of the actual IDF dispersibility test with respect to duplicate measurements prepared by the same person (excluding invalid measurements) was 1.9%. Despite the larger RMSE of the model dispersibility measurements than that of the reference method, it still falls within the acceptable range of less than 4%, according to IDF method repeatability criteria. The correlation between the predicted values and the actual measurements was 0.29. Also, the correlation between duplicated actual dispersibility tests was 0.76. The advantage of using a predictive model is that it facilitates rapid characterisation of powders, as it takes approximately ten minutes to conduct the test using the automated platform (with only two imaging rounds) versus about half an hour on the standard method to complete the dispersibility test.

Thus, the automated platform may be used as an at-line screening method, that in addition to estimating the three rehydration attributes, provides insight into powder dispersibility simultaneously, and samples whose dispersibility is flagged by the platform, may be sent to the laboratory for further analysis.

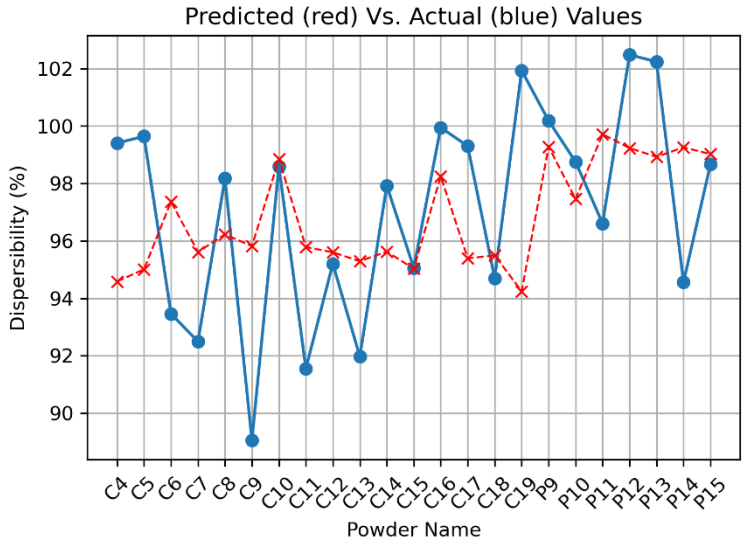

Figure 4-10 Results of the random forest regression model for predicting dispersibility

It is possible that the current model inputs do not fully represent all parameters affecting dispersibility. Incorporating powder properties such as powder particle size distribution, density, and chemical composition may enhance model generalisation. However, the current results demonstrate that machine learning techniques can potentially be used to predict complex rehydration attributes based on automated platform metrics. Consequently, this predictive model may serve as an objective and rapid method for benchmarking powder dispersibility before conducting time-consuming and subjective laboratory experiments.

4.4. Conclusions

The current study aimed to compare the rehydration properties of IF powders measured by an automated platform (using two agitation styles: swirl and shake) with those measured using commonly used reference methods. In addition, it examined the possibility of predicting the results of dispersibility reference test solely based on automated measurements. The platform's CV

algorithms for sediment height, foam height, and white particle counts showed good repeatability comparable to standard reference measurements. Key advantages of the automated approach include: (i) reduced subjectivity compared to qualitative human evaluations (repeatability of reference methods may also be decreased if different individuals perform the same test); (ii) provided a non-destructive method for monitoring the estimates of sediment and foam height over time as opposed to just endpoint measurements in the reference methods; (iii) provided higher degree of discretisation in the quantitative metrics for white particles versus coarse ordinal ratings in the reference test, and (iv) conducted the rehydration tests in the same baby bottle available off-the-shelf, to maintain a greater similarity between the tests and procedures used by end users when rehydrating powder.

By detecting subtle changes in foam and sediment height (missed by the reference methods), some insight could be gained into the kinetics of powder rehydration, in particular, clumping and sedimentation. These insights would suggest that flowability should be considered as an important rehydration stage in addition to previously four well-known rehydration stages. Therefore, the powder rehydration process will have five main stages: (i) flowing, (ii) wetting, (iii) sinking, (iv) dispersion, and (v) solubilisation. “Flowing” is directly associated with flowability (should be measured as flow index) and will be defined as the ability of powder particles to flow over one another during the period when the powder is exiting the scoop and hitting the water surface. To emphasise the importance of flow index compared to wettability, it is important to note that the flow index of powder provides information about how the powder behaves when scooped and poured into the water, which is normally not considered in wettability tests, where the powder is dropped into the water at once (GEA, 2009). In the wettability tests, the powder may already have been spread before the particles are dropped into the water, thereby disregarding the natural interaction between powder particles before they reach the water’s surface. In the literature, there has been a lack of adequate attention to the importance of flow index in the rehydration process, perhaps due to previous studies focusing on

conducting laboratory experiments that did not closely mimic the behaviour of end users, particularly scooping behaviour.

Using the platform rehydration properties estimations alone, a multivariate predictive model could predict the results of time-consuming dispersibility reference tests with acceptable accuracy, highlighting the potential of the platform for rapid screening applications. Data collected from the reference experiments and the automated platform also revealed some powder physicochemical parameters such as surface free fat, flowability, powder particle size, and density were correlated with the three studied rehydration attributes.

There is a possibility that the diversity, accuracy, and generalisability of predictions will continue to improve with the addition of new powder sets (the current study aimed to include all major commercial stage-1 infant formula powders available in Ireland and the Netherlands), additional rehydration properties metrics, and more advanced CV algorithms. However, this work demonstrated the potential of the automated platform concept for overcoming certain limitations associated with subjective qualitative testing. By providing rapid, quantitative, and objective rehydration data in a digitalised method. The integrated platform using robotics and CV techniques may enhance traceability and assist in optimising the infant formula manufacturing process.

Chapter 5: Towards standardised characterisation and robotic replication of human bottle agitation

5.1. Introduction

The present chapter aimed to characterise end-user bottle agitation behaviour and evaluate the possibility of using a robot to imitate this behaviour. Computer vision was used to observe human mixing, and robotics and a statistical learning method were used to learn and subsequently mimic two agitation styles demonstrated by humans. Characterising and replicating human agitation may assist in gaining valuable insight into the diversity of bottle agitation behaviour among participants and the main trends in their agitations. Understanding these patterns can be useful in developing rehydration quality tests that reflect the real-world usage of powders. For powder manufacturers, representative tests are needed to design products that rehydrate well across different mixing styles used in different cultures and locations. Additionally, a connection was made between this chapter and chapters three and four by evaluating the effects of the learned agitation on the rehydration attributes. In this chapter, the fluid dynamics of the mixture inside the bottle was not examined, as this requires analysis beyond the scope of the current thesis. Rather, the chapter focused on studying the movement of the bottle in 3D space during agitation, as demonstrated by participants or as replicated by the robot. No sensor was placed inside the bottle to avoid affecting natural fluid dynamics and to ensure realistic results, particularly for comparison of human-like swirl and shake agitations, and also comparison with results from chapters three and four.

5.1.1. Importance of understanding end-user bottle agitation behaviour

Mixing is a common operation in process engineering for material transfer (e.g., increasing homogeneity for infant formula). The duration and style of agitation can significantly impact the mixture quality (King, 1966; Richard et al., 2013). Thus, it is important, although difficult, to

understand how the powder will rehydrate when end-users rehydrate it (Richard et al., 2013). In some laboratory tests, the purpose is to simulate how well powder would dissolve in water upon rehydration by the end-user (Pisecky, 2012). However, since the tests are performed manually, the variability of human agitation highlights the need for more consistent methods to ensure that observed differences in rehydration behaviour reflect powder properties rather than variations in agitation. Also, as mentioned in Chapter 2, it is necessary to assess IF powder rehydration quality in a representative manner based on how the powder is rehydrated by the end-users (Lloyd et al., 2019).

For the food powder industry, it is important to characterise the impact of rehydration variables such as energy, fluid dynamics of solvent liquid (usually water), and even the shape of the container on the rehydration process (Richard et al., 2013). Better understanding the end-user rehydration behaviour, particularly considering possible diversity of rehydration practices in different geographies and cultures (O'Shea et al., 2021), can help powder manufacturers design and produce powders that meet the expected functionality. Despite the needs, there are limited studies in this area. However, considerable knowledge can be learned from other powder industries (Fitzpatrick and Ahrné, 2005).

Also, as discussed in chapters three and four, the agitation style can have a significant impact on the quality of rehydration, particularly the amount of dissolved solids. Some powder mixing parameters including water temperature and quality (King, 1966), agitation type and time (ADPI, 2023; Richard et al., 2013), or exact amount of water or scooped powder before mixture preparation (Farrent et al., 2021) can compromise mixture homogeneity. Although several studies have evaluated the impact of temperature, scooping and water measurement used by end-users on rehydration of infant formula (Farrent et al., 2021; Rosenkranz et al., 2024), agitation temperature and speed (Jeantet et al., 2010), and agitation style (Richard et al., 2013) are less studied. It has been shown that even with the same powder, temperature, and agitation duration, agitation style can have a significant impact on how much powder is dissolved in the mixture (Mozafari et al., 2024). In addition, although

more energetic agitation results in more dissolved powder (Fitzpatrick et al., 2016), it may also result in other rehydration attributes such as foam formation (Mozafari et al., 2024).

5.1.2. Limitation of current methods for characterising end-user bottle agitation behaviour

Research on agitation during rehydration of dairy powder may be viewed from two perspectives, namely from the perspective of chemical processing (mixing) (e.g., (Schober and Fitzpatrick, 2005), and from the perspective of end-user experience (e.g., (Altazan et al., 2019)).

To address the research gap in understanding rehydration from the perspective of end users, Lloyd et al., (2019) evaluated typical domestic rehydration processes by asking consumers to rehydrate a range of milk powders. They measured the residue in the rehydrated powders and adjusted a mixer to mimic participants mixing procedure by obtaining a similar level of residue. To obtain a "similar" level of residue, they rotated the mechanical mixer's mixing paddle 13 times clockwise and 13 times anticlockwise over eight seconds. The detail of their market research is not reported. Such a characterisation method does not directly measure the end-user agitation behaviour. Not characterising agitation behaviour introduces limits for the understanding of the agitation as it only considers the agitation process as a black box that only has inputs and outputs. Also, the method was affected by subjectivity as the implementation method for obtaining a similar sample quality only by adjusting the number of paddle rotations were subjective and may not consider the complexity of realistic fluid dynamics.

O'Shea et al., (2021) used a collaborative robot to approximate end-user bottle agitation as a more realistic alternative to the traditional mixers. However, the method of programming the robot was subjective. A more systematic approach is required to ensure inherent differences between human and robotic arms (such as degrees of freedom and the fundamental difference of the way they generate motions (Billard and Grollman, 2013)) do not hinder the replication of realistic agitations.

Despite the importance of characterisation of rehydration variables for the IF powder industry, there are only a few studies on the topic. However, understanding rehydration behaviour of a variety of powders (e.g., dairy, pharmaceuticals, or fertilisers) both for industrial and consumer applications has been studied (Cao, 2015; Richard et al., 2013). Because of complexity of understanding the liquid behaviour during agitations, many studies simulate dissolution or mass transfer behaviour during mixing in beaker using Computational Fluid Dynamics (CFD) methods (Hanspal et al., 2020; Hörmann et al., 2011; Wadnerkar et al., 2012). In the case of infant formula bottle agitation, simulations can be even more complex, considering the sensitivity of rehydration attributes to bottle shape (cf. Richard et al., 2013), higher complexity of fluid dynamics during bottle agitation (which may also result in a turbulent state in which simulations are much more complex if not impossible with currently available hardware) compared to stirrers in steady state, and the high diversity of human bottle agitation compared to mixing machines.

There are several studies that do not consider human participants and investigate the dissolution behaviour of powder under different agitation parameters such as shear and power produced by regular mixtures (Fitzpatrick et al., 2016; Jeantet et al., 2010; McCarthy et al., 2014; Schober and Fitzpatrick, 2005). They mainly have not considered realistic agitation parameters, perhaps due to challenges of realistic agitation characterisation. Despite the limited number of studies conducted to date, there is a need to measure end-user bottle agitation behaviour objectively (Hardy et al., 2002; Lloyd et al., 2019; O'Shea et al., 2021). However, digital data collection and data processing of diverse agitations between human agitations is a challenge of objective approaches.

5.1.3. Potential of adapting motion tracking techniques for rehydration studies

Although rare in the food powder industry, there are several studies characterising body limb movement behaviour, for example, for developing tools for assistant purposes such as in walking, running, or object grasping. The current techniques are either non-contact techniques based on vision or IR approaches, or wearable Micro-Electromechanical System (MEMS) sensors connected to the

human body (without being too heavy and interfering with the demonstrated motions) for motion tracing. Such techniques may have the potential to be adapted for characterising end-user behaviour during food powder rehydration. However, the available commercial solutions may be expensive, particularly those that can measure high-speed motions (Jensen et al., 2020). For the development of low-cost solutions, it is necessary to address the challenges associated with rehydration movements, such as high-speed agitations, which may require the development of tailored signal processing solutions.

Rehydration can be affected by many factors (e.g., powder properties, water penetration, changes in solubility resulting from environmental conditions such as pH (Siepmann and Siepmann, 2008), and mechanical energy (Richard et al., 2013)). Studies have examined how mixing conditions (mechanical input energy and duration (Fitzpatrick et al., 2016; Richard et al., 2013)) and system geometry (container and impeller design (Richard et al., 2013)) influence powder rehydration mechanism. The interaction of these mechanical factors can affect fluid dynamics including vortex formation, turbulence, and mass transfer (Fitzpatrick et al., 2016; Wadnerkar et al., 2012). Monitoring the bottle movements in 3D space using computer vision or sensors can provide insights into the trajectory of agitations, which can provide information about instantaneous or average agitation frequency and power (i.e., energy per unit of time). This can enable the possibility of mimicking the dominant agitation behaviour among participants, without needing to characterise or understand the fluid dynamics of the mixture inside the bottle. In this case, fluid dynamics inside the bottle can also be expected to be similar to those obtained in end-user agitations if the same bottle used by the end-user is used.

5.1.4. Motivation for replicating human bottle agitation with a robot

Although the selection of the cobot was not part of this thesis, Table 5-1 compares ten collaborative robots with a maximum payload of 5 kg manufactured by some major market players (M&M, 2023).

Table 5-1 Ten collaborative robots with payloads less than five kg (listed alphabetically by manufacturer name)

Cobot	Manufacturer	Maximum Payload (kg)	Degree of Freedom	Maximum Tool Speed (m/s)	Price (€)*	Reference
YuMi 14050	ABB	0.5	7	1.5	31,000	(ABB, 2021b)
AUBO-i3	AUBO	3	6	1.9	18,000	(AUBO, 2021)
COBOTTA	Denso	0.5	6	~ 0.13	15,000	(Denso, 2024)
E0509	Doosan Robotics	5	6	~ 1	16,000	(DOOSAN, 2024)
CRX-5iA	FANUC	5	6	1	32,000	(FANUC, 2023)
LBR iisy 3	KUKA	3	6	N/A	23,000	(KUKA, 2022)
Sawyer	Rethink Robotics	4	7	~ 1.5	33,000	(RR, 2020)
TM5 - 900	TECHMAN	4	6	1.4	26,000	(TM, 2019)
UR3	Universal Robots	3	6	~ 1	22,000	(UR, 2015)
MotoMINI	YASKAWA	0.5	6	N/A	13,000	(YASKAWA, 2022)

*Price information is approximate, may vary by market, and is not included in the provided references.

YuMi's small payload may limit the development of human-like agitation. However, its seven degrees of freedom may increase the likelihood of successful imitation of human arm movements. Since a human arm is believed to have seven degrees of freedom (Harthikote Nagaraja, 2019), the YuMi robot, which also has seven degrees of freedom, was expected be able to mimic the movements of the end users' arm.

The current rehydration tests that imitate end-user agitations are not widely automated; also, if automated, they are not developed systematically (Lloyd et al., 2019). If the test is not automated, an observed rehydration quality cannot directly be concluded to originate from changes in the formula or variability in human agitation. Obtaining such an objective rehydration platform can enable food powder manufacturers to mimic end-user agitation behaviour (as the agitation data is collected from humans) in a repeatable manner (as the agitation is performed by a robot). Using such a platform can have several benefits for researchers or powder manufacturers, including: i) standardisation of "realistic" agitations among the rehydration tests between different laboratories or manufacturing plants, especially considering the large diversity of the current rehydration methods, ii) enabling the

possibility to edit a specific characterised rehydration parameter (such as duration, amplitude, or frequency obtained from participants) and monitor its impact on the rehydration process; and iii) enabling characterisation of different human agitation styles and evaluating the impact of agitation style on rehydration attributes. Such controlled experiments on realistic motions can help in understanding the mechanisms linking agitation characteristics to rehydration performance. This can help identify practices that optimise rehydration and facilitate benchmarking the impact of deviations from the recommended rehydration procedure (usually available on the packaging) that can help the regularisation of the recommended rehydration methods.

5.1.5. Robotic learning from human demonstration

Learning rhythmic motions has traditionally been implemented using dynamical systems called Dynamic Movement Primitives (DMPs) (Ijspeert et al., 2002a, 2002b; Schaal et al., 2000), or probabilistic methods (Huang et al., 2021; Paraschos et al., 2018, 2013) that are based on sinusoidal basis functions and have limitations in capturing variations in phase, frequency, and amplitude (Kulak et al., 2020). To overcome these limitations, Fourier movement primitives that can extract multiple underlying frequencies in demonstrations were proposed by Kulak et al. (2020). As this method does not need an estimated dynamical model for the system and works based on the Fourier transform of the demonstrated signal, there is no subjectivity introduced during the selection and tuning of basis functions. Using this approach enabled the robot to wipe a whiteboard or draw figure-eight shapes starting from different initial positions.

Although learning based on FMPs is applicable to detect multiple frequencies in demonstrations, in the form implemented by Kulak et al. (2020), it has two limitations that prevent it being applicable in our case. First, although the learning approach allows the robot start from random points, the robot ultimately goes to the learned position which is not of interest in our study. The interest of our study is to learn the agitation behaviour as an isolated demonstration regardless of where in 3D space (or which position in front of the camera) participants agitate the bottle. Second,

the method learns all frequencies in the demonstration including frequencies of transferring from one cycle of the rhythmic demonstration to the other. Although this is an advantage of the method to detect these patterns, it might not be of interest in some applications, particularly in industrial environments.

5.2. Experiment to track and characterise human bottle agitation

Regardless of the robot performing the agitations, to understand variation intra and inter demonstration by humans, their agitations were evaluated in terms of their frequency and amplitude. As it is the first time such data have been collected, this analysis was expected to help obtain a better understanding of the expected variations in human agitations. Thus, this section presents the methods for bottle pose detection demonstrated by participants, data processing, and characterising human bottle agitation behaviour. The section aims to characterise two widely used (cf. WHO, 2007) end-user baby bottle agitation styles, swirl and shake, performed by participants, and evaluate variations inter and intra human agitation and find their basic agitation parameters (e.g., amplitude and frequency) and determine whether the human variations are significantly different.

5.2.1. Participants

Ten participants were randomly recruited for this study by sending internal email at Maynooth University. The participants included five males and five females, aged between 18 and 54, and they gave their informed consent to participate. Some participants reported having prior experience preparing infant formula; however, this was not a formal question or inclusion criterion. The only inclusion criterion was being above 18 years old.

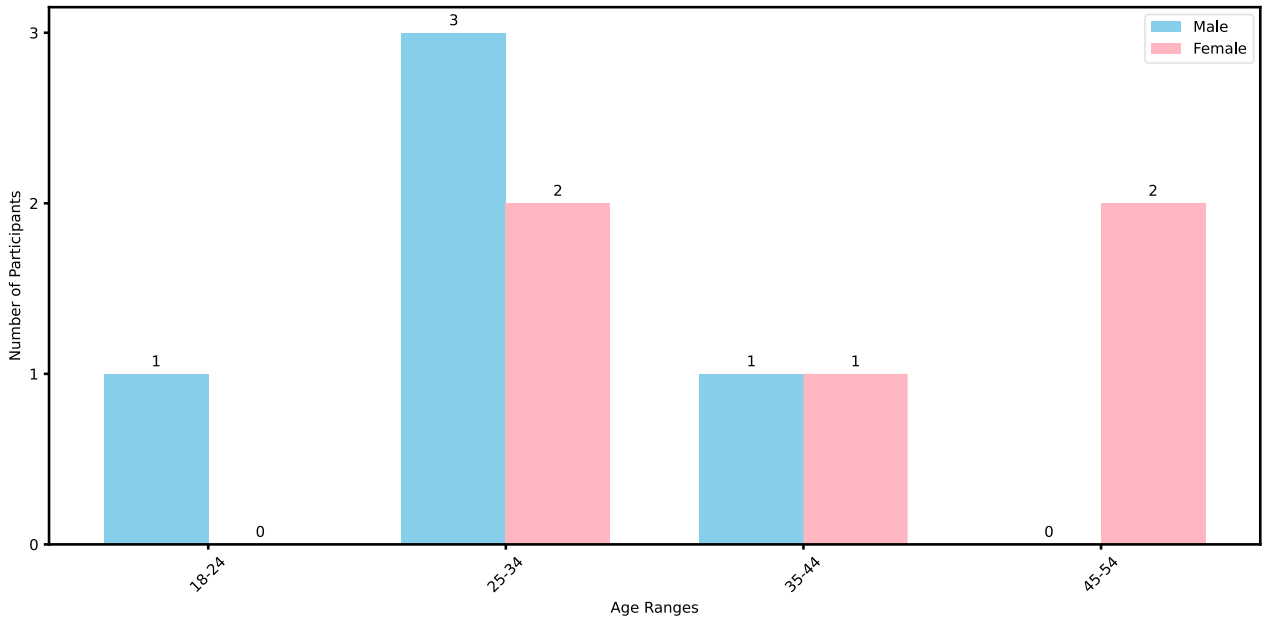

Figure 5-1 Age and gender distribution of ten participants in bottle agitation study

Since the present study was a preliminary assessment of human bottle agitation behaviour, a preliminary evaluation by the author was used to estimate the number of participants required. It was expected that a larger pool of participants may need to be recruited in the future depending on the outcomes of this study (the current sample of ten participants, however, was sufficient for the purposes of this study).

5.2.2. Motion capture apparatus

A 260 ml commercial Philips Avent baby bottle (Philips Avent, Glemsford, England) was instrumented with custom 3D-printed components Figure 5-2, AprilTags (Olson, 2011), and an Inertial Measurement Unit (IMU) sensor (Shimmer3 IMU unit, Dublin, Ireland). The design goal was to track bottle motions during agitation with two independent approaches: using an IMU and computer vision. To instrument the bottle for computer vision, five tag holders were designed using FreeCAD (FreeCAD, 2022), 3D printed from PLA, and attached to the bottle. According to Figure 5-2, the first and biggest tag holder was in the middle of the bottle (and designed to also hold the IMU sensor), two tag holders were on the right and left, and two tag holders were on the top and bottom.

The five AprilTags were from the tag36h11 class which is reported to have acceptable detectability from small angles that limit the camera's view of tags (cf. Olson, 2011).

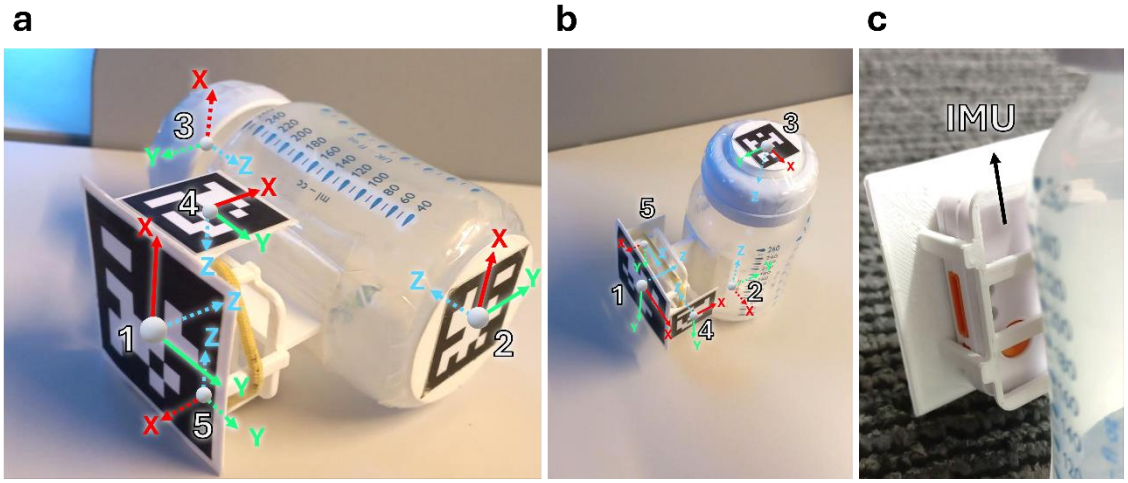

Figure 5-2 (a) and (b) show the five AprilTags connected to the sensor holder (tag 1) and tag holders (tags 2 to 5). (c) shows how the IMU sensor slides into the holder (the two side AprilTag holders are removed for demonstration purposes). Dotted lines show hidden axes.

A unique tag was used for each side of the bottle. The chosen tag arrangement allows up to three tags to be visible at the same time as the tags were attached to five unique faces perpendicular to each other (can be imagined as five unique faces of a Rectangular Prism). The sensor holder weighed 14 g and the sensor weighed 23.6 g, a total of 37.6 g.

The bottle was filled with 180 ml of milk to mimic a similar condition used in our previous studies which used 180 ml of water plus an average of 29 g of powder. Although the added powder in our previous study increases the overall mixture volume, this increase was ignored in the current study to not increase the bottle weight considering a sensor was attached to it. Here two simplifications are considered:

i) The added powder will increase the volume of the mixture in our previous study which results in mixture more than 180 ml. However, this was not considered since in this study, the sensor and sensor/tag holder need to be added and increasing the milk volume would increase the total bottle weight resulting in deviation from natural bottle weight.

ii) Sensor was placed outside the bottle, and its weight would generate a parameter of moment of inertia which is different from that of the natural agitation. But this deviation was ignored since attaching the IMU to the bottle was an important alternative plan for ensuring any agitation data from participants was not missed.

The 180 ml volume was chosen to not deviate too much from the realistic fluid dynamics inside the bottle and how the bottle feels in participants' hands (resulting from fluid dynamics and participants' perception from the presence of liquid) during agitations.

The sensor holder was designed to have a light weight and keep the sensor as close as possible to the bottle while still allowing participants to hold the bottle naturally. The centre of the sensor was 65 mm away from the centre of the bottle. The impact of moments of inertia of the attached sensor and the tag/sensor holders were ignored since they were lightweight and were not expected to have a significant impact on agitation dynamics. Considering the bottle mass was around 35 grams and it contained 180 ml of milk (with density of around 1.03 kg/L at 20° C) plus around 38 grams for the sensor and sensor holder, and the bottle cap, the overall bottle weight agitated by participants can be estimated at around 265 grams.

5.2.3. Bottle pose and motion estimation

Given that the relative position of bottle to the tags was known, the AprilTags were used to facilitate feature extraction for estimating the location of the bottle in 3D space. To detect the tags, the pupil_apriltags (Pupil Labs, 2022a) library was used in Python. Although detection of smaller tags may have more noise due to camera resolution limitations (especially at high frame rates), there was a space limit for the tags not to increase the moment of inertia and the tag holder vibrations, as well as not to interfere with the natural way participants may hold the bottle. As a result, except for the left and right tags (tags number 4 and 5), the tags had to have different sizes. Where possible, efforts were made to have a larger tag for better detection of edges, especially when camera ISO rating had been

increased to compensate for the limited lighting in the laboratory that could increase noise level. The sizes of tag1 to tag5 (which is defined as the distance of detection corners (AprilRobotics, 2024)) were 52, 37, 23, 28, and 28 mm. The distance of the centre of the tags to the centre of the bottle was known, and the tags were in planes perpendicular to each other.

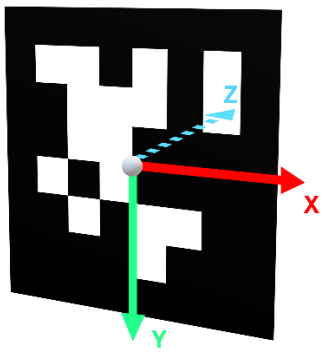

Figure 5-3 Coordinate system of AprilTags used to determine the bottle centre relative to each tag (here only the first tag is shown as an example)

The corners of an "ideal" tag are at (-1, 1), (1, 1), (1, -1), and (-1, -1) (Pupil Labs, 2022b). The tag coordinate system follows the right-hand rule with x to right and y to down (AprilRobotics, 2024), which is shown in Figure 5-3, and the distance of the bottle to the tag coordinate system relative to each tag shown in Figure 5-2 (a) and (b) for tag1 to 5 in the tags' coordinate systems respectively were (0, 0, 70), (0, 0, 50), (0, 0, 75), (54, 0, 29), (-54, 0, 29). Also, according to Figure 5-2, the rotations of the bottle relative to the coordinate system of tags 1 to 5 are respectively (0, 0, 0), (-π/2, 0, 0), (π/2, 0, 0), (0, π/2, 0), (0, -π/2, 0).

The algorithm pipeline for estimating the position of the bottle centre is as follows:

Algorithm1: Estimating Bottle Pose from Videos

Input: *video of bottle agitation in a participant's hand*

Output: *a time series of estimated position and orientation of bottle in camera coordinate system during the agitation demonstration video*

```
load camera calibration parameters
initialise AprilTag detector and pose data storage lists based on each tag
for (each frame in video):
    detect AprilTags in image
    if (any tags found):
        calculate bottle centre position and orientation based on each tag
        store estimated pose based on each tag
    else:
        store NaN (Not a Number) values in data storage lists
    end
end
for (each timepoint t in estimated poses based on all tags): (i.e., aggregating bottle position and orientation across tags)
    calculate mean position and orientation from detected tags at each t and store in bottle pose lists (i.e., bottle position and orientation)
end
for (each timepoint t in bottle pose): (i.e., computing bottle velocities):
    bottle linear velocity = (position[t+1] - position[t]) / (time[t+1] - time[t])
    bottle angular velocity = (orientation[t+1] - orientation[t]) / (time[t+1] - time[t])
end
```

Using this algorithm, bottle position, orientation, linear speed, and angular velocity were obtained at each frame of the recorded 240 fps video (i.e., time steps of 1/240 s).

5.2.4. Data collection procedure and motion capture setup

An SOP was developed for participants on expectations from the study and how to agitate the bottle (attached in Appendix 2). As there are two agitation styles of Shake and Swirl instructed in the

guideline provided by World Health Organisation (WHO, 2007), this study only measured these two agitation styles (however, measurement of any other agitation style should be possible with the same approach described in this study but potentially with modification of the sensor, camera, and bottle tag positions to avoid interfering with the way participants would naturally hold the bottle). To avoid inauthentic instructions, the SOP was designed to mimic the agitation guidelines on the packaging of commercially available IF powders. In the SOP, participants were communicated that "Your personal preferences will ultimately determine the details of the motion". Similar to manufacturer guidance, no additional instructions were provided regarding the exact Shake or Swirl method to ensure capturing natural bottle agitations according to participants' preferences.

Participants were asked to demonstrate each agitation style three times with a duration of 15 s per demonstration. As a result, there were three shake and three swirl agitations demonstrated by each participant. To minimise the impact of fatigue, participants had the option to take a rest between the demonstrations as much as they needed. Verbal cues were provided to indicate the start and end time of each demonstration. They stood in front of a table mounted with a GoPro Hero 8 Black camera (GoPro Inc., USA) in the robotics laboratory at Maynooth University to demonstrate the bottle agitation movements. The video was recorded at a frame rate of 240 fps with a resolution of 1080p which was the maximum resolution of the camera at this frame rate. The camera ISO was set to 1600 to ensure the frames were bright enough for tag detection using image analysis. Because increasing ISO will increase the chance of noise absorption, the possibility of detection of the tags in these settings was tested under the fastest possible range of agitations. There was no need to change the normal lighting or background (white wall) available in the room.

5.2.5. Data analysis

The video frames were processed using the OpenCV (Bradski, 2000) library in Python. The learning algorithm was also developed in Python. We used the NumPy library (Harris et al., 2020) to work with FFT, and the Scikit library (Pedregosa et al., 2011) to handle Gaussian Mixtures and implement

the grid search. To find the peak and trough in signals of individual demonstrations (for inter and intra demonstration analysis), the SciPy library (Virtanen et al., 2020) was used. The results were plotted using the Matplotlib library (Hunter, 2007).

5.3. Learning a single agitation cycle from human demonstrations

This section discusses how an LfD technique was developed and used to obtain one representative (dominant) agitation cycle for both swirl and shake styles from all participants' demonstrations. Moreover, it discusses how the two learned cycles were mapped onto the robot to simulate human-like agitations. This section also extracts the dominant agitation parameters from the learned agitation cycles as a statistical approach (in addition to the averaging approach described in section 5.3). The movements humans make when agitating a bottle in 3D space can occur in several layers, including rhythmic cycles we are interested in studying, as well as larger and slower movements (such as drifting from side to side). Rather than reproducing these large movements, our robot should be able to reproduce the rhythmic movement for as long as required by the robot operator. For this platform, only one agitation cycle should be obtained out of all demonstrated agitations in each agitation style because the platform aims to analysis the rehydration performance of different powders systematically, and it should perform identical agitations regardless of the time. For example, if the rehydration time is set to 5 s or 10 s, the only variable should be time, so that the platform is able to show the impact of agitation duration on the rehydration attributes while the other parameters, including the agitation path and agitation cycles, remain identical.

Considering participants may have large variation in swirling/shaking the bottle (as there was no limitation for them on shaking/swirling the bottle horizontally, vertically, or clockwise or counterclockwise), detecting a single cycle that represents all possible behaviours requires a statistical approach. The learning algorithm must be capable of handling situations in which some individuals shake the bottle horizontally (left-right) and others shake it vertically (top-down). In the same manner, opposite agitations (e.g., left-to-right and right-to-left, or clockwise and counterclockwise) must be

learnable without the opposite motions cancelling each other out. To obtain the most likely occurring agitation, bottle velocity was used rather than bottle position. After the representative velocity was learned, bottle position was calculated from the representative velocity. The reason for not using bottle position was that , despite many robotic problems that need to be solved for moving from point A to B, in the case of this study, it is important to understand how the bottle moves (i.e., its position relative to its previous state) rather than focusing on where the bottle is exactly located in 3D space. Working with bottle position needs data shifting (e.g., to bring all data to a certain point for learning) or data cleaning while it is best in LfD problems to take an approach without using these stages. As a result, position may not contain clean features for learning as participants may hold the bottle anywhere in space which is not a useful parameter for agitation. Moreover, finding the agitation cycles based on position data can be challenging because the agitation cycles cannot be clearly determined using this data (e.g., the bottle may change direction in the x-axis while not yet changing direction in the y-axis).

There were three requirements for the outcome of the learned agitations in this study:

1. Only one representative agitation cycle (from each style) needed to be learned out of demonstrations from all participants (because standardised human-like agitation was needed).
2. It was essential that the agitation cycle could be repeated smoothly. In other words, the bottle position, speed, and acceleration must be the same at the beginning and the end of the cycle (to ensure the robot could perform the human-like agitation smoothly for any duration desired).
3. The amplitude and frequency of the outcome of the learning algorithm must be scalable to any desired size (to provide platform users with the capability to evaluate the impact of different agitation parameters on rehydration quality).

Also, in LfD problems, there is a tendency to minimise preprocessing the demonstration data as much as possible to ensure the outcome is as objective as possible (Kulak et al., 2020).

To satisfy the first requirement, it is necessary to find at least one feature in the signals that indicates the start and end of the agitation cycle. The velocity signal was used for this purpose. Since agitation is a rhythmic movement, the velocity signal needs to change direction to return for the next repeat. Therefore, in any agitation cycle there must be two points in which velocity is zero. Also, for the same reason, velocity signal automatically oscillates around zero and does not need any preprocessing. This also helps to satisfy the second requirement because less preprocessing of data means less signal warp and a closer gap between the learned path start and end.

An alternative solution for finding such a feature is to find minimum or maximum of bottle position on any of the three axes. However, since the bottle position can be anywhere in the 3D space (provided it is in camera viewpoint), it would be necessary to process the position signal to remove the low frequency and bring all demonstrations to a known coordinate system. Additionally, the extremum may not happen simultaneously in the three axes.

To satisfy the third requirement, not only must a single closed and smooth agitation cycle have been obtained (the first two requirements must be already satisfied), but also the time of agitations must be included in the learning algorithm to obtain a trajectory. Then it will be possible to scale robotic agitation frequency since the learned timing is based on equal intervals (determined by the camera frame rate).

Three techniques were used to satisfy the three requirements at the same time:

1. Velocity signal was used instead of position signal. By learning the velocity signal for a single agitation cycle, it will be possible to find the position from integration of velocity.
2. Fast Fourier transform (FFT) was used to encode the agitation velocity signals for the agitation cycles.
3. A Gaussian Mixture Model (GMM) was used on the first two largest FFT components to learn the FFT parameters for the dominant velocity signal that represents all the demonstrated velocities.

We define m as the number of frequencies we select for each component, $(v_x, v_y, v_z, \omega_x, \omega_y, \omega_z)$ as the linear and angular velocity components in each demonstration (i.e., agitation cycle), M as the number of data points in a single cycle, and N as the number of demonstrations (agitation cycles).

For each cycle in each of the 6 signal components $(v_x, v_y, v_z, \omega_x, \omega_y, \omega_z)$, we perform an FFT:

$$X(f) = \mathcal{F}\{x(t)\} \tag{5.1}$$

where $x(t)$ is the time-domain signal and $X(f)$ is its frequency-domain representation.

We select the top two frequencies $(m = 2)$ with the largest magnitude in the frequency spectrum, along with their corresponding amplitudes:

$$|X(f)| = \sqrt{Re\big(X(f)\big)^2 + Im\big(X(f)\big)^2} \tag{5.2}$$

The most important components of $\mathcal{F}$ are identified as the m largest values in $|X(f)|$.
For each component, we find the m frequencies and amplitudes corresponding to the m largest magnitude peaks in the spectrum using Equations (*5.3*) and (*5.4*):

$$f_i = argmax_f |X(f)| \tag{5.3}$$

$$A_i = \frac{2|X(f_i)|}{M} \tag{5.4}$$

Then we create a feature vector for each cycle:

$$F_{fa} = [f_1, \dots, f_n, A_1, \dots, A_n] \tag{5.5}$$

where $n = m \times 6$ (m frequencies for each of the 6 components), and F_{fa} represents the frequency and amplitude feature components.

We fit a GMM to the frequencies and amplitudes components of the feature vectors.

$$P\big(F_{fa}\big) = \sum_{k=1}^{K} w_k \mathcal{N}\big(F_{fa}\big|\mu_k, \Sigma_k\big) \tag{5.6}$$

where K is the number of components in the GMM, w_k are the mixture weights, with $\sum_{k=1}^{K} w_k = 1$, and $\mathcal{N}(F_{fa}|\mu_k, \Sigma_k)$ are Gaussian distributions with means μ_k and covariances Σ_k.

The idea is to group similar patterns regardless of their starting point in the agitation cycle. For example, two agitation cycles from two different participants might have the same fundamental shape but start at different phases. By ignoring phase at this stage, we can recognise such signals as similar signals.

We select the GMM component whose sum of posterior probabilities across all cycles is highest, as the representative pattern in the agitation cycle:

$$k^* = \underset{k}{argmax} \sum_{i=1}^{N} P(k|F_{fa,i}) \tag{5.7}$$

where N is the number of demonstrations (agitation cycles), k^* is the index of the GMM component that maximises the sum of posterior probabilities across all cycles, and $P(k|F_{fa,i})$ is the posterior probability of component k given the frequency and amplitude features of cycle i.

This equation can identify a representative pattern by selecting the GMM component that has the highest sum of posterior probabilities, regardless of whether those probabilities are distributed across many cycles or concentrated in fewer cycles.

Now, we consider the phase to be able to reconstruct the representative agitation cycle, as it was not included in the learning features. We compute and circular average the signal phases for each j from 1 to n:

$$\phi_i = arctan\,2\left(Im(X(f_i)), Re(X(f_i))\right) \tag{5.8}$$

$$\phi_{avg,j} = \angle\left(\frac{1}{N}\sum_{i=1}^{N} e^{j\phi_{i,j}}\right) \tag{5.9}$$

Finally, for each of the 6 components, we reconstruct the learned signal using:

$$x_{\text{reconst}}(t) = \sum_{i=1}^{m} A_i \cos(2\pi f_i t + \varphi_i) \tag{5.10}$$

where f_i and A_i are from the representative GMM component k^*, and ϕ_i are the averaged phases.

As a result, the learning approach was designed so that scaling the amplitude and frequency of agitations (Equation (5.10)) was possible in case the user of the platform needs to evaluate the impact of frequency and amplitude on rehydration attributes.

The following paragraphs provide a mathematical analysis showing how a closed loop arises from this learning method so that the robot can repeat the agitation cycles smoothly. The analysis demonstrates how both GMM clustering and FFT calculations work together to achieve this result.

If agitation cycles are split at zero crossings, for each demonstration i:

$$v_i(0) = v_i(T_i) = 0 \tag{5.11}$$

where T_i is the period of demonstration cycle i.

According to the Central Limit Theorem, when sufficient demonstrations exist ($N \to \infty$), the distribution of agitation cycle periods converges to a normal distribution with mean denoted as T^*:

$$T^* = \lim_{N \to \infty} \left(\frac{1}{N}\right) \sum_{i=1}^{N} T_i \tag{5.12}$$

This mean (i.e., T^*) is identified by our GMM (using the most probable pattern k^* in Equation (5.7)) as a unique dominant period of human bottle agitations.

Since all demonstration cycles are periodic, their FFT representations contain frequencies that are multiples of their fundamental frequency $\frac{1}{T_i}$. As $N \to \infty$, these frequencies converge to multiples of $\frac{1}{T^*}$ through GMM clustering. Therefore, the FFT frequency components (f_i in Equation (*5.10*)) that generate the learned agitation cycle are integer multiples (harmonics) of the dominant frequency $\frac{1}{T^*}$:

$$f_i = \frac{i}{T^*}, \qquad i = 1, \ldots, m \tag{5.13}$$

As a result, for any reconstituted component in Equation (*5.10*):

$$cos(2\pi f_i T^* + \phi_i) = cos(2\pi i + \phi_i) = cos(\phi_i) = cos(2\pi f_i \cdot 0 + \phi_i) \tag{5.14}$$

This means that the reconstructed signal returns to its starting value:

$$x_{\text{reconst}}(T^*) = x_{\text{reconst}}(0) \tag{5.15}$$

For any reconstructed signal using Equation (5.10) (particularly $v_x, v_y, v_z, \omega_x, \omega_y$, and ω_z in our case), the derivatives or integrations remain periodic and preserve the harmonic relationships. As a result, given sufficient agitation demonstrations, the obtained position, velocity, acceleration, and jerk will remain closed smooth trajectories.

The method for learning a single agitation cycle that can represent all demonstrated agitation cycles is as follows:

Algorithm2: Learning a Single Agitation Cycle from Participants' Demonstrations

Input: *the time series of bottle position and orientation during demonstrations (derived from Algorithm1)*

Output: *a time series of bottle position and orientation during a single learned agitation cycle*

1 *import bottle position and orientation from the bottle pose estimation algorithm (Algorithm1)*

2 ***for (each agitation style (swirl and shake in our case)):*** *(i.e., feature extraction)*

3 *apply a 3rd-order Butterworth filter from the SciPy library with a normalised cutoff frequency of 0.04 (equivalent to 4.8 Hz, i.e., upper bound of the expected agitation frequency range, calculated as 0.04 × 120, where 120 is the Nyquist frequency)*

4 *calculate linear velocity (v_x, v_y, v_z) and angular velocity ($\omega_x, \omega_y, \omega_z$) from bottle position and orientation using NumPy's gradient function*

5 *calculate and identify the linear velocity component whose cycles have the highest average pairwise cross-correlation between each other (which was v_y for swirl and v_z for shake, as expected)*

6 ***for (each datapoint in the identified signal):***

find and store the indices of zero crossings where the signal changes from negative to positive (i.e., marking the beginning of each agitation cycle)

end

for (indices of zero crossings):

split the six signals (i.e., linear and angular velocities) into individual agitation cycles

end

for ($v_x, v_y, v_z, \omega_x, \omega_y$, and ω_z):

for (each split cycle):

perform FFT using Equations (5.1) and (5.2)

extract and store the top 2 frequency and amplitude components (not phases) of FFT

end

end

combine the extracted components into a single feature array (size: number of demonstrations × 24 (i.e., 6 motion components × top 2 of × the 2 FFT components))

for ($v_x, v_y, v_z, \omega_x, \omega_y$, and ω_z):

compute and store the circular average of the signal phase (to be used when reconstructing the signals)

end

end

for (each array of extracted features (swirl and shake in our case)): *(i.e., training a model for clustering agitation patterns that are similar)*

identify the optimal GMM using cross-validation and testing 1-10 Gaussian distributions and 4 covariance types

fit the identified model to the feature array

end

for (each trained model (swirl and shake in our case)): *(i.e., reconstructing the learned $v_x, v_y, v_z, \omega_x, \omega_y$, and ω_z)*

find the most common cluster of the trained model and use its mean as the representative frequency and amplitude

for ($v_x, v_y, v_z, \omega_x, \omega_y$, and ω_z):

reconstruct the learned signal by summing 2 sinusoids using the representative frequencies and amplitudes, and average phases (calculated at line 20)

end

end

for learned $v_x, v_y, v_z, \omega_x, \omega_y$ ***and*** ω_z ***in each agitation style:*** *(i.e., reconstructing the learned bottle position and orientation)*

obtain the learned bottle position by integrating the learned linear velocity (v_x, v_y, v_z)

obtain the learned bottle orientation by integrating the learned angular velocity $(\omega_x, \omega_y, \omega_z)$

calculate median starting angles $(\theta_x, \theta_y, \theta_z)$ *from original agitation cycles and add them to the reconstituted orientation data as initial orientation values*

end

5.3.1. Mapping the two learned agitation cycles onto the robot

The current section aimed to: i) update robot agitation programmes to perform "human-like" agitations, and ii) validate the updated agitations compared to the learned trajectory from humans.

To map the learned position of the bottle to the robot, matrix transformation was used. Since the robot tool for holding the bottle was on its left arm (i.e., similar to a left-handed person), in case a participant was right-handed, before mapping to the robot coordinate system, their demonstration was reflected relative to the XZ plane in the World's coordinate system with the following transformation:

$$M_{reflect,XZ}^{World} = \begin{bmatrix} 1 & 0 & 0 & 0 \\ 0 & -1 & 0 & 0 \\ 0 & 0 & 1 & 0 \\ 0 & 0 & 0 & 1 \end{bmatrix} \tag{5.16}$$

We define the following coordinate systems:

W: World

C: Camera

T_i: Tags $(i = 1, \dots, 5)$

B: Bottle (representing human hand)

R: Robot base

$WObj$: Work Object

EE: End Effector

TCP: Tool Centre Point

Figure 5-4 illustrates the defined coordinate systems required for transformations from the camera to the robot space.

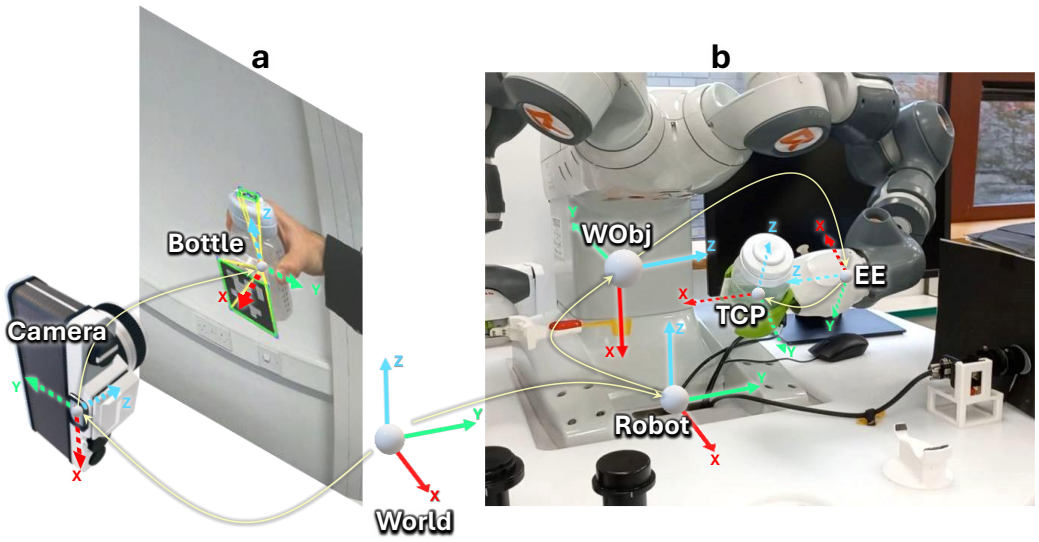

Figure 5-4 (a): Bottle pose relative to camera coordinate system (which is calculated from bottle pose in tag(s) coordinate system(s) and then the tag pose(s) in camera coordinate system). Camera coordinate system is defined based on ideal tag coordinate system as explained in the text. (b): The coordinate systems for Robot and EE are defined as default by robot controller. The coordinate systems for WObj and TCP in (b) were defined to respectively match those of the camera and bottle in (a). Dotted lines show hidden axes.

When transforming from any coordinate system P to Q, if the translation matrix is t_P^Q and the Rotation matrix is R_P^Q, then the transformation Matrix is:

$$T_P^Q = \begin{bmatrix} R_P^Q & t_P^Q \\ 0 & 1 \end{bmatrix} \tag{5.17}$$

For simplicity, first, we imagine only one random tag is identified. Afterwards, we will expand the equation to handle more identified tags.

In case of detecting only one random tag, the transformation Matrix for the bottle in human hand is as:

$$T_W^B = T_W^C \cdot T_C^{T_i} \cdot T_{T_i}^B \tag{5.18}$$

And the transformation for robot TCP (where the bottle is in robot gripper) is as:

$$T_W^{TCP} = T_W^R \cdot T_R^{WObj} \cdot T_{WObj}^{EE} \cdot T_{EE}^{TCP} \tag{5.19}$$

The learning approach allows scaling of human demonstration before mapping the movements to the robot, in case an operator wishes to scale down or up the robotic movements while mimicking the path of human demonstrations. The scaling Matrix from human demonstration for robot mimicking can be defined with option to scale agitation in any of the axes in World 3D space as:

$$S = \begin{bmatrix} s_x & 0 & 0 & 0 \\ 0 & s_y & 0 & 0 \\ 0 & 0 & s_z & 0 \\ 0 & 0 & 0 & 1 \end{bmatrix} \tag{5.20}$$

For the robot to mimic agitations learned from participants' demonstration, the goal is to match the relative position and orientation of the Bottle to the World with the relative position and orientation of the TCP to the World, after (if required) scaling and reflection applied:

$$T_W^{TCP} = M_{reflect,XZ}^{World} \cdot T_W^B \cdot S \cdot \left(M_{reflect,XZ}^{World}\right)^{-1} \tag{5.21}$$

Expanding this using the full transformation matrices will result in:

$$T_W^R \cdot T_R^{WObj} \cdot T_{WObj}^{EE} \cdot T_{EE}^{TCP} = M_{reflect,XZ}^{World} \cdot T_W^C \cdot T_C^{T_i} \cdot T_{T_i}^B \cdot S \cdot \left(M_{reflect,XZ}^{World}\right)^{-1} \tag{5.22}$$

In case more than one random tag is identified, the estimation of the bottle position based on each tag is averaged among the tags. Therefore, the transformation Matrix for the bottle in human hand will be:

$$T_W^B = \frac{1}{n}\sum_{i=1}^{n} T_W^C \cdot T_C^{T_i} \cdot T_{T_i}^B \tag{5.23}$$

where n is the number of visible tags.

Inputting this to equation for transformations on the robot side, and considering the reflection and scaling (if required), the equation will be:

$$T_W^{TCP} = M_{reflect,XZ}^{World} \cdot \left(\frac{1}{n} \sum_{i=1}^{n} T_W^C \cdot T_C^{T_i} \cdot T_{T_i}^B \right) \cdot S \cdot \left(M_{reflect,XZ}^{World} \right)^{-1} \tag{5.24}$$

Therefore, if there are more than one tag visible, the expanded equation will be:

$$T_W^R \cdot T_R^{WObj} \cdot T_{WObj}^{EE} \cdot T_{EE}^{TCP} = M_{reflect,XZ}^{World} \cdot \left(\frac{1}{n} \sum_{i=1}^{n} T_W^C \cdot T_C^{T_i} \cdot T_{T_i}^B \right) \cdot S \cdot \left(M_{reflect,XZ}^{World} \right)^{-1} \tag{5.25}$$

Defining the $Wobj$ coordinate system and calculating the inverse kinematics in this system is a cleaner approach in programming the robot as any future changes in robot arm configuration will be as simple as changing the position and orientation of this coordinate system. This enables the robot to perform the learned trajectory starting from any desirable point in its workspace (as long as the entire trajectory falls within robot workspace). To make the calculations straightforward, defining the $Wobj$ relative to TCP coordinate system was done in a way to resemble the relative orientation of the Bottle to Camera coordinate system. To implement the motions on YuMi robot, its native software (RobotStudio) was used to ensure all the safety features of the robot controller remain available. The robot native language is RAPID (ABB, 2024). To map the learned agitations to the robot space, all the points of the representative agitations (i.e., the learned points) were inputted into RAPID as "*robtarget"* datatype which is a common way to define points for the YuMi robot that also includes orientation of the robot end effector at that point as well as the preferred robot configuration to access the point. Python was used to generate *robtarget* points (the format required for RAPID) from the learned points.

As agitation is relatively a high frequency movement for the robot capability, the robot movements were implemented in joint space which needs command *MoveAbsJ()* in RAPID. There are also some other syntaxes for controlling robot arm including linear (*MoveL()*) or curved (*MoveJ()*) paths, but these syntaxes are performed slower as they need more calculations on the robot controller. Also, to get the full advantage of high-speed performance using the *MoveAbsJ()*, the robot position in joint space was already calculated and stored to be ready for use without spending more time for calculating the inverse kinematics during performing the agitations. For this, the inverse kinematics embedded inside the *CalcJointT()* in RAPID was used. In case there are several solutions for the inverse kinematics, the preferred robot configurations must be input. An identical preferred configuration was used in all points which was also the same as the old agitations (i.e., before update; the same agitations used in Chapter 3 and 4) so that the arm was in the same configuration of the past and therefore there was no need to modify the positions of objects already made on the table (bottle, IF can, etc.) for safety and preventing possible collisions.

5.3.2. Evaluation of robotic agitation performance

Although it may be possible to access the joint states of the actual YuMi robot in RobotStudio, only the robot position in the simulation environment was used for the evaluation of the learning method for the following reasons. First, there was an access error for monitoring the live motor states perhaps due to organisation limited level of access to the robot controller or network firewall rules. Second, as will be discussed in results section, the motor torque was insufficient to perform the high frequency acceleration change of the learned agitations. Consequently, as expected, the agitations for the robot needed to be scaled up to be adapted to the robot capabilities and make a similar agitation power as the learned agitations. This needed trial and error in the simulation environment to obtain the closest agitation power to that of the learned agitation the robot can perform. Consequently, for validation purposes, we relied solely on the simulation environment of the robot, which is an official digital replica of the robot that utilises the same controller software as the real robot. The controller version

of the robot was identical to that of the simulation environment. Therefore, the simulation environment was used to obtain the path of robot end effector to be compared with the learned paths. By extracting the trajectory of the robot end effector from the simulations in different scaled trajectories, the applied power to the bottle was calculated and compared with the power that would be applied if the robot could perform the original learned agitation trajectory.

5.3.2.1. Rehydration power calculations

Rehydration power, either from the learned trajectories or from the trajectories generated in the simulation software (and exported as trajectories in an Excel file), was calculated by finding the instantaneous speed and acceleration at each timestamp, using the following equations.

$$v(t) = \sqrt{v_x(t)^2 + v_y(t)^2 + v_z(t)^2} \tag{5.26}$$

$$a_x(t) = \frac{dv_x(t)}{dt}, \quad a_y(t) = \frac{dv_y(t)}{dt}, \quad a_z(t) = \frac{dv_z(t)}{dt} \tag{5.27}$$

$$a(t) = \sqrt{a_x(t)^2 + a_y(t)^2 + a_z(t)^2} \tag{5.28}$$

And instantaneous power being transferred to or from the bottle is determined using the scalar magnitudes of speed and acceleration as:

$$P(t) = m \cdot v(t) \cdot a(t) \tag{5.29}$$

Therefore, the average power over the time T is calculated as:

$$\bar{P} = \frac{1}{T}\int_0^T P(t)\ dt \tag{5.30}$$

$$= \frac{1}{T}\int_0^T m \cdot v(t) \cdot a(t)\, dt \tag{5.31}$$

As a result, in the current problem that contains discrete (digitalised) measurements, the average power transferred to or from the bottle can be calculated as:

$$\bar{P} \approx \frac{1}{N_p}\sum_{i=1}^{N} P(t_i) = \frac{1}{N_p}\sum_{i=1}^{N} m \cdot v(t_i) \cdot a(t_i) \tag{5.32}$$

Where N_p is the number of datapoints during the agitation for which we calculate the average power.

In the above formulations, the bottle and the liquid together are studied as a system. The average amplitude of the agitations was calculated as:

$$A_{avg} = \frac{1}{N_h}\sum_{i=1}^{N} \sqrt{x_i^2 + y_i^2 + z_i^2} \tag{5.33}$$

where N_h is the number of half agitation cycles (from peak to trough and vice versa). Variables x, y, and z are the distance bottle travelled in the three axes in space, and the peak for x, y, and z do not necessarily happen at the same time.

5.4. Assessment of rehydration attributes

The last part of this chapter evaluated whether the learned robotic agitations from human demonstrations resulted in different level of rehydration attributes compared to the agitations used in Chapters 3 and 4. The rehydration attributes estimated by the same computer vision algorithms developed in Chapter 3. Also, the percentage of dissolved solids was measured using a SmartTrac™ (CEM Corporation, NC, USA) as another supportive method (in addition to sediment level) for evaluating significance of powder solubility as a result of the updated agitations. The powders used in this chapter were P11 to P15, and each was rehydrated in duplicate using both agitation styles.

5.5. Results and discussion

5.5.1. Characterisation of human agitation behaviours

A few of the participants were observed to change the regime of agitation in the middle of their demonstration (e.g., changing the bottle orientation from vertical to horizontal and vice versa during

shake, or changing the swirling direction). However, they did not change the hand they were using for demonstration. This observation was the unique challenge for the robot learning from demonstrations in the present study. As explained in the methodology section, the learning algorithm was designed to handle variations of this nature.

5.5.1.1. Agitation amplitude patterns

The agitation amplitude in swirl style was significantly ($p < 0.001$) lower than the shake style, with average of 66.6 mm and 99.2 mm for swirl and shake respectively.

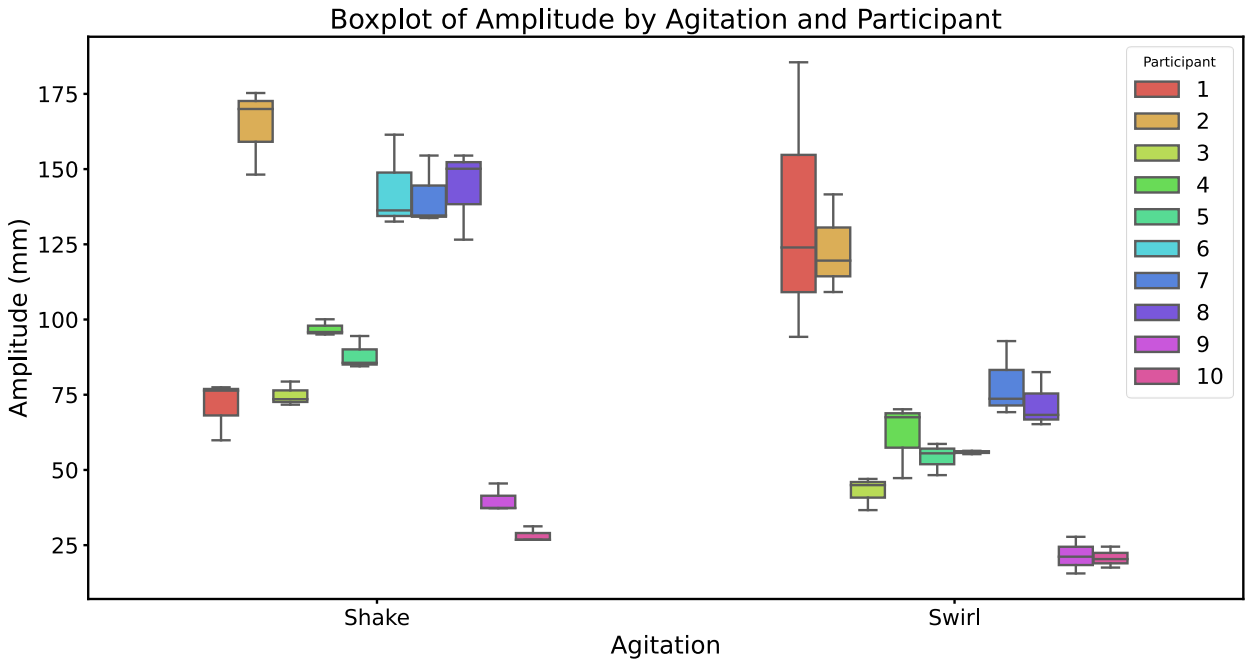

Figure 5-5 Individual boxplot of agitation amplitudes demonstrated by participants

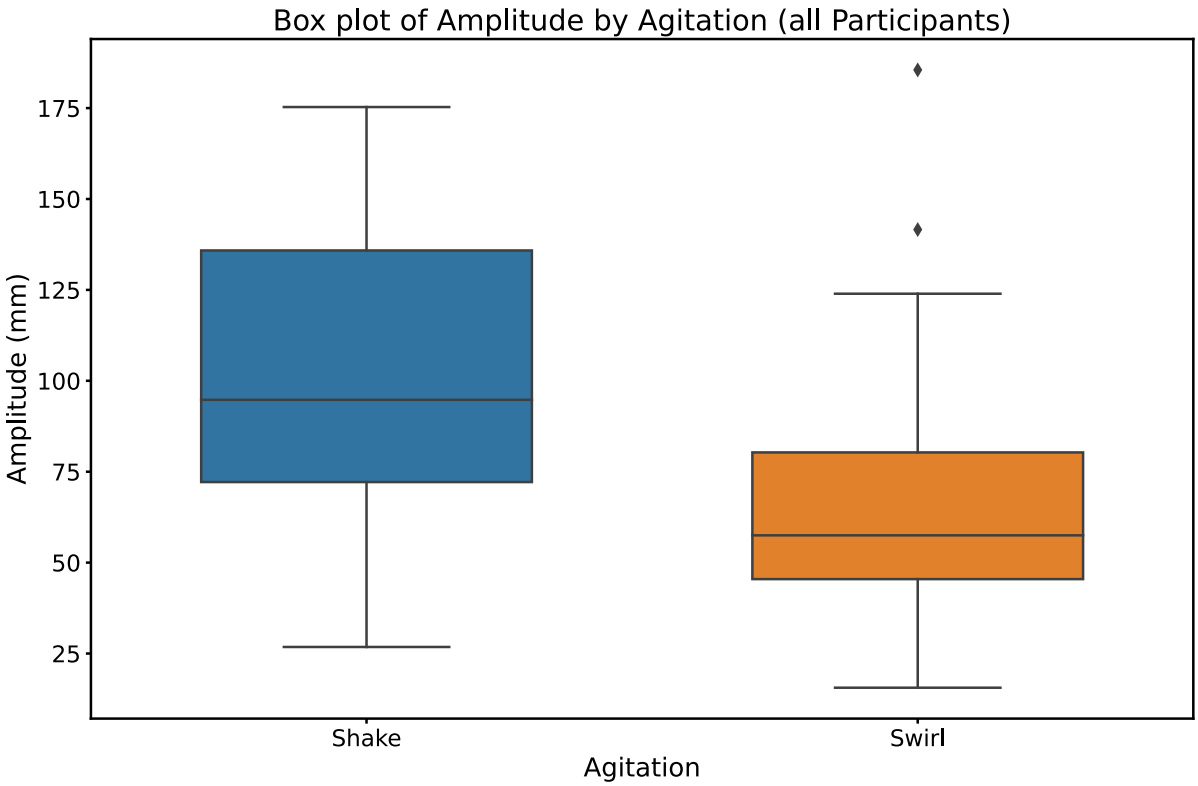

Figure 5-6 Overall boxplot of agitation amplitudes demonstrated by participants

5.5.1.2. Agitation frequency patterns

Interestingly, there was no significant difference ($p = 0.28$) between agitation frequency in swirl and shake styles, with average of 3.66 Hz and 3.77 Hz for swirl and shake respectively. As expected (given the significantly different agitation amplitudes), the amount of power transferred during swirl agitation was significantly lower than during shake agitation ($p < 0.001$), with an average of 1.31 W for swirl and 2.98 W for shake.

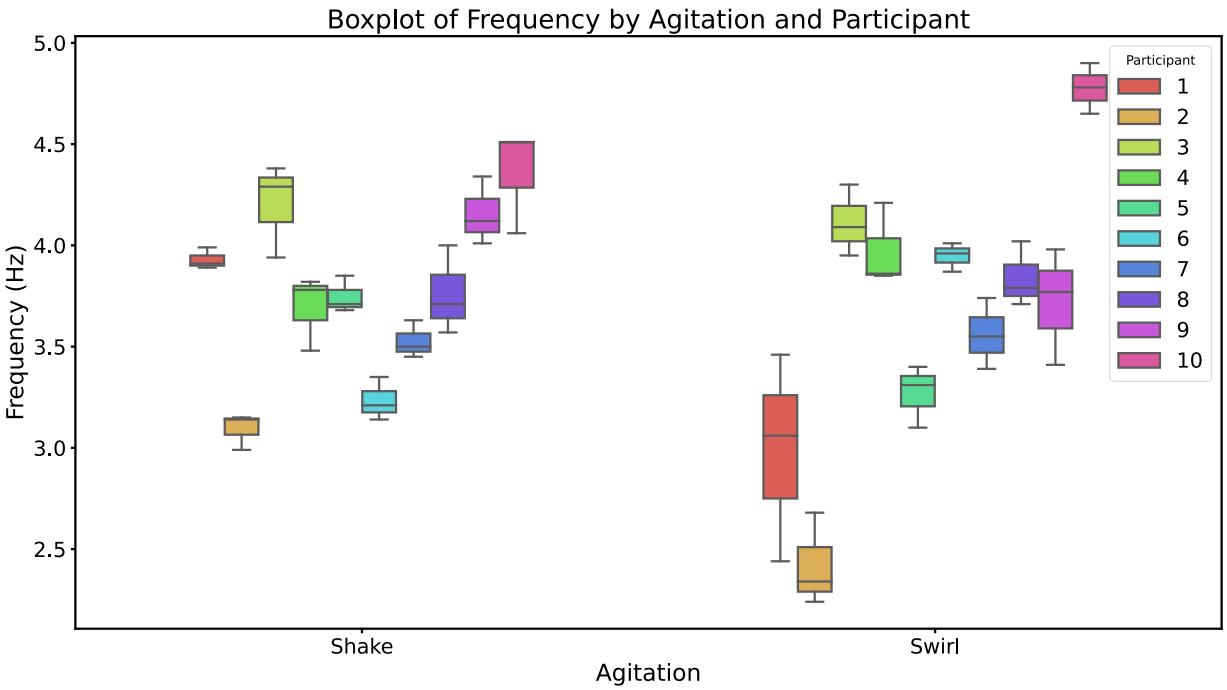

Figure 5-7 Individual boxplot of agitation frequencies demonstrated by participants

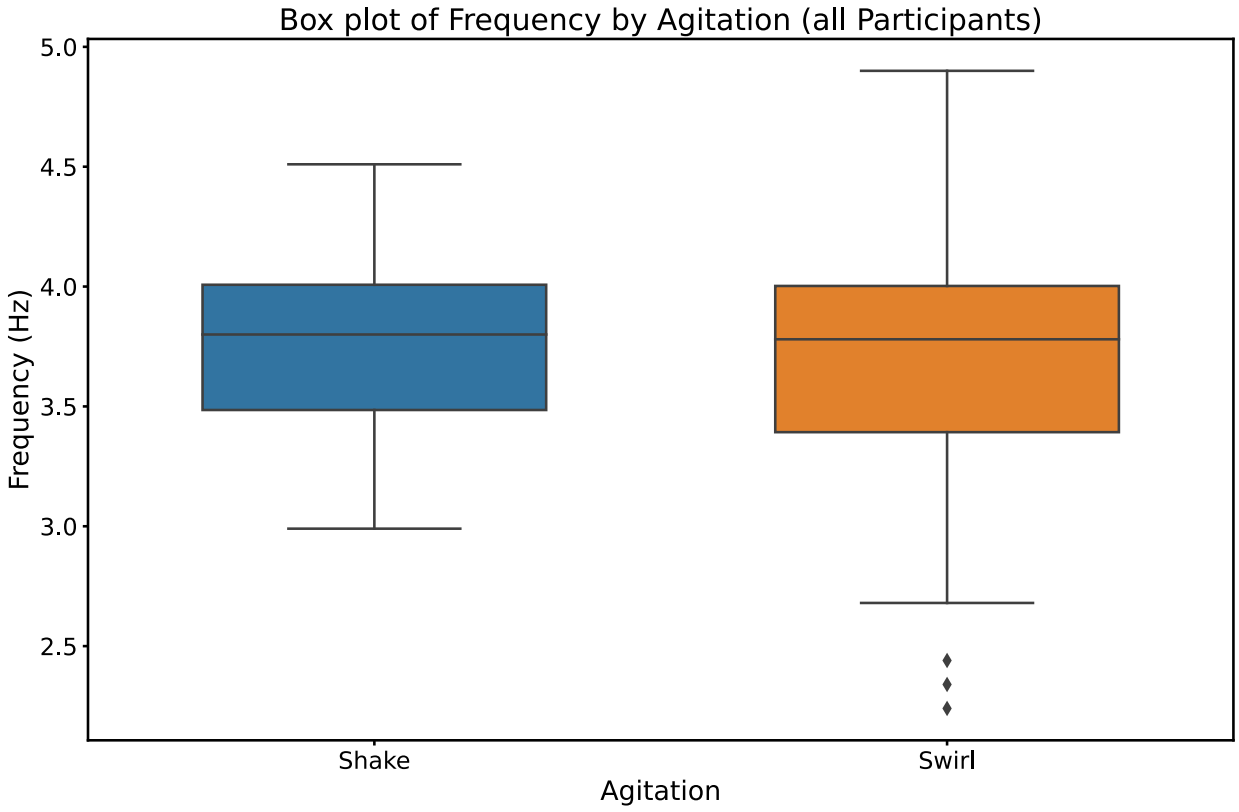

Figure 5-8 Overall boxplot of agitation frequencies demonstrated by participants

5.5.1.3. Inter-participant variability analysis

Another interesting observation was that both in swirl and shake, the higher the amplitude of an agitation, the lower the frequency of agitation. This relationship had correlations ($p < 0.001$) of 0.8 for swirl and 0.86 for shake agitations (Figure 5-9). Additionally, it was observed that the agitation performed by various individuals can differ significantly. For instance, there was a significant difference between participants two and nine in the amplitude and frequency of their agitations, both for swirl ($p < 0.001$ and $p < 0.003$, respectively) and shake ($p < 0.001$ and $p < 0.001$, respectively).

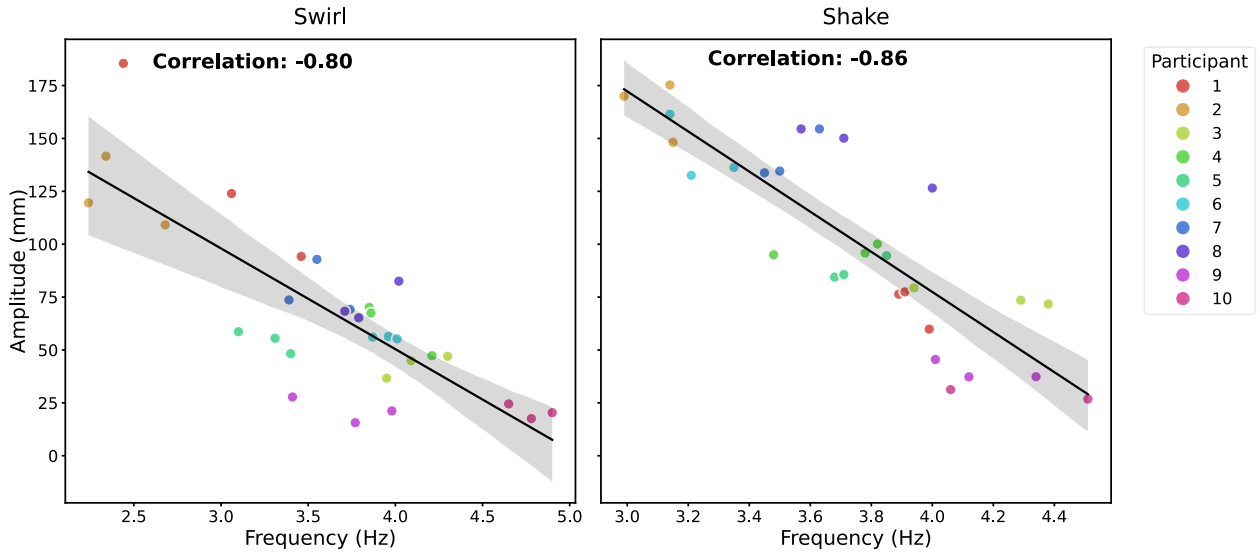

Figure 5-9 Relationship between frequency and amplitude of all swirl and shake agitation demonstrations

The inverse relationship between amplitude and frequency could be because simultaneously increasing the frequency and amplitude of agitations requires an increase in both speed and acceleration of the bottle, which demands more power from participants' muscles. Studying the limitations of applying more power is outside the scope of this thesis, as it would result in a deviation from the natural way a participant agitates the bottle.

5.5.2. Outcome of the learned cycles

The graphs of the six learned signals for swirl agitation are illustrated in Figure 5-10.

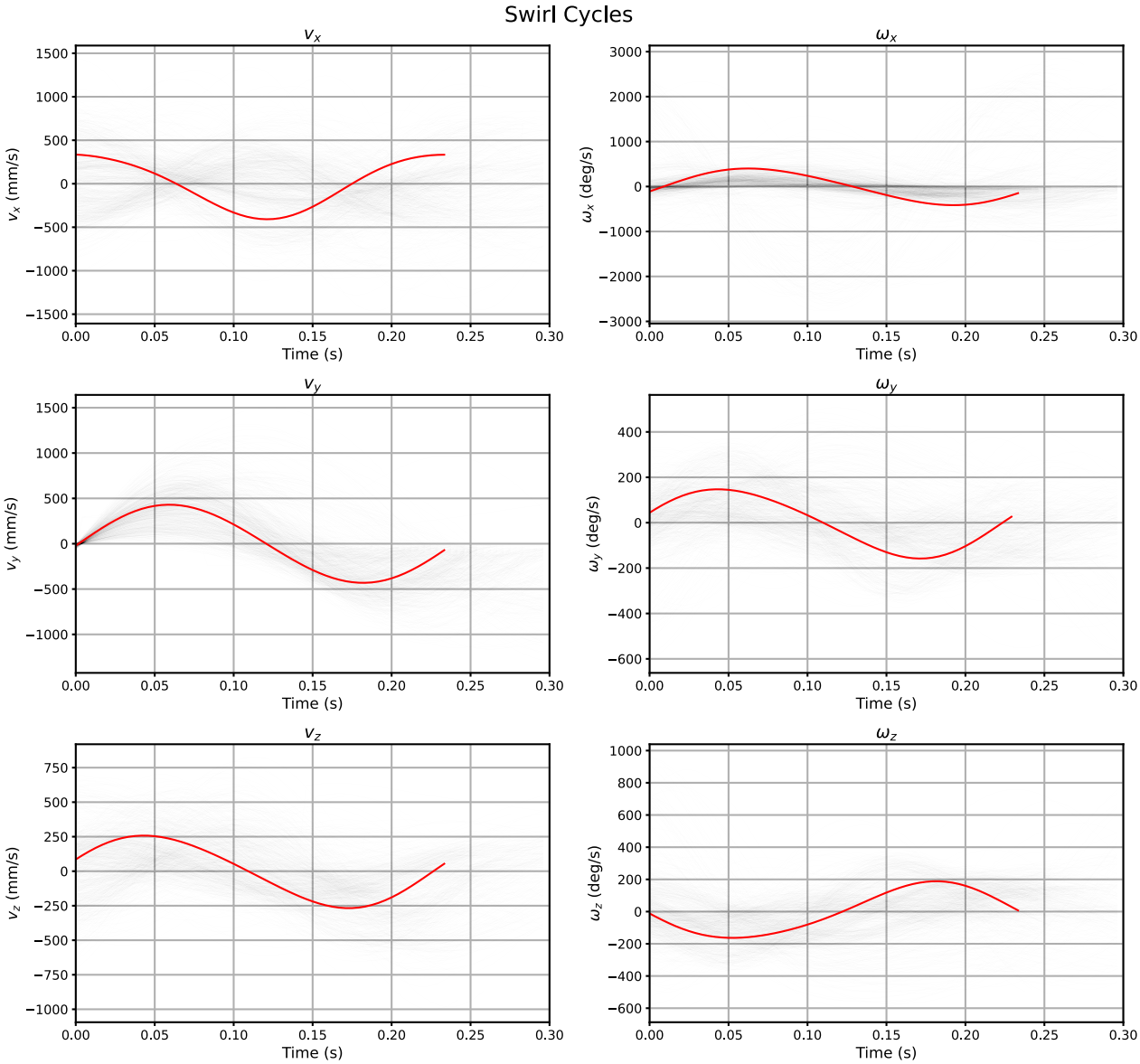

Figure 5-10 The six components of all swirl agitation cycles (transparent black) and the learned components (solid red)

As expected, all six learned velocity signals for swirl agitation are complete cycles that end where they start. After the integration of the learned signals from the velocities, the bottle position was obtained as shown in Figure 5-11. According to the figure, the trajectory points of one swirl agitation cycle end at the starting point and the transition from the last trajectory point to the starting point (i.e., one agitation cycle to the next when the robot repeats them) is also smooth. This is in accordance with the analysis from Equations (*5.11*) to (*5.15*) and the smooth complete velocity cycles illustrated

in Figure 5-10. As a result, the obtained trajectory points satisfy all three requirements for smooth swirl agitation over any desired time

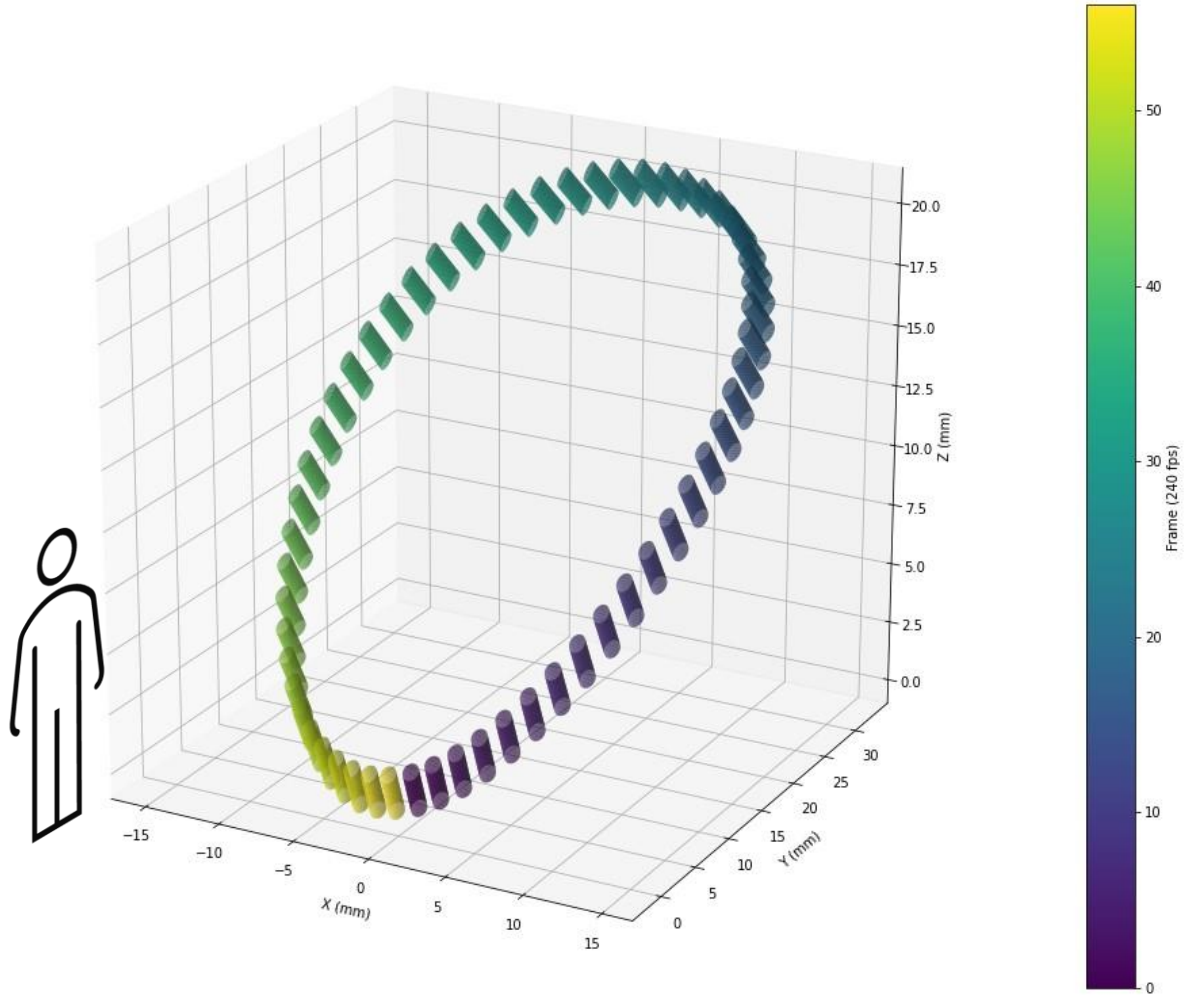

Figure 5-11 A representative swirl agitation cycle based on all demonstrations. The orientation of human demonstrator(s) is illustrated relative to the 3D bottle orientation.

Regarding the shake agitation, the graphs of the six learned velocity signals are shown in Figure 5-12. In the same way, the learned signals end at the same point at which they were started, and they are smooth complete cycles. A notable difference is the vertical linear velocity (i.e., v_z), which has larger absolute peak and trough values than swirl agitation (Figure 5-10).

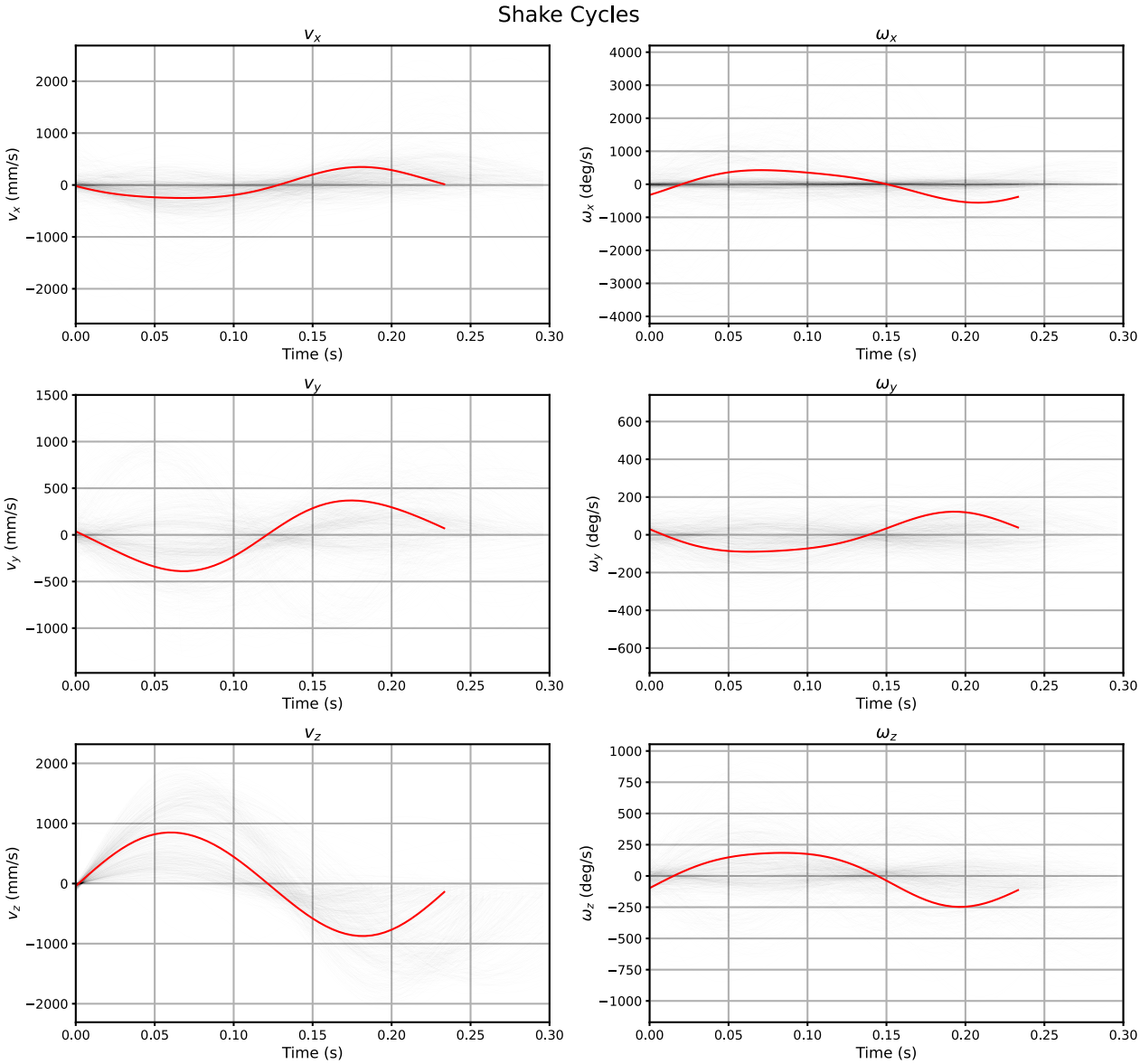

Figure 5-12 The six components of all shake agitation cycles (transparent black) and the learned components (solid red)

After the integration of the learned signals from the velocities, the bottle trajectory for the shake agitation was obtained according to Figure 5-13. Again, it is noteworthy that the learned trajectory cycle for shake is a complete and smooth cycle that ends at its starting point as expected. This figure also illustrates the learned change in the orientation of the bottle during the shaking process. In an interesting observation, the vertical axis of the bottle aligns more closely to the trajectory path when the bottle is moving down (i.e., towards the ground) than when it is moving up (i.e., against the ground). This may be due to the anatomy of the human wrist or to the fact that gravity contributes to

the downward movement of the bottle, which helps humans achieve a straight bottle path more quickly.

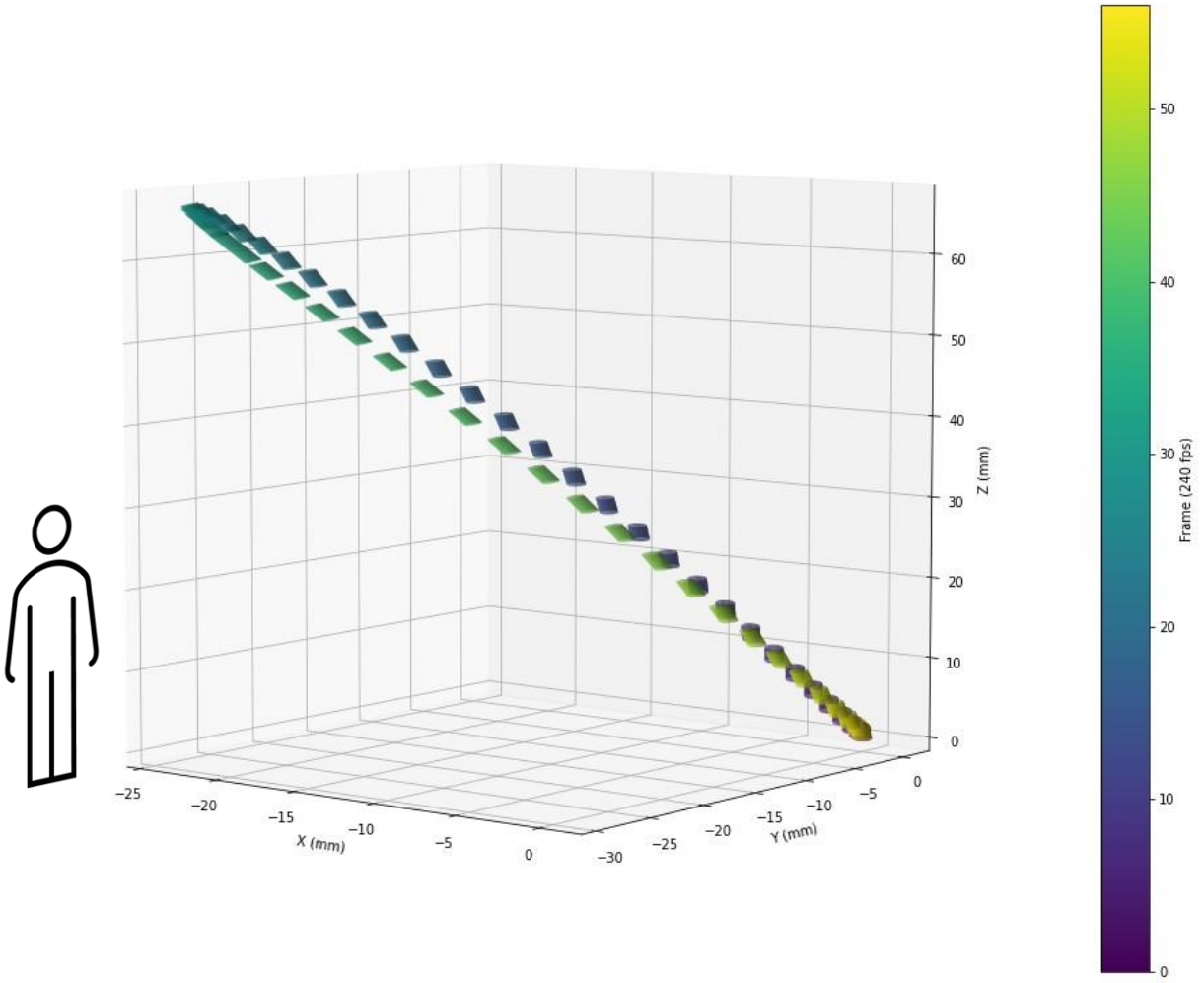

Figure 5-13 A representative shake agitation cycle based on all demonstrations. The orientation of human demonstrator(s) is illustrated relative to the 3D bottle orientation.

Another interesting observation is that the shake agitation follows a narrow, twisted figure-eight shape in 3D space. This might be due to the anatomy of the human arm and the fact that the bottle needs to return to its starting point before beginning the next agitation cycle in a smooth, feasible manner for human performance. While it is also possible that this observation could be influenced by larger and slower side-to-side movements that occur during natural human motion, this seems less likely given that such movements would need to follow a consistent rhythmic pattern to create artifacts in the FFT analysis, and such patterns were not consistently observed across participants. However, these

observations require further investigation by monitoring the exact position of arm joints involved, which is outside the scope of the current thesis.

5.5.2.1. Dominant motion features in the two learned agitation cycles

Learning from demonstration technique resulted in a single agitation cycle for each of the demonstrated agitations (the learned trajectories and bottle orientations were already presented in Figure 5-11 and Figure 5-13). It is a contribution of the present study that a single swirl or shake agitation cycle was obtained despite the variety of human demonstrations and the fact that there were no restrictions imposed on how participants would like to swirl or shake the bottle. These cycles are a novelty of the present study for obtaining a single swirl or shake agitation cycle despite the large diversity of demonstrations and the fact that the provided SOP did not restrict participants. The dominant participants' shake and swirl agitation behaviours are represented by these two cycles. In this section, the dominant features (i.e., total bottle displacement, speed, acceleration, and agitation power and cumulative energy) of agitation motions in swirl and shake styles are compared. As explained in methodology, now the mass of the bottle can be applied to the learned kinematics of the bottle to find bottle dynamics and transferred power.

The average of applied power during the learned swirl agitation was 1.34 W with 0.32 J cumulative energy transfer in an agitation cycle:

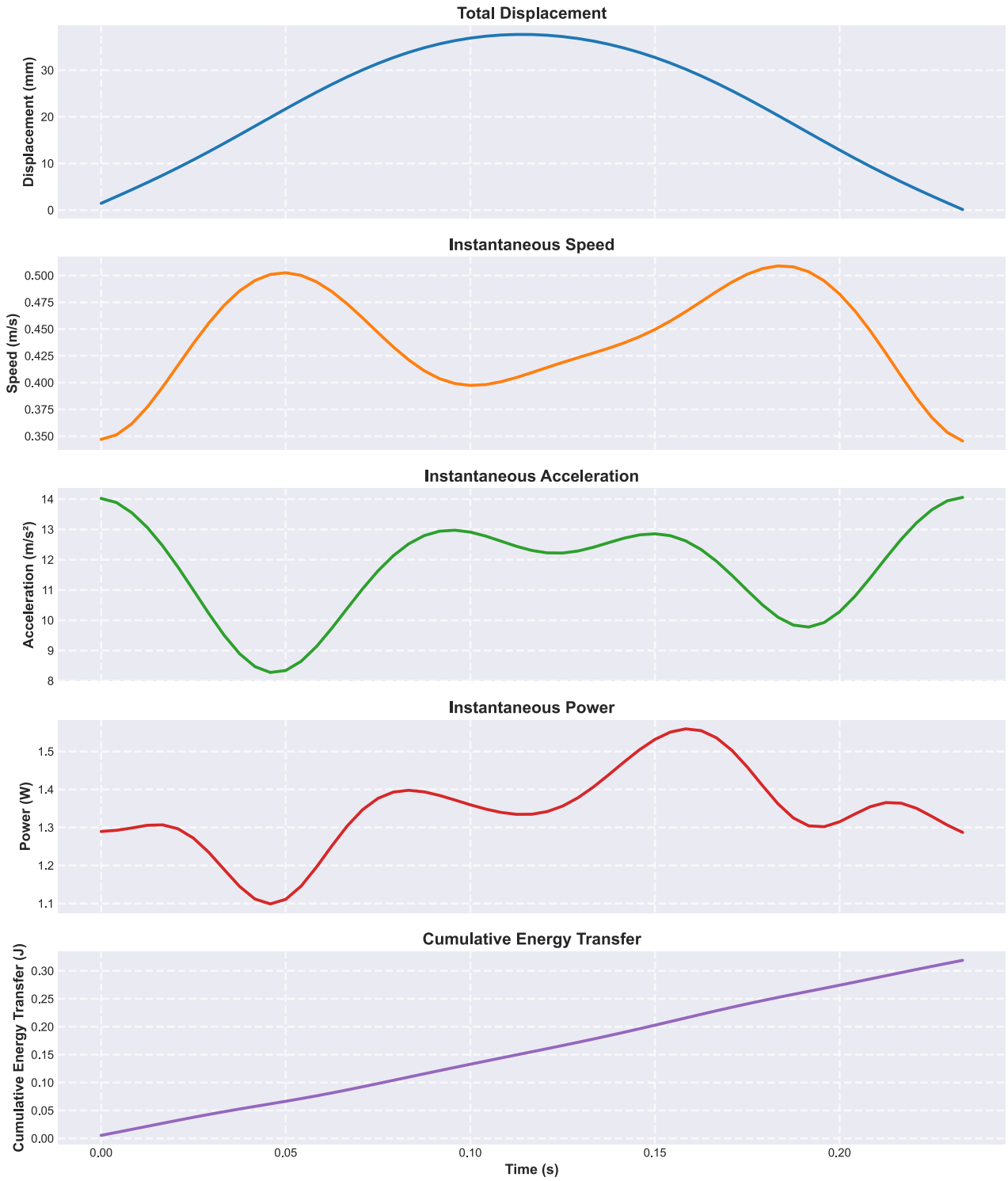

Figure 5-14 Analysing the learned cycle for swirl agitation. Based on bottle displacement (top), instantaneous speed and acceleration are calculated. The instantaneous power is calculated by multiplying the bottle speed, acceleration, and mass. Finally, cumulative transferred energy is obtained from instantaneous power. Note: power fluctuates around 1.3 W, and the cumulative energy is not linear even though it appears to be linear.

For shake, the average instantaneous power was 2.24 W with a 0.53 J cumulative energy transfer in an agitation cycle:

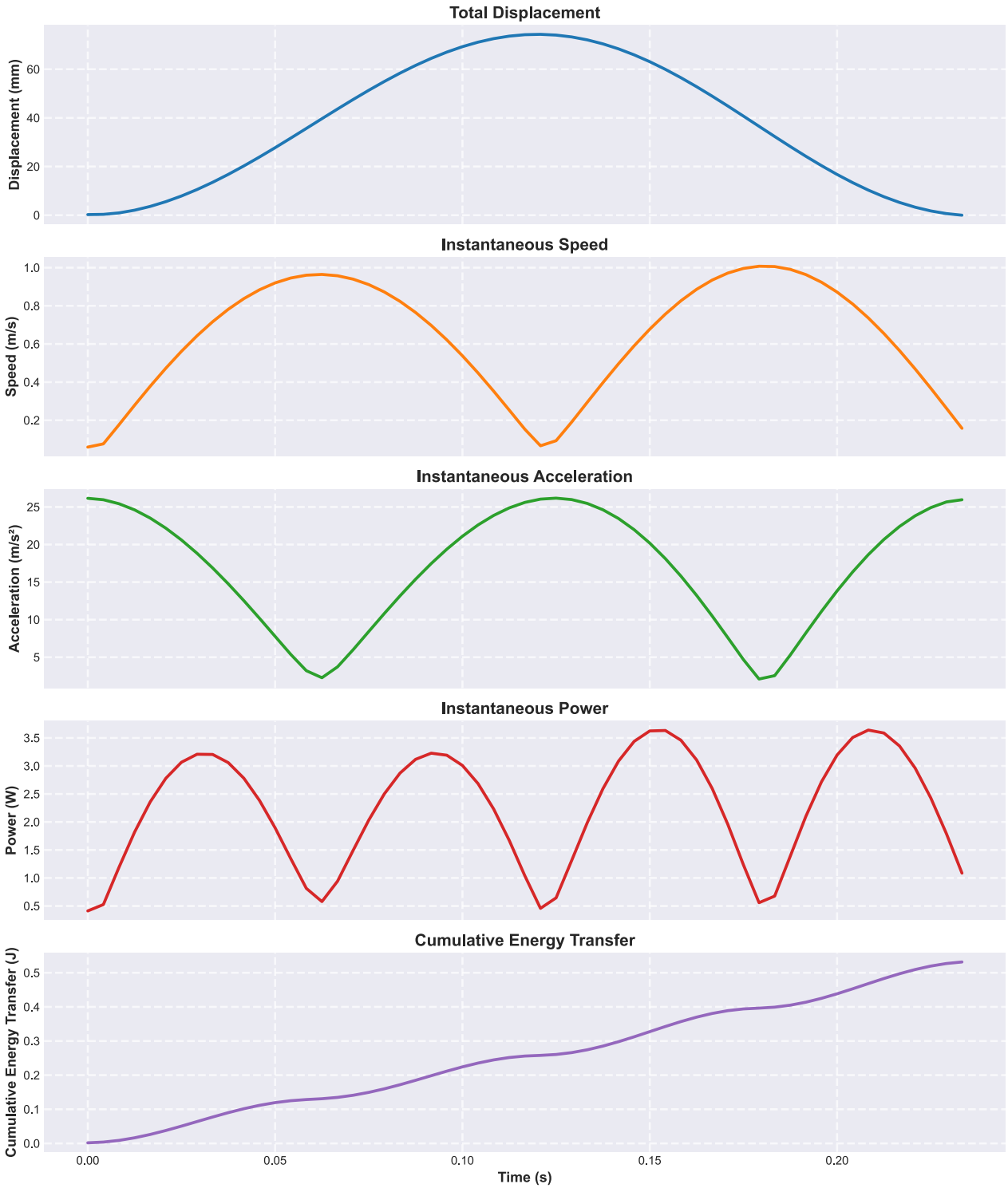

Figure 5-15 Analysing the learned cycle for shake agitation. Based on bottle displacement (top), instantaneous speed and acceleration are calculated. The instantaneous power is calculated by multiplying the bottle speed, acceleration, and mass. Finally, cumulative transferred energy is obtained from instantaneous power. Note: the cumulative energy is not linear.

According to the Figure 5-14 and Figure 5-15, during an agitation cycle for shake agitation there are larger power changes with clear rhythmic behaviour that maximises two times during forward and two times during backward motion. In each course of the motion, the first maximum power is for increasing the bottle speed and the second one is for stopping it until the bottle reaches the end of the course (a half agitation cycle). For swirl however the power is more uniform and oscillates around its average power as the bottle speed in this agitation does not get close to zero. Therefore, although the energy transfer in swirl has smaller values than shake, it is more uniform. Also, even though the speed and acceleration in shake motion come close to zero in a rhythmic manner, the maximum values still compensate the overall power with a higher average compared to swirl. It remains an open question whether high peak powers or high average powers are responsible for better powder rehydration.

As expected from energy formulation in the methodology section, the maximum energy transfer happens at the peak of instantaneous power. According to Figure 5-14 and Figure 5-15, for both agitations, power has four local maxima in an agitation cycle. This indicates that the transferred energy in human agitations, as expected, is not steady. This behaviour is particularly visible in the shake agitation cycle. The peak of energy transfer is at the times when both bottle speed and acceleration are high simultaneously, but not at their peak, because the acceleration is at its lowest point when the speed is at its peak (for example in shake, these points are not at the beginning or middle of the agitation cycle where the speed and acceleration are zero respectively). However, this observation cannot provide any information about the state of the fluid inside the bottle. This study only aimed to characterise the bottle agitation movement, and any information about the fluid state (e.g., laminar or turbulent, or the amount of shear forces) at the points with maximum power are out of the scope of this study (and can be complex considering the increase in fluid viscosity during powder rehydration).

5.5.3. Validating the programmed "human-like" agitations

Although there was no requirement for participants to be right or left-handed (and they were not asked about it), they all demonstrated the agitations with their right hand. Therefore, as the robot was expected to agitate the bottle with its left hand, all the demonstrations were reflected for the robotic demonstration, according to Equations (5.16) and (5.25). After programming the robot, it was discovered that, although the robot was able to follow and repeat the learned swirl and shake agitation cycles smoothly, the motors could not produce enough torque to match the agility of human bottle agitations. However, given there was a significant inverse correlation between participants' agitation amplitude and frequency (Figure 5-9), and given the learning approach was flexible to scaling the outcome of the learned trajectories, the amplitudes of the learned agitation cycles were increased on the same observed trend as human demonstrations while maintaining the robot's maximum agitation frequency (Figure 5-16). Scaling up the learned amplitudes was intended to, as a response to robot limitations, simulate people who agitate the bottle with a greater amplitude and smaller frequency. Scaling up the amplitudes was carried out until the robot could produce the same agitation energy as the originally learned agitation cycles (i.e., the same agitation energy as if the robot had been able to perform the original agitation cycles without scaling). This procedure required a trial-and-error approach in the robot's native programming software (mentioned in section 5.3.1). For the robot used in this study, the agitation energy equal to the learned energies (Figure 5-14 and Figure 5-15) occurred approximately at 155 mm for the shake style and 150 mm for the swirl style.

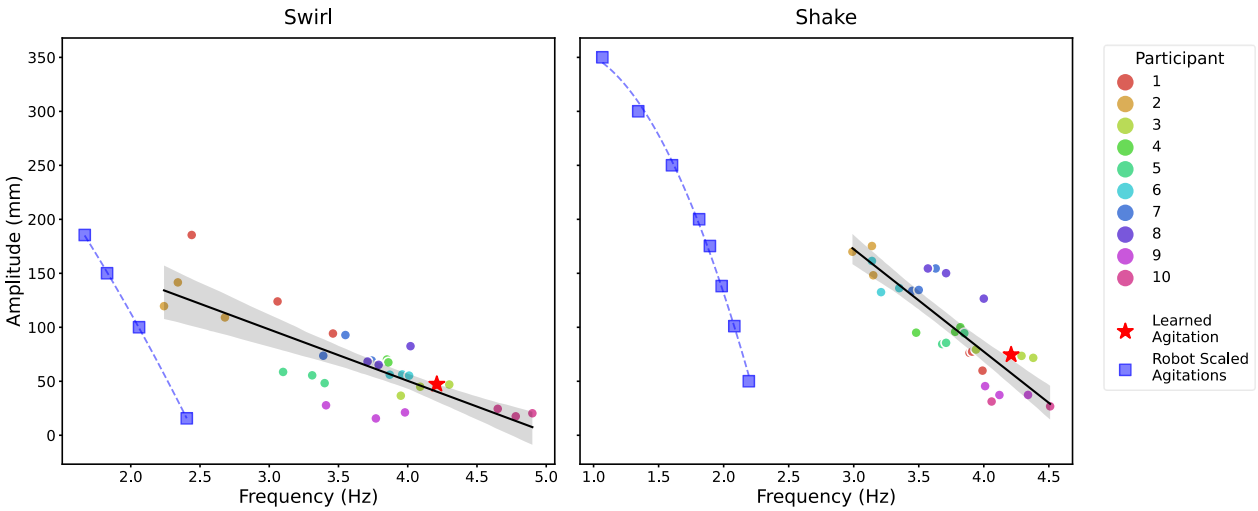

Figure 5-16 The frequency and amplitude of participants' agitations (circles) in comparison to the amplitudes achieved by robot at its maximum speed (blue squares) illustrating the robot limit in performing the learned trajectories. The red stars indicate the learned agitations from human demonstrations. Data is shown for both swirl (left) and shake (right) agitation styles.

After scaling up the trajectory amplitudes, for shake agitation, there was also a robot controller processing limitation regarding handling the three requirements of agility, accuracy, and safety in the trajectory points in real-time. This was expected due to the higher amplitude/speed in shake agitation compared to swirl agitation. Thus, to reduce the load on the controller, the number of trajectory points for shake agitation had to be reduced to two trajectory points which had the greatest distance from each other. This was accomplished at the cost of the robot not reproducing every detail of the learned shake style. For the swirl style, the exact trajectory was maintained after scaling up as a reduction in the number of trajectory points was not required.

5.5.4. Evaluating the impact of "human-like" robotic agitations on rehydration attributes

It was observed that for all rehydration attributes, there was a significant difference ($p < 0.001$) before and after updating the robotic movements to human-like agitations. As the updated motions were more energetic than the old motions, and in accordance with the findings in Chapters 3 and 4, for both

agitation styles, the average of CV estimates increased for foam height and decreased for sediment height (Table 5-2).

Table 5-2 CV shows an increase in foam height estimates and decrease in sediment height estimates for both swirl and shake agitation styles after the movements are updated to "human-like" agitations

	CV foam height estimates (mm)		CV sediment height estimates (mm)	
	swirl	shake	swirl	shake
With human-like agitations	4.1	5.4	2.9	2.3
Without human-like agitations	3.8	4.9	5.4	2.6

Also, the percentage of dissolved solids was significantly higher for shake agitation compared to swirl agitation ($p < 0.05$). The reason for these observations is that, according to section 5.5.3, the learned agitations are more energetic than those manually programmed into the robot previously. The more energetic agitation is usually expected to dissolve more powder, produce less sediment, and create more foam by introducing more air to the more energetically agitated mixture.

5.6. Conclusion

Although agitation is an important parameter in food/dairy powder rehydration, it is not well studied how agitation motions applied by end-user of powders can impact rehydration quality. This is perhaps due to challenges associated with studying fluid dynamics, particularly in complex states of agitations which can also vary widely in different humans and even different countries. This study, first, aimed to provide insights into human bottle agitation movements. It quantified some dynamical parameters in bottle agitation behaviour of ten human participants for the first time in the literature. It was found that the energy applied during swirl agitation is significantly lower than the shake agitation. Also, participants' swirl agitations had a significantly smaller amplitude than shake agitations, although frequencies of agitations were not significantly different. In both agitation styles, frequency and

amplitude of participants' agitations were negatively correlated (i.e. higher frequency resulted in lower amplitude). The second aim of the present study was to evaluate the possibility of obtaining dominant agitation behaviours out of all demonstrations and reproduce the dominant shake and swirl agitations with a robot. The method for finding the dominant agitation was based on the state-of-the-art techniques used in robot learning from demonstrations. Our developed LfD technique was able to extract a single representative agitation cycle out of all demonstrations, which was a requirement for our platform aiming to evaluate rehydration quality. Also, our learning approach guaranteed flexibility for multiplying the learned trajectories to any desired scale (reachable for the robot) to study the impact of changes in frequency or amplitude of agitations on rehydration attributes. Although the robot in our study was not as agile as human demonstrators, the flexibility of the learning approach made it possible to increase the amplitude of the learned agitations for the robot to obtain the same transferred power to the bottle as the demonstrated agitations. The updated robotic agitations both for swirl and shake resulted in significantly more foam and less sediment compared to the old robotic agitations before they were updated to be "human-like". This was expected because the previous robotic agitations were less powerful than the updated "human-like" agitations, and also, in the old movements, only a limited number of motors were being utilised on the robot arm, which can result in a different fluid dynamic inside the bottle.

Future studies may increase the number of participants and diversify their demographics. It will be particularly beneficial to study the effects of agitations in different regions or countries on rehydration quality. The robotic limitations in the present study may be addressed by using a different robot, which is beyond the scope of this thesis. Nevertheless, since human bottle agitations were examined for the first time in this study, future research is expected to have a clearer picture of whether a selected robot can produce such human-like movements. Also, based on the results of this study, with the availability of a robot generating editable human-like agitations, further research may benefit from studying the impact of specific parameters of human-like bottle agitations (e.g.,

amplitude or frequency) on the rehydration quality of IF or other food/dairy powders. Here, only visible rehydration attributes were used to assess the impact of agitation on rehydration quality. However, in-bottle sensors (e.g., conductivity sensors) may be used to obtain real-time information regarding agitation's impact on rehydration. Finally, it is expected that the methodology developed for generating identical human-like agitations may also apply to other types of food or pharmaceutical powders that are intended for rehydration by end-users.

Chapter 6: Concluding remarks

6.1. Introduction

The present thesis examined potential improvements in automating IF rehydration quality tests, both in terms of sample preparation and rehydration quality measurement. Several issues were found in literature regarding commonly used rehydration tests. The tests are mostly subjective, time-consuming, and prone to error (Selomulya et al., 2023). Additionally, there are sometimes different tests for measuring the same rehydration attribute, some developed in-house and potentially confidential (Pisecky, 2012), thus not useful to the research community. These make the findings dependent on the method and the analyst who performed the test. Consequently, it can be difficult to gain a deeper understanding of how powder physicochemical properties impacts its rehydration.

Several studies have attempted to improve the tests using alternative methods. For example, using laser diffraction and measuring particle size, Boiarkina et al. (2017) investigated powder dispersibility in a less time-consuming method. Another study by Lloyd et al. (2019) demonstrated further improvements in test discretisation by counting slowly dissolving particles using computer vision rather than manually comparing them to five reference images. Ideally, the improved tests are expected to provide insights into the optimal parameters for powder rehydration and powder production (e.g., drying parameters), saving energy, time, and material resources (Munir et al., 2017).

The work described in this thesis aimed to address the issues identified by means of an automated platform that integrated a cobot and computer vision system. The cobot was used to scoop and rehydrate the mixtures consistently in addition to rotating and presenting the bottle to the computer vision system. The computer vision system made estimates of visible rehydration properties (foam, sediment, and white particles) objectively. Finally, the automated platform also replicated key aspects of the end-user rehydration practice (i.e., the use of a baby bottle and performing the agitation styles that are usually instructed on the packaging of powders).

6.2. Summary of contributions

This thesis made the following seven contributions to the automation and understanding of powder rehydration.

1. In Chapter 3, an automated rehydration quality measurement platform was developed by integrating a cobot with a CV system (Mozafari et al., 2024). The author is not aware of any comparable system being described in literature. A primary objective of the platform was to replicate the end-user rehydration procedure as closely as possible, for example rehydrating the powders and assessing the quality of rehydrated powders in a commercially available baby bottle. The platform ratings of three key rehydration properties (foam height, sediment height, and number of white particles) were compared to human participants in an evaluation experiment. The results indicated ratings that were comparable to those of human participants except for sediment height using shake agitation. Considering some commonly used tests are based on human visual inspection, this was a significant result. Also, this is the first report to use CV to measure these attributes in IF rehydration. A key benefit of the automated platform is that it could be used in different laboratories around the world and provide reproducible results that are not impacted by the subjectivities that may be introduced by geographical agitation style preferences or the variations in quality interpretation or energetic rehydration of the analyst who performs the test. Additionally, the platform may be used to ensure that powder does not lose its rehydration quality during storage or transportation from the production plant to the repackaging facility, such as in another country. More standardised and objective methods using the integration of emerging technologies can contribute to gaining a better understanding of rehydration (Crowley et al., 2016). Moreover, obtaining objective measurements can offer a better comparison of research findings and quicker convergence to common understandings and shared opinions about rehydration.

2. In Chapter 3, “digitally generated” reference images for evaluating the numbers of white particles were developed (Mozafari et al., 2024, 2022). As part of the evaluation of the platform based on participants’ ratings, it was necessary to design experiments that allowed humans to rate the images captured by the automated platform. The subjectivity issue associated with traditional reference images (e.g., the scores assigned to the reference images are not systematically explained, and the reference images may not reflect all observations) has already been raised in the literature (Lloyd et al., 2019). The present study addressed two of these limitations by: (i) developing the reference images in a systematic manner and (ii) based on observations from several extreme samples (that contained a large number of undissolved particles). The developed reference images or the method used for their systematic development can be used by the research community going forward.
3. As explained in Chapter 4, the modification of “sludge” (Pisecky, 2012) and “slowly dissolving particles” (Lloyd et al., 2019) tests to improve their repeatability for the benchmarking purposes was the third contribution of this PhD. For example, regarding the modified sludge test, it was observed that it is not only more robust for benchmarking purposes, but it also exhibits higher correlations with other commonly used laboratory tests, such as the percentage of targeted but undissolved solids. Thus, the modified tests could provide the research community with more valuable insight into rehydration.
4. In Chapter 4 an important relationship between powder flowability and sediment formation (which is possibly related to clump formation and clump sedimentation) was reported for the first time in the literature. Our findings suggest that rehydration stages can be more complex than previously thought, having five stages rather than four. As a result, good flowability is not only important in the production line but also important in rehydration when powder particles flow on top of each other quickly to reach the water surface faster as the first step in rehydration (followed by wetting, and the additional rehydration stages).

5. As dispersibility is an important rehydration quality test that requires a complicated and time-consuming procedure, alternative methods for predicting it are of interest (Boiarkina et al., 2017). In Chapter 5, a random forest model was developed to more easily and quickly predict the results of the dispersibility test based on rehydration property ratings from the automated platform. Although predicting dispersibility using some measurements from the mixture is already reported (Boiarkina et al., 2017; Nugroho et al., 2021), this was the first time in the literature that a CV method applied to the prepared mixture (not powder (Ding et al., 2020b)) was used to predict dispersibility. Also, this was the first time in the literature a computer vision approach was used to monitor the sediment height change over time in the intact bottle in which the sample was prepared. The monitoring of sediment height change was necessary to predict dispersibility.
6. In Chapter 5, the natural bottle agitations of ten human participants using two agitation styles mentioned by WHO (2007), swirl and shake, were characterised. To the best of the author's knowledge, this was the first time in the literature that such a characterisation has been reported. For this purpose, we designed a custom CV and IMU-based approach to detect agitation movement in a reliable and economically feasible manner. It was shown that the natural swirl agitation performed by humans was significantly less energetic than the shake agitation. As a result, the amount of agitation power applied by humans depends on the agitation style. It suggests that end-user instructions regarding bottle agitation should be improved. Also, it was observed that, interestingly, the frequencies of swirl and shake agitations were not significantly different, but the amplitudes were significantly different, and the amplitude of agitations is negatively correlated with their frequency
7. In Chapter 5, the seventh contribution of this thesis was the development of a statistical learning method that was used to obtain the dominant swirl or shake agitation trajectory as a single closed path that was smoothly repeatable for the robot. It was a unique challenge for

the present study compared with previous studies to learn such a cycle without constraining the natural agitation behaviour of participants (despite the observed significant variations in demonstrations). It was also shown that it is possible to use a 7 DOF robotic arm to mimic the learned trajectory. The flexibility of the learning method allowed scaling up the learned trajectory so that the robot could apply a similar power to that of humans during the bottle agitation despite having to use a lower agitation frequency due to robot limitations. The learned swirl agitation was less energetic than the learned shake agitation, resulting in a greater sediment height and a smaller foam height on average. Additionally, both in the case of swirl and shake agitation styles, the updated robotic agitations (i.e., the learned "human-like" agitations) were significantly more energetic than the previous robotic agitations which attempted to subjectively and approximately replicate human agitations. As expected, both in the case of swirl and shake agitations, updating the robotic agitations resulted in higher foam height and lower sediment height than had been measured in Chapter 3.

6.3. Potential research impact

There is considerable similarity between food powders and powders in other industries (Fitzpatrick and Ahrné, 2005). In fact, some of the methods used in the current study were inspired by studies on food and pharmaceutical powders. Therefore, although this study focused on infant formula powder, its findings may be of relevance for future studies in a wider range of powder rehydration applications, such as high protein dairy powders (Ji et al., 2016b). The current platform can not only rehydrate infant formula powder and estimate the rehydration quality in a reproducible manner (using a robot and a CV system) but can also rehydrate the samples in a "human-like" manner, using swirl and shake agitations learned from humans. This enables the platform to be used as an objective method for evaluating the rehydration process while using a rehydration energy and style that is similar to end users of the powder. The same methods used for characterising the baby bottle agitations could be

applied to other applications, such as agitation of protein shake bottles or rehydration of pharmaceutical powders, with appropriate modifications.

6.4. Opportunities for future work

During the work described in this thesis, several opportunities for additional work were identified. Although these were outside the scope of the present work, they are collected here in the form of potential limitations and research questions that deserve further attention.

1. The computer vision approach used in this work could not detect features that are invisible to cameras (and perhaps the human eye). One example of this is the exact sediment topology inside the bottle, rather than sediment height detection just from the bottle sidewall. Additionally, the type of camera used, an RGB camera, was limited to registering features that manifest in the visible range of the electromagnetic spectrum. Hyperspectral, thermal, or UV cameras may be able to provide richer information for all three rehydration attributes automatically rated in this study, particularly for distinguishing white particles from small droplets and foam pieces. Furthermore, additional research could be conducted with an RGB camera on the impact of variations in the colour of the light source (wavelength), use of a movable light source rather than a fixed source, and the number and variety of imaging viewpoints around the bottle used to generate ratings.
2. Computer vision algorithms developed in the present study were based on classical techniques, which may prove beneficial in certain tasks, such as in detecting nuanced sediment changes in the present study. However, a method based on ML may be more flexible when dealing with unseen data, such as detecting particles that are slightly larger than expected. An ML based method may also provide greater tolerance of lighting and colour variations. However, more images may be needed to develop an ML algorithm. In this stage of the study, the collected images may provide sufficient data for developing a more flexible method, particularly for white particle detection. The development of a vision approach based on ML

and the comparison of its results with those of the present study would be an interesting research direction.

3. It was outside the scope of this thesis to determine if the water preparation used within the experiments introduced any variability into the results. Precautions were taken (as far as possible) to ensure that identical water was provided to the automated platform during our work (e.g., with the analyst's eye level aligned with the marking on the bottle for accurate volume measurement and starting the robotic experiments within thirty seconds of dispensing the water to minimise the possibility of a drop in water temperature). Nevertheless, the process of filling the bottle with water is still a manual task, which introduces some possibility for variability and error, and this could be investigated. If it were a problem, it may be possible to achieve more consistent results by integrating an automated water dispenser with the automated platform that can heat the water and control the temperature and volume of water dispensed.
4. The robot platform used in this work was a bimanual cobot with a relatively low maximum payload and some limits on the maximum movement speeds. The robot specifications affect the cost of the robot (e.g., bimanual robots are often more expensive than single arm robots), and the ability of the robot to fully mimic human movements (characterised in Chapter 5). In the context of the work in this thesis the feasibility of using a single arm robot was briefly examined (but not reported). While the bimanual robot used in this study used the right arm for scooping the powder and the left arm for levelling the powder in the scoop and agitating the bottle, a single arm robot could perform the actions if appropriate jigs were provided to hold the bottle in place. A single arm solution could be a valuable step towards developing a more cost-effective platform at a higher technology readiness level.
5. The impact of the scooping method on the dissolved solids has been studied before (Rosenkranz et al., 2024), but there is a need for deeper studies (Mozafari et al., 2024), for

example, to consider the impact of scoop shape (not just volume) on the amount of powder the scoop can fit, considering the high compressibility of dairy powders. Even the size of the holes on the scoop may be responsible for consistency in the weight of powder in scoops, as they should let the trapped air out of the scoop to fully fill it with powder. Such studies would assist IF processors in improving scoop shapes for optimal rehydration. Also, further research may be conducted to determine how humans scoop powder naturally, using a method similar to that used for characterising human bottle agitation in the present study. To gain insight into the natural force applied during scooping (which, again, may affect the amount of powder scooped as dairy powders are highly compressible).

6. Further investigation of the formation of clumps using the automated platform (e.g., identical powder scooping and bottle agitations) could provide a deeper insight into the observed behaviour in sediment height change. Although some observed relationships between sedimentation, flowability, and dispersibility were discussed in Chapter 4, a more in-depth (e.g., quantified) examination of clumps (e.g., based on their weight and volume) might provide more insights into the impact of flowability on clump formation and clump sedimentation.
7. Quantification of scorched particles may provide some insight into the possible impact of particle size and agglomeration on the number and size distribution of scorched particles. A relationship may also exist between the number and distribution of scorched particles and the number of white particles (possibly damaged particles) examined in this study. Using a high-resolution camera (such as that used in the present study), colour segmentation, and connected component analysis, it is possible to identify scorched particles on a white colour filter disc (called sediment disc). As a result, their size distribution can be determined. During the current study, a preliminary analysis of this approach was conducted, which allowed us to both count the particles and estimate their size. However, it was not pursued further, and its results were

not presented since the integration of the computer vision approach to scorched particles test, which involves filtration and high-speed agitation, was outside the scope of this thesis.

8. It has already been reported that powder particle size is related to dispersibility (Boiarkina et al., 2017). During the experiments conducted in Chapter 4, there were also some initial observations that a larger powder particle size, particularly D10, may reflect the presence of more white particles that may be damaged during agglomeration and fines return (which can increase D10). For further evaluations of this observation, improvements will need to be made both in terms of the CV algorithm and the traditional test as a reference. As mentioned in the previous paragraph, this observation may also be related to the size distribution of scorched particles.
9. Although the number of participants in human bottle agitation experiments was sufficient to examine whether there were significant differences in swirl and shake agitations, a larger number of participants could provide additional insights, such as understanding agitation behaviour across different cultures or geographical regions.
10. Further research could examine the impact of human-like agitation parameters (such as amplitude and frequency) on powder rehydration. Although the present study developed a platform capable of replicating human-like agitations with the ability to scale the agitation parameters, the relationship between specific agitation parameters and rehydration outcomes remains to be determined. For example, it was observed in Chapter 5 that the average and peak power of shake agitation are higher than those of swirl agitation. Further research could be conducted to determine whether peak power or average power is more crucial to the complete rehydration of powder. It may be possible to establish optimal practices for powder rehydration by understanding how agitation parameters affect rehydration.

6.5. Conclusion

The work in this thesis represents a first attempt to address two major issues in powder rehydration quality measurements: subjectivity and lack of representative sample preparation. To address these challenges, an automated rehydration quality measurement approach that mimics the bottle agitation behaviour of end-users was developed in the thesis. It was shown that the automated platform can serve as an example of the potential of emerging technologies and interdisciplinary research in gaining novel insights into long-standing research questions about powder rehydration. The insights gained regarding the complex process of powder rehydration as well as end-users' powder rehydration behaviour and replication of this behaviour can lead to consistent and improved product quality and process efficiency for IF powders. Ultimately, these advances can pave the way to the innovation in powder technology as a whole, and the development of powders with enhanced performance in other industries such as dairy, food, and pharmaceutical powders.

References

ABB, 2024. Technical reference manual RAPID Instructions, Functions and Data types Document ID: 3HAC050917-001 Revision: X.

ABB, 2021a. Product manual IRB 14000 gripper IRC5 Document ID: 3HAC054949-001 Revision: M.

ABB, 2021b. YuMi [WWW Document]. URL https://search.abb.com/library/Download.aspx?DocumentID=9AKK107046A3807&LanguageCode=en&DocumentPartId=&Action=Launch

ADPI, 2023. Reconstituting Dairy powders Handbook. American Dairy Product Institute.

Aggarwal, A.K., Mohan, R., 2010. Aspect ratio analysis using image processing for rice grain quality. Int. J. Food Eng. 6. https://doi.org/10.2202/1556-3758.1788

Akyazi, T., Goti, A., Oyarbide, A., Alberdi, E., Bayon, F., 2020. A guide for the food industry to meet the future skills requirements emerging with industry 4.0. Foods 9, 1–16. https://doi.org/10.3390/foods9040492

Altazan, A.D., Gilmore, L.A., Guo, J., Rosenberg, D.M., Toupo, D., Gowins, A., Burton, J.H., Beyl, R.A., Chow, C.C., Hall, K.D., Redman, L.M., 2019. Unintentional error in formula preparation and its simulated impact on infant weight and adiposity. Pediatr. Obes. 14, 2–7. https://doi.org/10.1111/ijpo.12564

Andersson, I.M., Millqvist-Fureby, A., Sommertune, J., Alexander, M., Hellström, N., Glantz, M., Paulsson, M., Bergenståhl, B., 2019. Impact of protein surface coverage and layer thickness on rehydration characteristics of milk serum protein/lactose powder particles. Colloids Surfaces A Physicochem. Eng. Asp. 561, 395–404. https://doi.org/10.1016/j.colsurfa.2018.10.073

AprilRobotics, 2024. AprilTag.

AUBO, 2021. AUBO-i3 [WWW Document]. URL https://aubo.co.th/wp-

content/uploads/2021/10/aubo_i3_gerenga_manual_brochure.pdf

Bader, F., Rahimifard, S., 2020. A methodology for the selection of industrial robots in food handling. Innov. Food Sci. Emerg. Technol. 64, 102379. https://doi.org/10.1016/j.ifset.2020.102379

Bader, F., Rahimifard, S., 2018. Challenges for industrial robot applications in food manufacturing. ACM Int. Conf. Proceeding Ser. https://doi.org/10.1145/3284557.3284723

Bakshi, S., Paswan, V.K., Yadav, S.P., Bhinchhar, B.K., Kharkwal, S., Rose, H., Kanetkar, P., Kumar, V., Al-Zamani, Z.A.S., Bunkar, D.S., 2023. A comprehensive review on infant formula: nutritional and functional constituents, recent trends in processing and its impact on infants' gut microbiota. Front. Nutr. 10. https://doi.org/10.3389/fnut.2023.1194679

Bals, A., Kulozik, U., 2003. Effect of pre-heating on the foaming properties of whey protein isolate using a membrane foaming apparatus. Int. Dairy J. 13, 903–908. https://doi.org/10.1016/S0958-6946(03)00111-0

Bélanger, J., Venne, P., Paquin, J.-N., others, 2010. The what, where and why of real-time simulation. Planet Rt 1, 25–29.

Benkovic, M., Bauman, I., 2009. Flow Properties of Commercial Infant Formula Powders. Int. J. Nutr. Food Eng. 3, 304–308. https://doi.org/10.5281/zenodo.1080486

Bhandari, B., Bansal, N., Zhang, M., Schuck, P., 2013. Handbook of Food Powders: Processes and Properties, Handbook of Food Powders: Processes and Properties. https://doi.org/10.1533/9780857098672

Billard, A., Grollman, D., 2013. Robot learning by demonstration. Scholarpedia 8, 3824.

Bloss, R., 2016. Collaborative robots are rapidly providing major improvements in productivity, safety, programing ease, portability and cost while addressing many new applications. Ind. Rob. 43, 463–468. https://doi.org/10.1108/IR-05-2016-0148

Bock, J.E., Milliken, G.A., Schmidt, K.A., 2007. Best Mixing Practices to Minimize the Particle

Size in Reconstituted Nonfat Dry Milk. J. Food Process. Preserv. 32, 60–74. https://doi.org/10.1111/j.1745-4549.2007.00164.x

Bogue, R., 2009. The role of robots in the food industry: A review. Ind. Rob. 36, 531–536. https://doi.org/10.1108/01439910910994588

Boiarkina, I., Depree, N., Prince-Pike, A., Yu, W., Wilson, D.I., Young, B.R., 2018. Using Big Data in Industrial Milk Powder Process Systems, Computer Aided Chemical Engineering. Elsevier Masson SAS. https://doi.org/10.1016/B978-0-444-64241-7.50377-3

Boiarkina, I., Depree, N., Yu, W., Wilson, D.I., Young, B.R., 2017. Rapid particle size measurements used as a proxy to control instant whole milk powder dispersibility. Dairy Sci. Technol. 96, 777–786. https://doi.org/10.1007/s13594-016-0302-5

Bradski, G., 2000. The OpenCV Library. Dr. Dobb's J. Softw. Tools 25, 120–123.

Brito, T., Queiroz, J., Piardi, L., Fernandes, L.A., Lima, J., Leitão, P., 2020. A machine learning approach for collaborative robot smart manufacturing inspection for quality control systems. Procedia Manuf. 51, 11–18. https://doi.org/10.1016/j.promfg.2020.10.003

Brosnan, T., Sun, D.W., 2004. Improving quality inspection of food products by computer vision - A review. J. Food Eng. 61, 3–16. https://doi.org/10.1016/S0260-8774(03)00183-3

Brown, M., Laitano, F., Williams, C., Gibson, B., Haw, M., Sefcik, J., Johnston, K., 2019. "Curdling" of soymilk in coffee: A study of the phase behaviour of soymilk coffee mixtures. Food Hydrocoll. 95, 462–467. https://doi.org/10.1016/j.foodhyd.2019.04.032

Caldwell, D., 2013. Robotics and automation in the food industry: Current and future technologies.

Caldwell, D.G., 2023. Automation in Food Manufacturing and Processing, in: Springer Handbooks. Springer, Cham, pp. 949–971. https://doi.org/10.1007/978-3-030-96729-1_44

Cao, H., 2015. Simulations of Dissolution of Structured Particles. The University of Leeds.

CFR, 2024. Code of Federal Regulations, Title 21, Chapter I, Subchapter B, Part 107—Infant Formula. [WWW Document]. Code Fed. Regul. URL https://www.ecfr.gov/current/title-

21/chapter-I/subchapter-B/part-107

Chapman, T., 2003. Lab automation and robotics: Automation on the move. Nature.

Chen, X.D., Lloyd, R.J., 1994. Some aspects of measuring the size and rate of dispersion of milk powder agglomerates using the Malvern Particle Sizer 2600c. J. Dairy Res. 61, 201–208.

Cimini, A., Pallottino, F., Menesatti, P., Moresi, M., 2016. A Low-Cost Image Analysis System to Upgrade the Rudin Beer Foam Head Retention Meter. Food Bioprocess Technol. 9, 1587–1597. https://doi.org/10.1007/s11947-016-1743-9

Codex, 2023. Standard for Infant Formula and Formulas for Special Medical Purposes Intended for Infants (CXS 72-1981) [WWW Document]. Codex Aliment. URL https://www.fao.org/fao-who-codexalimentarius/sh-proxy/en/?lnk=1&url=https%253A%252F%252Fworkspace.fao.org%252Fsites%252Fcodex%252FStandards%252FCXS%2B72-1981%252FCXS_072e.pdf

Condé, B.C., Fuentes, S., Caron, M., Xiao, D., Collmann, R., Howell, K.S., 2017. Development of a robotic and computer vision method to assess foam quality in sparkling wines. Food Control 71, 383–392. https://doi.org/10.1016/j.foodcont.2016.07.020

Crowley, S. V., 2016. Physicochemical characterisation of protein ingredients prepared from milk by ultrafiltration or microfiltration for application in formulated nutritional products. University College Cork.

Crowley, S. V., Kelly, A.L., Schuck, P., Jeantet, R., O'Mahony, J.A., 2016. Rehydration and Solubility Characteristics of High-Protein Dairy Powders. Adv. dairy Chem.

Crowley, S. V, Gazi, I., Kelly, A.L., Huppertz, T., O'Mahony, J.A., 2014. Influence of protein concentration on the physical characteristics and flow properties of milk protein concentrate powders. J. Food Eng. 135, 31–38.

Crumpton, M., Rice, C.J., Atkinson, A., Taylor, G., Marangon, M., 2018. The effect of sucrose addition at dosage stage on the foam attributes of a bottle-fermented English sparkling wine. J.

Sci. Food Agric. 98, 1171–1178. https://doi.org/10.1002/jsfa.8570

Cubero, S., Aleixos, N., Moltó, E., Gómez-Sanchis, J., Blasco, J., 2011. Advances in Machine Vision Applications for Automatic Inspection and Quality Evaluation of Fruits and Vegetables. Food Bioprocess Technol. 4, 487–504. https://doi.org/10.1007/s11947-010-0411-8

Daelemans, S., Peeters, L., Hauser, B., Vandenplas, Y., 2018. Recent advances in understanding and managing infantile colic. F1000Research 7. https://doi.org/10.12688/f1000research.14940.1

Demartini, M., Pinna, C., Tonelli, F., Terzi, S., Sansone, C., Testa, C., 2018. Food industry digitalization: from challenges and trends to opportunities and solutions. IFAC-PapersOnLine 51, 1371–1378. https://doi.org/10.1016/j.ifacol.2018.08.337

Denso, 2024. COBOTTA [WWW Document]. URL https://www.densorobotics.com/products/collaborative/cobotta/

Derossi, A., Di Palma, E., Moses., J.A., Santhoshkumar, P., Caporizzi, R., Severini, C., 2023. Avenues for non-conventional robotics technology applications in the food industry. Food Res. Int. 173. https://doi.org/10.1016/j.foodres.2023.113265

Ding, H., 2021. Image Processing Applications on Milk Powder Measurement. The University of Auckland.

Ding, H., Li, B., Boiarkina, I., Wilson, D.I., Yu, W., Young, B.R., 2020a. Effects of morphology on the bulk density of instant whole milk powder. Foods 9, 1–19. https://doi.org/10.3390/foods9081024

Ding, H., Wilson, D.I., Yu, W., Young, B.R., 2021. An investigation of the relative impact of process and shape factor variables on milk powder quality. Food Bioprod. Process. 126, 62–72. https://doi.org/10.1016/j.fbp.2020.12.010

Ding, H., Yu, W., Boiarkina, I., Depree, N., Young, B.R., 2020b. Effects of morphology on the dispersibility of instant whole milk powder. J. Food Eng. 276, 109841.

https://doi.org/10.1016/j.jfoodeng.2019.109841

DOOSAN, 2024. E0509 [WWW Document]. URL https://manual.doosanrobotics.com/en/user/2.10.3/3.-E-Series/e0509

Duan, Q., Jiang, S., Chen, F., Li, Z., Ma, L., Song, Y., Yu, X., Chen, Y., Liu, H., Yu, L., 2023. Fabrication, evaluation methodologies and models of slow-release fertilizers: A review. Ind. Crops Prod. 192, 116075. https://doi.org/https://doi.org/10.1016/j.indcrop.2022.116075

Duong, L.N.K., Al-Fadhli, M., Jagtap, S., Bader, F., Martindale, W., Swainson, M., Paoli, A., 2020. A review of robotics and autonomous systems in the food industry: From the supply chains perspective. Trends Food Sci. Technol. 106, 355–364. https://doi.org/10.1016/j.tifs.2020.10.028

Ernesti, J., Righetti, L., Do, M., Asfour, T., Schaal, S., 2012. Encoding of periodic and their transient motions by a single dynamic movement primitive. IEEE-RAS Int. Conf. Humanoid Robot. 57–64. https://doi.org/10.1109/HUMANOIDS.2012.6651499

Estolatan, E., Geuna, A., 2019. Looking forward via the Past: An Investigation of the Evolution of the Knowledge Base of Robotics Firms.

EUR-Lex, 2016. Commission Delegated Regulation (EU) 2016/127 [WWW Document]. EUR-Lex. URL https://eur-lex.europa.eu/legal-content/EN/TXT/PDF/?uri=CELEX:02016R0127-20190612&from=EN

Ewert, J., Claaßen, W., Glück, C., Zeeb, B., Weiss, J., Hinrichs, J., Stressler, T., Fischer, L., 2016. A non-invasive method for the characterisation of milk protein foams by image analysis. Int. Dairy J. 62, 1–9. https://doi.org/10.1016/j.idairyj.2016.06.012

Fang, Y., Selomulya, C., Ainsworth, S., Palmer, M., Chen, X.D., 2011. On quantifying the dissolution behaviour of milk protein concentrate. Food Hydrocoll. 25, 503–510. https://doi.org/10.1016/j.foodhyd.2010.07.030

Fang, Y., Selomulya, C., Chen, X.D., 2008. On Measurement of food powder reconstitution

properties. Dry. Technol. 26, 3–14. https://doi.org/10.1080/07373930701780928

FANUC, 2023. CRX-5iA [WWW Document]. URL https://crx.fanuc.eu/wp-content/uploads/2023/12/MDS-04892-EN.20231215110957254.pdf

Farrent, S., Coppin, B., Morris, S., 2021. Call for infant formula reconstitution uniformity and improvements in manufacturer feeding guides. Med. J. Aust. 214, 107-110.e1. https://doi.org/10.5694/mja2.50760

Farrera-Rebollo, R.R., de la Salgado-Cruz, M.P., Chanona-Pérez, J., Gutiérrez-López, G.F., Alamilla-Beltrán, L., Calderón-Domínguez, G., 2012. Evaluation of Image Analysis Tools for Characterization of Sweet Bread Crumb Structure. Food Bioprocess Technol. 5, 474–484. https://doi.org/10.1007/s11947-011-0513-y

FDA, 2024. Handling Infant Formula Safely: What You Need to Know [WWW Document]. FDA. URL https://www.fda.gov/food/buy-store-serve-safe-food/handling-infant-formula-safely-what-you-need-know

Fechner, G.T., Boring, E.G., Howes, D.H., 1966. Elements of psychophysics. New York, Holt, Rinehart and Winston.

Fein, S.B., Falci, C.D., 1999. Infant Formula Preparation, Handling, and Related Practices in the United States. J. Am. Diet. Assoc. 99, 1234–1240. https://doi.org/10.1016/S0002-8223(99)00304-1

Felfoul, I., Burgain, J., Perroud, C., Gaiani, C., Scher, J., Attia, H., Petit, J., 2020. Impact of spray-drying conditions on physicochemical properties and rehydration ability of skim dromedary and cow's milk powders. https://doi.org/10.1080/07373937.2020.1828448 40, 665–677. https://doi.org/10.1080/07373937.2020.1828448

Fermier, A.M., Troisi, J., Heritage, E.C., Drexel, M.A., Gallea, P., Swinney, K.A., 2003. Powder dispensing robot for sample preparation. Analyst 128, 790–795. https://doi.org/10.1039/b300274h

Fernando, Y., Mathath, A., Murshid, M.A., 2016. Improving Productivity: A Review of Robotic Applications in Food Industry. Int. J. Robot. Appl. Technol. 4, 43–62. https://doi.org/10.4018/ijrat.2016010103

Finnegan, E.W., Mahomud, M.S., Murphy, E.G., O'Mahony, J.A., 2021. The influence of pre-heat treatment of skim milk on key quality attributes of fat filled milk powder made therefrom. Int. J. Dairy Technol. 74, 404–413. https://doi.org/10.1111/1471-0307.12758

Fitzpatrick, J.J., Ahrné, L., 2005. Food powder handling and processing : Industry problems , knowledge barriers and research opportunities. Chem. Eng. Process. Process Intensif. 44, 209–214. https://doi.org/10.1016/j.cep.2004.03.014

Fitzpatrick, J.J., Salmon, J., Ji, J., Miao, S., 2017. Characterisation of the wetting behaviour of poor wetting food powders and the influence of temperature and film formation. KONA Powder Part. J. 2017, 282–289. https://doi.org/10.14356/kona.2017019

Fitzpatrick, J.J., van Lauwe, A., Coursol, M., O'Brien, A., Fitzpatrick, K.L., Ji, J., Miao, S., 2016. Investigation of the rehydration behaviour of food powders by comparing the behaviour of twelve powders with different properties. Powder Technol. 297, 340–348. https://doi.org/10.1016/j.powtec.2016.04.036

Forny, L., Marabi, A., Palzer, S., 2011. Wetting, disintegration and dissolution of agglomerated water soluble powders. Powder Technol. 206, 72–78. https://doi.org/10.1016/j.powtec.2010.07.022

FreeCAD, 2022. FreeCAD Project.

Freudig, B., Hogekamp, S., Schubert, H., 1999. Dispersion of powders in liquids in a stirred vessel. Chem. Eng. Process. Process Intensif. 38, 525–532. https://doi.org/10.1016/S0255-2701(99)00049-5

Fu, X., Huck, D., Makein, L., Armstrong, B., Willen, U., Freeman, T., 2012. Effect of particle shape and size on flow properties of lactose powders. Particuology 10, 203–208.

https://doi.org/10.1016/j.partic.2011.11.003

Gaiani, C., Banon, S., Scher, J., Schuck, P., Hardy, J., 2005. Use of a turbidity sensor to characterize micellar casein powder rehydration: Influence of some technological effects. J. Dairy Sci. 88, 2700–2706. https://doi.org/10.3168/jds.S0022-0302(05)72948-9

Gaiani, C., Boyanova, P., Hussain, R., Murrieta Pazos, I., Karam, M.C., Burgain, J., Scher, J., 2011. Morphological descriptors and colour as a tool to better understand rehydration properties of dairy powders. Int. Dairy J. 21, 462–469. https://doi.org/10.1016/j.idairyj.2011.02.009

Gaiani, C., Schuck, P., Scher, J., Desobry, S., Banon, S., 2007. Dairy powder rehydration: Influence of protein state, incorporation mode, and agglomeration. J. Dairy Sci. 90, 570–581. https://doi.org/10.3168/jds.S0022-0302(07)71540-0

Galet, L., Vu, T.-O., Oulahna, D., Fages, J., 2004. The wetting behaviour and dispersion rate of cocoa powder in water. Food Bioprod. Process. 82, 298–303.

GEA, 2009. GEA Niro Method No. A 5 b: Wettability IDF Method [WWW Document]. URL https://www.gea.com/fr/binaries/A 5 b - Wettability IDF Method_tcm29-30910.pdf

GEA, 2006a. GEA Niro Method No. A 1 a: Powder Moisture Accurate Standard Method [WWW Document]. URL https://www.gea.com/en/binaries/A 1 a - Powder Moisture Accurate Standard Method_tcm11-30900.pdf

GEA, 2006b. GEA Niro Method No. A 11 a: Particle Density, Occluded Air and Interstitial Air by Air Pycnometer [WWW Document]. URL https://www.gea.com/en/binaries/A 11 a - Particle Density%2C Occluded Air and Interstitial Air by Air Pycnometer_tcm11-30919.pdf

GEA, 2006c. GEA Niro Method No. A 2 b: Powder Bulk Volume [WWW Document]. URL https://www.gea.com/en/binaries/A 2 b - Powder Bulk Volume_tcm11-30906.pdf

GEA, 2006d. GEA Niro Method No. A 3 a: Insolubility Index [WWW Document]. URL https://www.gea.com/en/binaries/A 3 a - Insolubility Index_tcm11-30907.pdf

GEA, 2006e. GEA Niro Method No. A 4 a: Scorched Particles [WWW Document]. URL

https://www.gea.com/en/binaries/A 4 a - Scorched Particles_tcm11-30908.pdf

GEA, 2005a. GEA Niro Method No. A 6 a: Powder Dispersibility IDF Method [WWW Document]. URL https://www.gea.com/en/binaries/A 6 a - Powder Dispersibility IDF Method_tcm11-30911.pdf

GEA, 2005b. GEA Niro Method No. A 10 a: Surface Free Fat of Powder [WWW Document]. URL https://www.gea.com/en/binaries/A 10 a_Surface Free Fat of Powder_tcm11-30918.pdf

GEA, 2005c. GEA Niro Method No. A 7 a: Slowly Dispersible Particles in Agglomerated Milk Powder [WWW Document]. URL https://www.gea.com/en/binaries/A 7 a - Slowly Dispersible Particles in Agglomerated Milk Powder_tcm11-30912.pdf

Gonzalez Viejo, C., Fuentes, S., Li, G.J., Collmann, R., Condé, B., Torrico, D., 2016. Development of a robotic pourer constructed with ubiquitous materials, open hardware and sensors to assess beer foam quality using computer vision and pattern recognition algorithms: RoboBEER. Food Res. Int. 89, 504–513. https://doi.org/10.1016/j.foodres.2016.08.045

Gonzalez Viejo, C., Fuentes, S., Torrico, D., Howell, K., Dunshea, F.R., 2018. Assessment of beer quality based on foamability and chemical composition using computer vision algorithms, near infrared spectroscopy and machine learning algorithms. J. Sci. Food Agric. 98, 618–627. https://doi.org/10.1002/jsfa.8506

Grant, A., Jones, S., Sibson, V., Ellis, R., Dolling, A., McNamara, T., Cooper, J., Dvorak, S., Breward, S., Buchanan, P., Yhnell, E., Brown, A., 2024. The safety of at home powdered infant formula preparation: A community science project. Matern. Child Nutr. 20. https://doi.org/10.1111/mcn.13567

Gribble, K., Berry, N., Kerac, M., Challinor, M., 2017. Volume marker inaccuracies: A cross-sectional survey of infant feeding bottles. Matern. Child Nutr. 13, 1–7. https://doi.org/10.1111/mcn.12388

Han, J., Fitzpatrick, J., Cronin, K., Maidannyk, V., Miao, S., 2022. Investigation of breakage

behavior and its effects on spray-dried agglomerated whey protein-lactose powders: Effect of protein and lactose contents. J. Dairy Sci. 105, 8750–8764. https://doi.org/10.3168/jds.2021-21452

Han, J., Fitzpatrick, J., Cronin, K., Maidannyk, V., Miao, S., 2021. Particle size, powder properties and the breakage behaviour of infant milk formula. J. Food Eng. 292, 110367. https://doi.org/10.1016/j.jfoodeng.2020.110367

Hanspal, N., Chai, N., Allen, B., Brown, D., 2020. Applying multiple approaches to deepen understanding of mixing and mass transfer in large-scale aerobic fermentations. J. Ind. Microbiol. Biotechnol. 47, 929–946. https://doi.org/10.1007/s10295-020-02307-2

Hardy, J., Scher, J., Banon, S., 2002. Water activity and hydration of dairy powders. Lait 82, 441–452. https://doi.org/10.1051/lait:2002022

Harris, C.R., Millman, K.J., van der Walt, S.J., Gommers, R., Virtanen, P., Cournapeau, D., Wieser, E., Taylor, J., Berg, S., Smith, N.J., Kern, R., Picus, M., Hoyer, S., van Kerkwijk, M.H., Brett, M., Haldane, A., del Río, J.F., Wiebe, M., Peterson, P., Gérard-Marchant, P., Sheppard, K., Reddy, T., Weckesser, W., Abbasi, H., Gohlke, C., Oliphant, T.E., 2020. Array programming with NumPy. Nature 585, 357–362. https://doi.org/10.1038/s41586-020-2649-2

Harthikote Nagaraja, V., 2019. Motion Capture and Musculoskeletal Simulation Tools to Measure Prosthetic Arm Functionality.

Hauke, J., Kossowski, T., 2011. Comparison of values of pearson's and spearman's correlation coefficients on the same sets of data. Quaest. Geogr. 30, 87–93. https://doi.org/10.2478/v10117-011-0021-1

Hazlett, R., Schmidmeier, C., O'Mahony, J.A., 2021. Approaches for improving the flowability of high-protein dairy powders post spray drying – A review. Powder Technol. 388, 26–40. https://doi.org/10.1016/j.powtec.2021.03.021

Henihan, L.E., O'Donnell, C.P., Esquerre, C., Murphy, E.G., O'Callaghan, D.J., 2019.

Fluorescence-based analyser as a rapid tool for determining soluble protein content in dairy ingredients and infant milk formula. Innov. Food Sci. Emerg. Technol. 52, 75–79. https://doi.org/10.1016/j.ifset.2018.11.014

Henihan, L.E., O'Donnell, C.P., Esquerre, C., Murphy, E.G., O'Callaghan, D.J., 2018. Quality Assurance of Model Infant Milk Formula Using a Front-Face Fluorescence Process Analytical Tool. Food Bioprocess Technol. 11, 1402–1411. https://doi.org/10.1007/s11947-018-2112-7

Hentout, A., Aouache, M., Maoudj, A., Akli, I., 2019. Human–robot interaction in industrial collaborative robotics: a literature review of the decade 2008–2017. Adv. Robot. 33, 764–799. https://doi.org/10.1080/01691864.2019.1636714

Ho, T.M., Bhandari, B.R., Bansal, N., 2021. Functionality of bovine milk proteins and other factors in foaming properties of milk: a review. Crit. Rev. Food Sci. Nutr. 0, 1–21. https://doi.org/10.1080/10408398.2021.1879002

Hogekamp, S., Schubert, H., 2003. Rehydration of food powders. Food Sci. Technol. Int. 9, 223–235. https://doi.org/10.1177/1082013203034938

Hong, J., Zhang, Z., Enayati, A.M.S., Najjaran, H., 2023. Human-Robot Skill Transfer with Enhanced Compliance via Dynamic Movement Primitives. arXiv Prepr. arXiv2304.05703.

Hörmann, T., Suzzi, D., Khinast, J.G., 2011. Mixing and dissolution processes of pharmaceutical bulk materials in stirred tanks: Experimental and numerical investigations. Ind. Eng. Chem. Res. 50, 12011–12025. https://doi.org/10.1021/ie2002523

Huang, Y., Abu-Dakka, F.J., Silverio, J., Caldwell, D.G., 2021. Toward Orientation Learning and Adaptation in Cartesian Space. IEEE Trans. Robot. 37, 82–98. https://doi.org/10.1109/TRO.2020.3010633

Huang, Y., Kangas, L.J., Rasco, B.A., 2007. Applications of Artificial Neural Networks (ANNs) in food science. Crit. Rev. Food Sci. Nutr. 47, 113–126. https://doi.org/10.1080/10408390600626453

Hunter, J.D., 2007. Matplotlib: A 2D graphics environment. Comput. Sci. \& Eng. 9, 90–95. https://doi.org/10.1109/MCSE.2007.55

Huppertz, T., 2010. Foaming properties of milk: A review of the influence of composition and processing. Int. J. Dairy Technol. 63, 477–488. https://doi.org/10.1111/j.1471-0307.2010.00629.x

Ijspeert, A.J., Nakanishi, J., Schaal, S., 2002a. Learning rhythmic movements by demonstration using nonlinear oscillators. IEEE Int. Conf. Intell. Robot. Syst. 1, 958–963. https://doi.org/10.1109/irds.2002.1041514

Ijspeert, A.J., Nakanishi, J., Schaal, S., 2002b. Movement imitation with nonlinear dynamical systems in humanoid robots, in: Proceedings 2002 IEEE International Conference on Robotics and Automation (Cat. No. 02CH37292). pp. 1398–1403.

Iqbal, J., Islam, R.U., Abbas, S.Z., Khan, A.A., Ajwad, S.A., 2016. Automatzacija industrijskih poslova kroz mehatronicke sustave - Pregled robotike iz industrijske perspektive. Teh. Vjesn. 23, 917–924. https://doi.org/10.17559/TV-20140724220401

Jeantet, R., Schuck, P., Six, T., Andre, C., Delaplace, G., 2010. The influence of stirring speed, temperature and solid concentration on the rehydration time of micellar casein powder. Dairy Sci. Technol. 90, 225–236. https://doi.org/10.1051/dst/2009043

Jensen, G.W., der Smagt, P., Heiss, E., Straka, H., Kohl, T., 2020. Snakestrike: A low-cost open-source high-speed multi-camera motion capture system. Front. Behav. Neurosci. 14, 116.

Ji, J., Fitzpatrick, J., Cronin, K., Crean, A., Miao, S., 2016a. Assessment of measurement characteristics for rehydration of milk protein based powders. Food Hydrocoll. 54, 151–161. https://doi.org/10.1016/j.foodhyd.2015.09.027

Ji, J., Fitzpatrick, J., Cronin, K., Maguire, P., Zhang, H., Miao, S., 2016b. Rehydration behaviours of high protein dairy powders: The influence of agglomeration on wettability, dispersibility and solubility. Food Hydrocoll. 58, 194–203. https://doi.org/10.1016/j.foodhyd.2016.02.030

Kadalagere Sampath, S., Wang, N., Wu, H., Yang, C., 2023. Review on human-like robot manipulation using dexterous hands. Cogn. Comput. Syst. 5, 14–29. https://doi.org/10.1049/ccs2.12073

Kelly, A.L., O'connell, J.E., Fox, P.F., 2003. Manufacture and properties of milk powders, in: Advanced Dairy Chemistry—1 Proteins: Part A/Part B. Springer, pp. 1027–1061.

Kelly, James, Kelly, P.M., Harrington, D., 2002. Influence of processing variables on the physicochemical properties of spray dried fat-based milk powders. Lait.

Khadka, P., Ro, J., Kim, Hyeongmin, Kim, I., Kim, J.T., Kim, Hyunil, Cho, J.M., Yun, G., Lee, J., 2014. Pharmaceutical particle technologies: An approach to improve drug solubility, dissolution and bioavailability. Asian J. Pharm. Sci. 9, 304–316.

Khan, A., Munir, M.T., Yu, W., Young, B.R., 2020. A Review Towards Hyperspectral Imaging for Real-Time Quality Control of Food Products with an Illustrative Case Study of Milk Powder Production. Food Bioprocess Technol. 739–752. https://doi.org/10.1007/s11947-020-02433-w

Khan, Z.H., Khalid, A., Iqbal, J., 2018. Towards realizing robotic potential in future intelligent food manufacturing systems. Innov. Food Sci. Emerg. Technol. 48, 11–24. https://doi.org/10.1016/j.ifset.2018.05.011

Kim, E.H.-J., Chen, X.D., Pearce, D., 2009. Surface composition of industrial spray-dried milk powders. 2. Effects of spray drying conditions on the surface composition. J. Food Eng. 94, 169–181.

Kim, E.H.-J., Chen, X.D., Pearce, D., 2002. Surface characterization of four industrial spray-dried dairy powders in relation to chemical composition, structure and wetting property. Colloids Surfaces B Biointerfaces 26, 197–212. https://doi.org/10.1016/s0927-7765(01)00334-4

Kim, E.H.J., Xiao, D.C., Pearce, D., 2005. Effect of surface composition on the flowability of industrial spray-dried dairy powders. Colloids Surfaces B Biointerfaces 46, 182–187. https://doi.org/10.1016/j.colsurfb.2005.11.005

Kim, S., Cheikhali, M., Davé, R.N., 2022. Decoding Fine API Agglomeration as a Key Indicator of Powder Flowability and Dissolution: Impact of Particle Engineering. Pharm. Res. 39, 3079–3098. https://doi.org/10.1007/s11095-022-03293-z

King, N., 1966. Dispersibility and reconstitutability of dried milk.

Klerkx, L., Rose, D., 2020. Dealing with the game-changing technologies of Agriculture 4.0: How do we manage diversity and responsibility in food system transition pathways? Glob. Food Sec. 24, 100347. https://doi.org/10.1016/j.gfs.2019.100347

Ko, W.K.H., Wu, Y., Tee, K.P., Buchli, J., 2015. Towards industrial robot learning from demonstration. HAI 2015 - Proc. 3rd Int. Conf. Human-Agent Interact. 235–238. https://doi.org/10.1145/2814940.2814984

KUKA, 2022. LBR iisy 3 R760 [WWW Document]. URL https://www.kuka.com/-/media/kuka-downloads/imported/8350ff3ca11642998dbdc81dcc2ed44c/0000320854_en.pdf

Kulak, T., Silvério, J., Calinon, S., 2020. Fourier movement primitives: an approach for learning rhythmic robot skills from demonstrations. Robot. Sci. Syst. https://doi.org/10.15607/RSS.2020.XVI.056

Kulak, T.A., 2021. Learning strategies and representations for intuitive robot learning from demonstration.

Kumar, R.A., Summaiya, Santanumal, James, A.C., 2018. Mixing Technologies in the Pharmaceutical Industries. J. Emerg. Technol. Innov. Res. 5, 606–609.

Kyrarini, M., Haseeb, M.A., Ristić-Durrant, D., Gräser, A., 2019. Robot learning of industrial assembly task via human demonstrations. Auton. Robots 43, 239–257. https://doi.org/10.1007/s10514-018-9725-6

Le Roux, L., Mejean, S., Chacon, R., Lopez, C., Dupont, D., Deglaire, A., Nau, F., Jeantet, R., 2020. Plant proteins partially replacing dairy proteins greatly influence infant formula functionalities. Lwt 120, 108891. https://doi.org/10.1016/j.lwt.2019.108891

Leidenkrantz, A., Westbrandt, E., 2019. Implementation Of Machine Vision On A Collaborative Robot.

Lezoche, M., Panetto, H., Kacprzyk, J., Hernandez, J.E., Alemany Díaz, M.M.E., 2020. Agri-food 4.0: A survey of the Supply Chains and Technologies for the Future Agriculture. Comput. Ind. 117. https://doi.org/10.1016/j.compind.2020.103187

Lillienskiold, A., Rahal, R., Giordano, P.R., Pacchierotti, C., Misimi, E., 2022. Human-Inspired Haptic-Enabled Learning from Prehensile Move Demonstrations. IEEE Trans. Syst. Man, Cybern. Syst. 52, 2061–2072. https://doi.org/10.1109/TSMC.2020.3046775

Liu, L., Guo, F., Zou, Z., Duffy, V.G., 2022. Application, Development and Future Opportunities of Collaborative Robots (Cobots) in Manufacturing: A Literature Review. Int. J. Hum. Comput. Interact. 0, 1–18. https://doi.org/10.1080/10447318.2022.2041907

Liu, Y., Gupta, A., Abbeel, P., Levine, S., 2018. Imitation from Observation: Learning to Imitate Behaviors from Raw Video via Context Translation. Proc. - IEEE Int. Conf. Robot. Autom. 1118–1125. https://doi.org/10.1109/ICRA.2018.8462901

Liu, Z., Liu, Q., Xu, W., Wang, L., Zhou, Z., 2022. Robot learning towards smart robotic manufacturing: A review. Robot. Comput. Integr. Manuf. 77, 102360. https://doi.org/10.1016/j.rcim.2022.102360

Lloyd, R., Stewart, H., Bailey, D., 2019. Slowly dissolving particles in instant whole milk powder – Characterisation and quantitative analysis. Int. Dairy J. 97, 65–70. https://doi.org/10.1016/j.idairyj.2019.05.015

M&M, 2023. Collaborative Robot Market [WWW Document]. URL https://www.marketsandmarkets.com/Market-Reports/collaborative-robot-market-194541294.html

Ma, J., Sun, D.W., Qu, J.H., Liu, D., Pu, H., Gao, W.H., Zeng, X.A., 2016. Applications of Computer Vision for Assessing Quality of Agri-food Products: A Review of Recent Research

Advances. Crit. Rev. Food Sci. Nutr. 56, 113–127. https://doi.org/10.1080/10408398.2013.873885

Martin, C.R., Ling, P.R., Blackburn, G.L., 2016. Review of infant feeding: Key features of breast milk and infant formula. Nutrients 8, 1–11. https://doi.org/10.3390/nu8050279

Masum, A.K.M., Chandrapala, J., Huppertz, T., Adhikari, B., Zisu, B., 2020. Production and characterization of infant milk formula powders: A review. Dry. Technol. 0, 1–21. https://doi.org/10.1080/07373937.2020.1767645

Mc Carthy, U., Uysal, I., Badia-Melis, R., Mercier, S., O'Donnell, C., Ktenioudaki, A., 2018. Global food security – Issues, challenges and technological solutions. Trends Food Sci. Technol. 77, 11–20. https://doi.org/10.1016/j.tifs.2018.05.002

McCarthy, N.A., Kelly, P.M., Maher, P.G., Fenelon, M.A., 2014. Dissolution of milk protein concentrate (MPC) powders by ultrasonication. J. Food Eng. 126, 142–148. https://doi.org/10.1016/j.jfoodeng.2013.11.002

McSweeney, D.J., Maidannyk, V., O'Mahony, J.A., McCarthy, N.A., 2021. Rehydration properties of regular and agglomerated milk protein concentrate powders produced using nitrogen gas injection prior to spray drying. J. Food Eng. 305, 110597. https://doi.org/10.1016/j.jfoodeng.2021.110597

Meenu, M., Kurade, C., Neelapu, B.C., Kalra, S., Ramaswamy, H.S., Yu, Y., 2021. A concise review on food quality assessment using digital image processing. Trends Food Sci. Technol. 118, 106–124. https://doi.org/10.1016/j.tifs.2021.09.014

Mercan, E., Sert, D., Akın, N., 2018. Effect of high-pressure homogenisation on viscosity, particle size and microbiological characteristics of skim and whole milk concentrates. Int. Dairy J. 87, 93–99. https://doi.org/10.1016/j.idairyj.2018.07.017

Mery, D., Pedreschi, F., Soto, A., 2013. Automated Design of a Computer Vision System for Visual Food Quality Evaluation. Food Bioprocess Technol. 6, 2093–2108.

https://doi.org/10.1007/s11947-012-0934-2

Mimouni, A., Deeth, H.C., Whittaker, A.K., Gidley, M.J., Bhandari, B.R., 2009. Rehydration process of milk protein concentrate powder monitored by static light scattering. Food Hydrocoll. 23, 1958–1965. https://doi.org/10.1016/j.foodhyd.2009.01.010

Misimi, E., Olofsson, A., Eilertsen, A., Øye, E.R., Mathiassen, J.R., 2018. Robotic Handling of Compliant Food Objects by Robust Learning from Demonstration. IEEE Int. Conf. Intell. Robot. Syst. 6972–6979. https://doi.org/10.1109/IROS.2018.8594368

Mitchell, W.R., Forny, L., Althaus, T., Niederreiter, G., Palzer, S., Hounslow, M.J., Salman, A.D., 2020. Tracking of powder lump formation and dispersion with the use of FBRM technology and video recordings. Powder Technol. 367, 10–19. https://doi.org/10.1016/j.powtec.2020.03.035

Mitchell, W.R., Forny, L., Althaus, T.O., Niederreiter, G., Palzer, S., Hounslow, M.J., Salman, A.D., 2015. Mapping the rate-limiting regimes of food powder reconstitution in a standard mixing vessel. Powder Technol. 270, 520–527. https://doi.org/10.1016/j.powtec.2014.08.014

MOH, 2022. Feeding your baby infant formula - How to prepare infant formula safely. New Zealand Government.

Morelle, E., Rudolph, A., McHardy, C., Rauh, C., 2021. Detection and prediction of foam evolution during the bottling of noncarbonated beverages using artificial neural networks. Food Bioprod. Process. 128, 63–76. https://doi.org/10.1016/j.fbp.2021.03.017

Mozafari, B., O'Shea, N., Fenelon, M., Villing, R., 2022. Towards Image Processing-based Quantification of White Particles in Reconstituted Infant Formula. 2022 33rd Irish Signals Syst. Conf. ISSC 2022 2–7. https://doi.org/10.1109/ISSC55427.2022.9826210

Mozafari, B., Shea, N.O., Fenelon, M., Li, R., Daly, D.F.M., 2024. An automated platform for measuring infant formula powder rehydration quality using a collaborative robot integrated with computer vision. J. Food Eng. 383, 112229.

https://doi.org/10.1016/j.jfoodeng.2024.112229

Muhuri, P.K., Shukla, A.K., Abraham, A., 2019. Industry 4.0: A bibliometric analysis and detailed overview. Eng. Appl. Artif. Intell. 78, 218–235. https://doi.org/10.1016/j.engappai.2018.11.007

Müller, M., Kuhlenkötter, B., Nassmacher, R., 2014. Robots in food industry challenges and chances. Proc. Jt. Conf. ISR 2014 - 45th Int. Symp. Robot. Robot. 2014 - 8th Ger. Conf. Robot. ISR/ROBOTIK 2014 232–238.

Münchow, M., Jørgensen, L., Amigo, J.M., Sørensen, K., Ipsen, R., 2015. Steam-frothing of milk for coffee: Evaluation for foam properties using video analysis and feature extraction. Int. Dairy J. 51, 84–91. https://doi.org/10.1016/j.idairyj.2015.07.009

Munir, M.T., Wilson, D.I., Depree, N., Boiarkina, I., Prince-Pike, A., Young, B.R., 2017. Real-time product release and process control challenges in the dairy milk powder industry. Curr. Opin. Food Sci. 17, 25–29. https://doi.org/10.1016/j.cofs.2017.08.005

Munir, M.T., Wilson, D.I., Yu, W., Young, B.R., 2018. An evaluation of hyperspectral imaging for characterising milk powders. J. Food Eng. 221, 1–10. https://doi.org/10.1016/j.jfoodeng.2017.10.001

Murphy, E.G., Regost, N.E., Roos, Y.H., Fenelon, M.A., 2020. Powder and reconstituted properties of commercial infant and follow-on formulas. Foods 9, 1–17. https://doi.org/10.3390/foods9010084

National Academies Press, C. on the E. of the A. of I.N. to I.F., 2004. Infant formula: evaluating the safety of new ingredients. National Academies Press.

Nelson, R.D., 2012. Dispersing powders in liquids. Elsevier.

Nijdam, J.J., Langrish, T.A.G., 2006. The effect of surface composition on the functional properties of milk powders. J. Food Eng. 77, 919–925. https://doi.org/10.1016/j.jfoodeng.2005.08.020

Novak, P., Postulkova, M., Ruzicka, M.C., Branyik, T., 2015. Novel desaturation cell to quantify

gushing intensity: A preliminary study on model solutions. J. Am. Soc. Brew. Chem. 73, 185–189. https://doi.org/10.1094/ASBCJ-2015-0404-01

Nugroho, R.W.N., Outinen, M., Toikkanen, O., Rojas, O.J., 2021. Particle size and fat encapsulation define the colloidal dispersibility and reconstitution of growing-up milk powder. Powder Technol. 391, 133–141. https://doi.org/10.1016/j.powtec.2021.06.008

Nyarko, E.K., Glavaš, H., Habschied, K., Mastanjević, K., 2021. Determination of foam stability in lager beers using digital image analysis of images obtained using rgb and 3d cameras. Fermentation 7. https://doi.org/10.3390/fermentation7020046

O'Donoghue, L.T., Haque, M.K., Kennedy, D., Laffir, F.R., Hogan, S.A., O'Mahony, J.A., Murphy, E.G., 2019. Influence of particle size on the physicochemical properties and stickiness of dairy powders. Int. Dairy J. 98, 54–63. https://doi.org/10.1016/j.idairyj.2019.07.002

O'Mahony, N., Campbell, S., Carvalho, A., Harapanahalli, S., Hernandez, G.V., Krpalkova, L., Riordan, D., Walsh, J., 2019. Deep Learning vs. Traditional Computer Vision, in: Science and Information Conference. pp. 128–144. https://doi.org/10.1007/978-3-030-17795-9_10

O'Shea, N., Kennedy, D., Tobin, J.T., Fenelon, M.A., 2021. Reconstituting infant formula powder using a collaborative robot 'CoBoT' to mimic human biomechanical movements. Innov. Food Sci. Emerg. Technol. 67, 102562. https://doi.org/10.1016/j.ifset.2020.102562

Olson, E., 2011. AprilTag: A robust and flexible visual fiducial system, in: 2011 IEEE International Conference on Robotics and Automation. pp. 3400–3407.

Otto, S.A., 2019. How to normalize the RMSE [WWW Document]. URL https://www.marinedatascience.co/blog/2019/01/07/normalizing-the-rmse/

Panckow, R.P., McHardy, C., Rudolph, A., Muthig, M., Kostova, J., Wegener, M., Rauh, C., 2021. Characterization of fast-growing foams in bottling processes by endoscopic imaging and convolutional neural networks. J. Food Eng. 289, 110151.

https://doi.org/10.1016/j.jfoodeng.2020.110151

Paraschos, A., Daniel, C., Peters, J., Neumann, G., 2018. Using probabilistic movement primitives in robotics. Auton. Robots 42, 529–551. https://doi.org/10.1007/s10514-017-9648-7

Paraschos, A., Daniel, C., Peters, J., Neumann, G., 2013. Probabilistic movement primitives. Adv. Neural Inf. Process. Syst. 1–9.

Parthasarathi, S., Anandharamakrishnan, C., 2014. Modeling of shrinkage, rehydration and textural changes for food structural analysis: A review. J. Food Process Eng. 37, 199–210. https://doi.org/10.1111/jfpe.12073

Patel, K.K., Kar, A., Jha, S.N., Khan, M.A., 2012. Machine vision system: A tool for quality inspection of food and agricultural products. J. Food Sci. Technol. 49, 123–141. https://doi.org/10.1007/s13197-011-0321-4

Pedersen, L.D., 1991. Assessment of sensors used in the food industry. Food Control 2, 87–98. https://doi.org/10.1016/0956-7135(91)90144-L

Pedregosa, F., Varoquaux, G., Gramfort, A., Michel, V., Thirion, B., Grisel, O., Blondel, M., Prettenhofer, P., Weiss, R., Dubourg, V., Vanderplas, J., Passos, A., Cournapeau, D., Brucher, M., Perrot, M., Duchesnay, E., 2011. Scikit-learn: Machine Learning in Python. J. Mach. Learn. Res. 12, 2825–2830.

Pirisino, J.F., 1983. High Performance Liquid Chromatographic Determination of Lactose, Glucose, and Galactose in Lactose-Reduced Milk. J. Food Sci. 48, 742–744. https://doi.org/10.1111/j.1365-2621.1983.tb14887.x

Pisecky, J., 2012. Second Edition Handbook of Milk Powder Manufacture.

PR, 2023. Infant Formula Market [WWW Document]. Preced. Res. URL https://www.precedenceresearch.com/infant-formula-market

Prado, E.L., Dewey, K.G., 2014. Nutrition and brain development in early life. Nutr. Rev. 72, 267–284. https://doi.org/10.1111/nure.12102

Pugliese, A., Cabassi, G., Chiavaro, E., Paciulli, M., Carini, E., Mucchetti, G., 2017. Physical characterization of whole and skim dried milk powders. J. Food Sci. Technol. 54, 3433–3442. https://doi.org/10.1007/s13197-017-2795-1

Pupil Labs, 2022a. Pupil Labs [WWW Document]. URL https://github.com/pupil-labs/apriltags

Pupil Labs, 2022b. pupil-apriltags API Reference [WWW Document]. URL https://pupil-apriltags.readthedocs.io/en/stable/api.html

Quadro, 2015. Effective Powder Dispersion of Rheology Modifiers [WWW Document]. URL https://www.quadroliquids.com/blog/understanding-powder-dispersion-how-overcome-many-mixing-challenges

R Core Team, 2020. R: A Language and Environment for Statistical Computing.

Rahman, M.S., 2020. Handbook of food preservation. CRC press.

Rajendran, V., Debnath, B., Mghames, S., Mandil, W., Parsa, S., Parsons, S., Ghalamzan-E., A., 2023. Towards autonomous selective harvesting: A review of robot perception, robot design, motion planning and control. J. F. Robot. https://doi.org/10.1002/rob.22230

Ravichandar, H., Polydoros, A.S., Chernova, S., Billard, A., 2020. Recent Advances in Robot Learning from Demonstration. Annu. Rev. Control. Robot. Auton. Syst. 3, 297–330. https://doi.org/10.1146/annurev-control-100819-063206

Renfrew, M.J., Ansell, P., Macleod, K.L., 2003. Formula feed preparation: Helping reduce the risks; a systematic review. Arch. Dis. Child. 88, 855–858. https://doi.org/10.1136/adc.88.10.855

Richard, B., Le Page, J.F., Schuck, P., Andre, C., Jeantet, R., Delaplace, G., 2013. Towards a better control of dairy powder rehydration processes. Int. Dairy J. 31, 18–28. https://doi.org/10.1016/j.idairyj.2012.07.007

Rimpiläinen, V., Kaipio, J.P., Depree, N., Young, B.R., Wilson, D.I., 2015. Predicting functional properties of milk powder based on manufacturing data in an industrial-scale powder plant. J.

Food Eng. 153, 12–19. https://doi.org/10.1016/j.jfoodeng.2014.12.010

Rodriguez-Gonzalez, C.G., Herranz-Alonso, A., Escudero-Vilaplana, V., Ais-Larisgoitia, M.A., Iglesias-Peinado, I., Sanjurjo-Saez, M., 2019. Robotic dispensing improves patient safety, inventory management, and staff satisfaction in an outpatient hospital pharmacy. J. Eval. Clin. Pract. 25, 28–35. https://doi.org/10.1111/jep.13014

Rodríguez Arzuaga, M., Felix da Silva, D., Xanthakis, E., Aalaei, K., Czaja, T.P., Añón, M.C., Abraham, A.G., Ahrné, L., 2021. Impact of wet-mix total solids content and heat treatment on physicochemical and techno-functional properties of infant milk formula powders. Powder Technol. 390, 473–481. https://doi.org/10.1016/j.powtec.2021.05.093

Rosenkranz, R.R., Gonzalez-Alvarez, A., Acosta, C., Hooyman, A., Hidalgo, J.R., Ballesteros-Paniagua, C.R., Rosenkranz, S.K., 2024. Variability and error in measurement of infant formula powder and water: an experimental study. Front. Nutr. 11, 1–10. https://doi.org/10.3389/fnut.2024.1385496

RR, 2020. Sawyer [WWW Document]. URL https://www.rethinkrobotics.com/fileadmin/user_upload/brochure_en.pdf

Salazar-González, C.Y., Rodríguez-Pulido, F.J., Terrab, A., Díaz-Moreno, C., Fuenmayor, C.A., Heredia, F.J., 2018. Analysis of Multifloral Bee Pollen Pellets by Advanced Digital Imaging Applied to Functional Food Ingredients. Plant Foods Hum. Nutr. 73, 328–335. https://doi.org/10.1007/s11130-018-0695-9

Sane, Tanmay U., Sane, Tanuj U., 2021. Artificial Intelligence and Deep Learning Applications in Crop Harvesting Robots-A Survey. 3rd Int. Conf. Electr. Commun. Comput. Eng. ICECCE 2021 1–6. https://doi.org/10.1109/ICECCE52056.2021.9514232

Schaal, S., Kotosaka, S., Sternad, D., 2000. Nonlinear dynamical systems as movement primitives, in: IEEE International Conference on Humanoid Robotics. pp. 1–11.

Schmidmeier, C., O'Gorman, C., Drapala, K.P., Waldron, D.S., O'Mahony, J.A., 2019. Elucidation

of factors responsible for formation of white flecks in reconstituted fat filled milk powders. Colloids Surfaces A Physicochem. Eng. Asp. 575, 245–255. https://doi.org/10.1016/j.colsurfa.2019.03.034

Schneider, C.A., Rasband, W.S., Eliceiri, K.W., 2012. NIH Image to ImageJ: 25 years of image analysis. Nat. Methods 9, 671–675. https://doi.org/10.1038/nmeth.2089

Schober, C., Fitzpatrick, J.J., 2005. Effect of vortex formation on powder sinkability for reconstituting milk powders in water to high solids content in a stirred-tank. J. Food Eng. 71, 1–8. https://doi.org/10.1016/j.jfoodeng.2004.09.027

Schuck, P., Dolivet, A., Jeantet, R., 2012. Analytical Methods for Food and Dairy Powders. John Wiley & Sons, Ltd.

Schuck, P., Jeantet, R., Bhandari, B., Chen, X.D., Perrone, Í.T., Carvalho, A.F. de, Fenelon, M., Kelly, P., 2016. Recent advances in spray drying relevant to the dairy industry: A comprehensive critical review. Dry. Technol.

Schuck, P., Mejean, S., Dolivet, A., Gaiani, C., Banon, S., Schuck, P., Mejean, S., Dolivet, A., Gaiani, C., Banon, S., 2007. Water transfer during rehydration of micellar casein powders To cite this version : Short review Water transfer during rehydration of micellar. Lait 87, 425–432.

Selomulya, C., Fang, Y., Wang, Y., 2023. Food powder rehydration, Second Edi. ed, Handbook of Food Powders: Chemistry and Technology, Second Edition. Elsevier Ltd. https://doi.org/10.1016/B978-0-323-98820-9.00002-8

Serazetdinova, L., Garratt, J., Baylis, A., Stergiadis, S., Collison, M., Davis, S., 2019. How should we turn data into decisions in AgriFood? J. Sci. Food Agric. 99, 3213–3219. https://doi.org/10.1002/jsfa.9545

Seville, J.P., Tüzün, U., Clift, R., 2012. Processing of particulate solids. Springer Science \& Business Media.

Sharma, A., Atanu, H.J., Chavan, R.S., 2012. Functionality of milk powders and milk-based

powders for end use applications—a review. Compr. Rev. Food Sci. Food Saf. https://doi.org/10.1111/j.1541-4337.2012.00199.x

Siepmann, J., Siepmann, F., 2008. Mathematical modeling of drug delivery. Int. J. Pharm. 364, 328–343. https://doi.org/10.1016/j.ijpharm.2008.09.004

Skibsted, L.H., Risbo, J., Andersen, M.L., 2010. Chemical deterioration and physical instability of food and beverages. Elsevier.

Sunderland, R., Emery, J.L., 1979. Apparent disappearance of hypernatraemic dehydration from infant deaths in Sheffield. Br. Med. J. 2, 575–576. https://doi.org/10.1136/bmj.2.6190.575

Tai, Y.L., Chiu, Y.C., Chao, Y.W., Chen, Y.T., 2023. SCONE: A Food Scooping Robot Learning Framework with Active Perception. Proc. Mach. Learn. Res. 229.

Tamime, A.Y., 2009. Dairy Powders and Concentrated Products, Dairy Powders and Concentrated Products. https://doi.org/10.1002/9781444322729

Thompkinson, D.K., Kharb, S., 2007. Aspects of Infant Food Formulation. Compr. Rev. Food Sci. Food Saf. 6, 79–102.

TM, 2019. TM5.

Toikkanen, O., Outinen, M., Malafronte, L., Rojas, O.J., 2018. Formation and structure of insoluble particles in reconstituted model infant formula powders. Int. Dairy J. 82, 19–27. https://doi.org/10.1016/j.idairyj.2018.03.001

TP, 2016. 2 common powder mixing challenges - and how to solve them [WWW Document]. URL https://www.tetrapak.com/insights/cases-articles/common-powder-mixing-challenges

Uno, H., Tanaka, S., 1972. Adhesion of suspension particles on the wall surface of the container: II: Mechanism of particle adhesion. Kolloid-Zeitschrift und Zeitschrift für Polym. 250, 238–252. https://doi.org/10.1007/BF01507610

Uno, H., Tanaka, S., 1970. Adhesion of suspension particles on the wall surface of the container: I. Particle trapping and factors relating with adhesion. Kolloid-Zeitschrift und Zeitschrift für

Polym. 242, 1186–1195.

UR, 2015. UR3 [WWW Document]. URL https://www.universal-robots.com/media/240787/ur3_us.pdf

Vignolles, M.-L., Jeantet, R., Lopez, C., Schuck, P., 2007. Free fat, surface fat and dairy powders: interactions between process and product. A review. Lait 87, 187–236.

Villani, V., Pini, F., Leali, F., Secchi, C., 2018. Survey on human–robot collaboration in industrial settings: Safety, intuitive interfaces and applications. Mechatronics 55, 248–266. https://doi.org/10.1016/j.mechatronics.2018.02.009

Villanueva, D., Posada, R., González, I., García, Á., Martínez, A., 2015. Monitoring of a sugar crystallization process with fuzzy logic and digital image processing. J. Food Process Eng. 38, 19–30. https://doi.org/10.1111/jfpe.12122

Virtanen, P., Gommers, R., Oliphant, T.E., Haberland, M., Reddy, T., Cournapeau, D., Burovski, E., Peterson, P., Weckesser, W., Bright, J., van der Walt, S.J., Brett, M., Wilson, J., Millman, K.J., Mayorov, N., Nelson, A.R.J., Jones, E., Kern, R., Larson, E., Carey, C.J., Polat, \.Ilhan, Feng, Y., Moore, E.W., VanderPlas, J., Laxalde, D., Perktold, J., Cimrman, R., Henriksen, I., Quintero, E.A., Harris, C.R., Archibald, A.M., Ribeiro, A.H., Pedregosa, F., van Mulbregt, P., SciPy 1.0 Contributors, 2020. SciPy 1.0: Fundamental Algorithms for Scientific Computing in Python. Nat. Methods 17, 261–272. https://doi.org/10.1038/s41592-019-0686-2

Vogt, D., Stepputtis, S., Grehl, S., Jung, B., Ben Amor, H., 2017. A system for learning continuous human-robot interactions from human-human demonstrations. Proc. - IEEE Int. Conf. Robot. Autom. 2882–2889. https://doi.org/10.1109/ICRA.2017.7989334

Wadnerkar, D., Utikar, R.P., Tade, M.O., Pareek, V.K., 2012. CFD simulation of solid-liquid stirred tanks. Adv. Powder Technol. 23, 445–453. https://doi.org/10.1016/j.apt.2012.03.007

Wakchaure, Y.B., Patle, B.K., Pawar, S., 2023. Prospects of robotics in food processing: an overview. J. Mech. Eng. Autom. Control Syst. 4, 17–37.

https://doi.org/10.21595/jmeacs.2023.23209

Wallin, P.J., 1997. Robotics in the food industry: An update. Trends Food Sci. Technol. 8, 193–198. https://doi.org/10.1016/S0924-2244(97)01042-X

Wallin, P.J., 1995. Review of the use of robotics and opportunities in the food and drinks industry. Ind. Rob. 22, 9–11. https://doi.org/10.1108/01439919510104085

Walshe, E.J., O'Regan, J., O'Mahony, J.A., 2021. Influence of protein content and profile on the processing characteristics and physical properties of model infant formula powders. Int. J. Dairy Technol. 74, 592–599. https://doi.org/10.1111/1471-0307.12788

Walstra, P., 1989. Principles of Foam Formation and Stability, in: Foams: Physics, Chemistry and Structure. pp. 1–15. https://doi.org/10.1007/978-1-4471-3807-5_1

Wang, H.H., Sun, D.W., 2002. Melting characteristics of cheese: Analysis of effects of cooking conditions using computer vision technology. J. Food Eng. 51, 305–310. https://doi.org/10.1016/S0260-8774(01)00072-3

Wang, Z., Hirai, S., Kawamura, S., 2022. Challenges and Opportunities in Robotic Food Handling: A Review. Front. Robot. AI 8, 1–12. https://doi.org/10.3389/frobt.2021.789107

Warncke, M., Kulozik, U., 2020. Impact of temperature and high pressure homogenization on the solubility and rheological behavior of reconstituted dairy powders of different composition. Powder Technol. 376, 285–295. https://doi.org/10.1016/j.powtec.2020.08.039

WHO, 2009. Acceptable medical reasons for use of breast-milk substitutes, WHO.

WHO, 2007. Safe preparation, storage and handling of powdered infant formula - Guidelines [WWW Document]. WHO. URL https://iris.who.int/bitstream/handle/10665/43659/9789241595414_eng.pdf

Wickham, H., 2016. ggplot2: Elegant Graphics for Data Analysis. Springer-Verlag New York.

Wilson, M., 2010. Developments in robot applications for food manufacturing. Ind. Rob. 37, 498–502. https://doi.org/10.1108/01439911011081632

Winter, W., Huber, L., 2000. Implementing 21 CFR Part 11 in analytical laboratories, Part 3: Ensuring data integrity in electronic records. BioPharm 13, 45 – 49.

Wu, D., Sun, D.W., 2013. Colour measurements by computer vision for food quality control - A review. Trends Food Sci. Technol. 29, 5–20. https://doi.org/10.1016/j.tifs.2012.08.004

Wu, S., Cronin, K., Fitzpatrick, J., Miao, S., 2021. Updating insights into the rehydration of dairy-based powder and the achievement of functionality. Crit. Rev. Food Sci. Nutr. 62, 6664–6681. https://doi.org/10.1080/10408398.2021.1904203

Xiong, X., Ho, M.T., Bhandari, B., Bansal, N., 2020. Foaming properties of milk protein dispersions at different protein content and casein to whey protein ratios. Int. Dairy J. 109, 104758. https://doi.org/10.1016/j.idairyj.2020.104758

Xu, G., Zaitoun, B.J., O'Shea, N., O'Donnell, C.P., Amamcharla, J.K., 2024. Investigation of the rehydration characteristics of dairy and infant formula powders using focused beam reflectance measurement and electrical resistance tomography. Int. J. Dairy Technol.

YASKAWA, 2022. MotoMINI.

Zaatari, S. El, Wang, Y., Hu, Y., Li, W., 2021. An improved approach of task-parameterized learning from demonstrations for cobots in dynamic manufacturing. J. Intell. Manuf. https://doi.org/10.1007/s10845-021-01743-w

Zacaron, T.M., Francisquini, J.D.A., Perrone, Í.T., Stephani, R., 2023. The effect of homogenisation pressure on the microstructure of milk during evaporation and drying: Particle-size distribution, electronic scanning microscopy, water activity and isotherm. J. Dairy Res. 90, 299–305. https://doi.org/10.1017/S0022029923000456

Zhou, L., Zhang, C., Liu, F., Qiu, Z., He, Y., 2019. Application of Deep Learning in Food: A Review. Compr. Rev. Food Sci. Food Saf. 18, 1793–1811. https://doi.org/10.1111/1541-4337.12492

Zhu, Z., Hu, H., 2018. Robot learning from demonstration in robotic assembly: A survey. Robotics

7. https://doi.org/10.3390/robotics7020017

Appendices

Appendix 1 Standard Operating Procedure for participants to rate cobot-taken images

Standard Operating Procedure for rating sample images

General Information

Thank you for taking the time to participate in this study.

There are three measurements from sample images that need to be reported by you:

- **Foam** height (reading the height using the ruler in the images)
- **Sediment** height (reading the height using the ruler in the images)
- Presence of **white particles** (comparing each image with six reference pictures and assigning a number between 1 to 6)

For each of the above defects, there is a unique folder including 36 images to be rated by you. Also, an "Excel File (measurement)" folder containing an Excel file is provided for entering the measurements (the numbers you assign). All images include their own specific label as shown in the red rectangular in Figure 1. In the **white particles** folder, to facilitate the comparison of the sample images with the reference pictures, a single webpage is provided that contains all 36 images, as well as the six reference pictures.

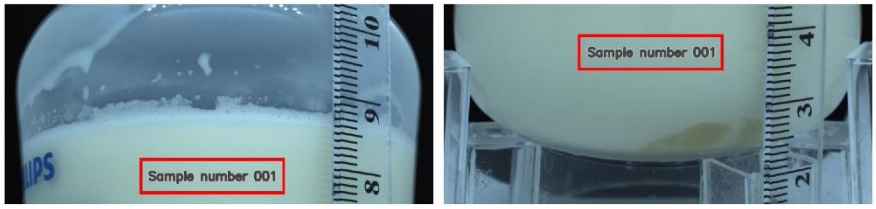

Figure 1 Position of labels in the images (red rectangular)

The following sections provide some guidelines for conducting the measurements.

1. Foam Height

For the foam height measurement, there are a total of 36 images to be measured by you. According to Figure 2, a metric ruler is placed alongside the bottle.

- You should report the foam height in mm read from the ruler.
- You can zoom into the images and count the number of ruler grades that show the presence of foam as millimeters (Figure 3).
- The region where you report foam height should be as close to the ruler as possible.
- The numbers on the ruler do not matter in this study, however, they might be used for easier reading.
- There can be an accuracy of 0.5 mm in the reported numbers (e.g., you might report the foam height equal to 3.5 mm).
- Important points regarding **foam appearance**:

1

- Some samples may contain both large and very small bubbles (for example, a foam layer may contain large bubbles on top and very small bubbles underneath). In this case:
  - All bubble sizes should be considered foam.
  - The color change may assist in detecting very small bubbles.
- Foam shape can vary greatly from sample to sample.
- Please do not consider unconnected foam regions as foam in case this occurs.

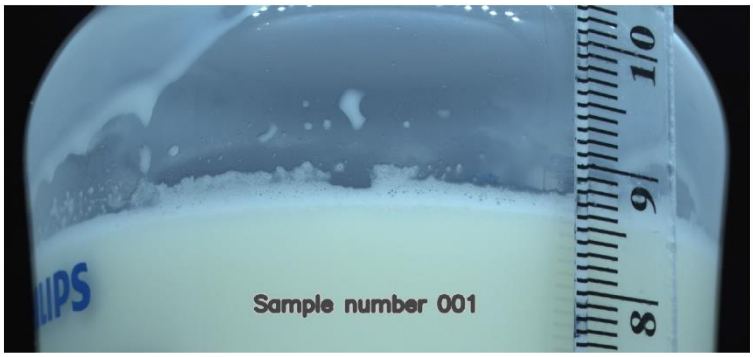

Figure 2 A sample image in the foam folder to be rated by you

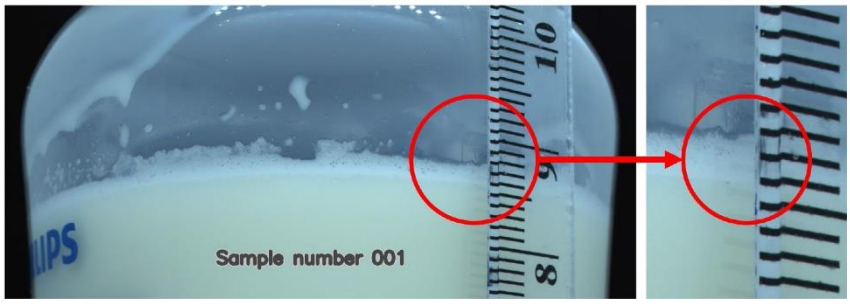

Figure 3 Measuring foam height

2. Sediment Height

For the sediment height measurement, similarly, there are a total of 36 images to be measured by you. According to Figure 4, a metric ruler is placed alongside the bottle.

- You should report the sediment height in mm based on the ruler.
- You can zoom into the images and count the number of ruler grades that show the presence of sediment as millimeters (Figure 5).
- The region where you report sediment height should be as close to the ruler as possible.
- The numbers on the ruler do not matter in this study, however, they might be used for easier reading.
- There can be an accuracy of 0.5 mm in the reported numbers (e.g., you might report the sediment height equal to 3.5 mm)
- Important points regarding **sediment appearance**:
    - Some samples may exhibit a clear boundary between sediment and liquid, while some samples may show a smooth boundary (Figure 6). In this case:
        - You should consider the highest visible boundary to be the upper boundary, and the bottom of the bottle (mixture) to be the lower boundary.
        - If the ruler creates shadows or reflections on the bottom of the bottle, you can use colour changes in regions farther away from the ruler to assist in locating the sediment boundary. However, please ensure that you measure the height next to the ruler.
    - Sediment colors can vary greatly between samples.

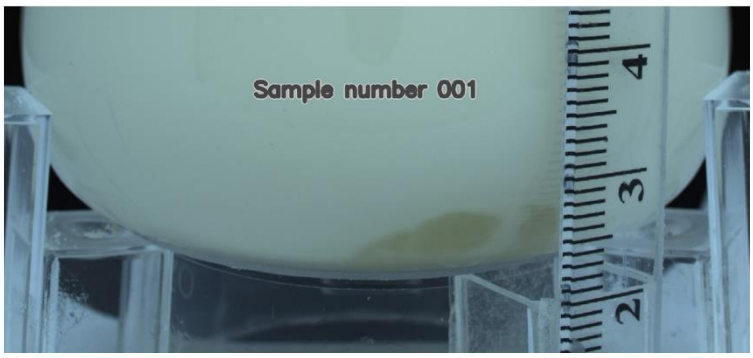

Figure 4 A sample image in the sediment folder to be rated by you

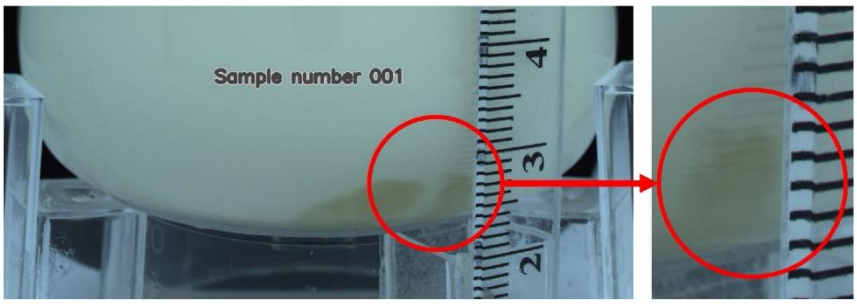

Figure 5 Measuring sediment height

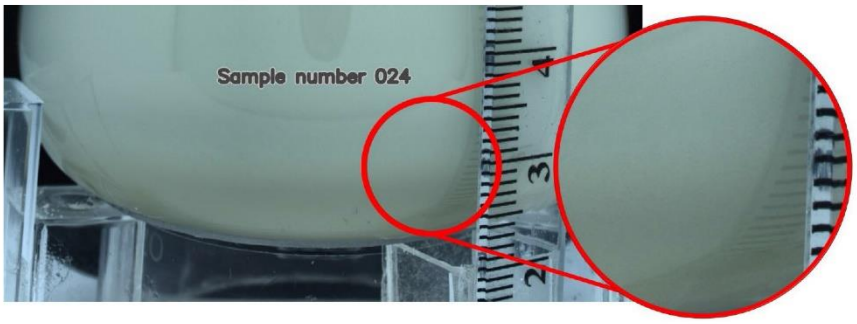

Figure 6 Sediment with smooth boundary around the 3 cm mark on the ruler

3. White Particles

Some samples may contain white particles adhered to the bottle sidewall at the top of the liquid (Figure 8). For the measurement of the white particles, there is a total of 36 images. The ruler in the images is not required for this measurement.

- A web page has been provided in the white particles folder to facilitate rating this defect. The sample images as well as the reference pictures can be viewed by opening the web page (Google Chrome is recommended for opening the web page). Based on the reference pictures shown in Figure 7, you should assign a score from 1 to 6 to each sample image to express your assessment of the presence of white particles (clicking on the left or right arrows changes the sample images, and scrolling down or up changes the reference pictures).
- Score 1 and score 6 respectively indicate the lowest and highest number of white particles.
- The presence of foam, mixture droplets, or water vapor in the bottle sidewall does not matter in this measurement and should not be reported as white particles (Figure 8).

- The region where you report white particles can be anywhere in the sidewall of the bottle above the liquid.

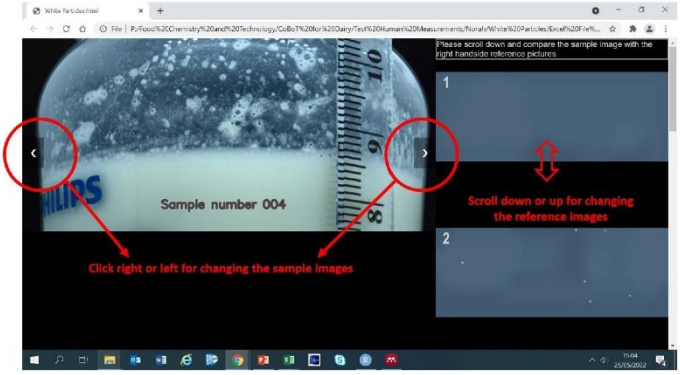

Figure 7 Sample images (left) and reference pictures (right) for rating white particles

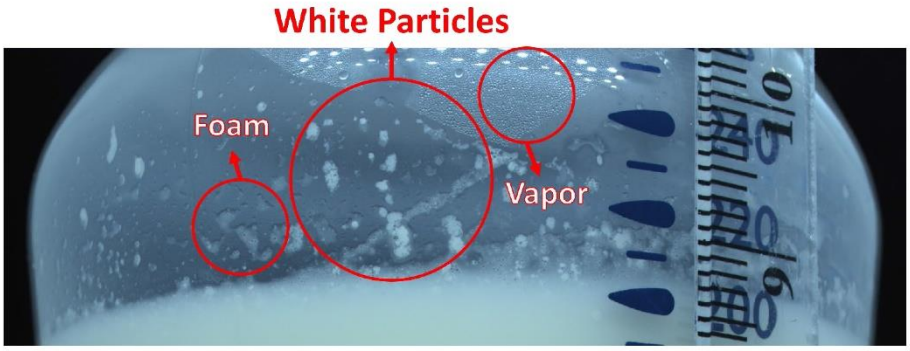

Figure 8 An example showing white particles which should be considered when rating and other observations such as foam and vapour which should be ignored

5

Standard Operating Procedure (SOP)

Standard Operating Procedure for Infant Formula Bottle Agitation

Thank you for taking the time to participate in this study.
In this study, you are being asked to agitate an infant formula bottle six times using two different agitation styles (three repetitions for each agitation style):

- Three repetitions of **Shake** style agitation
- Three repetitions of **Swirl** style agitation

Apparatus:

- An infant bottle containing milk will be provided to you.
- In order for us to measure bottle movements, a small sensor (2 × 3 × 1 cm) and some tags are already attached to the bottle.
- A camera will be used to film your arm and bottle movements.

Outline:
Figure 1 and Figure 2 illustrate the outlines of the two agitation styles. A sensor and a camera will record your arm's movements as you shake the bottle. Your arm will be the only part of your body visible to the camera (in the event that you move within the camera's field of view and your face is accidentally recorded, the video will be modified by cropping out or blocking out your face, and the original video will be deleted). You may use either hand. The mixture temperature will be room temperature. The camera data will be used for both image processing, which estimates the bottle pose, and for better visualizing the IMU sensor data.
Performing the agitations:
Performing each agitation style follows a general procedure as follows:
Shake Agitation:

- An infant bottle containing milk will be provided to you.
- Figure 1 illustrates the shaking motion. It should be noted that this is only an indicative illustration. Your personal preferences will ultimately determine the details of the motion.
- During the experiment, the experimenter will instruct you on how to proceed:
    1. Initially, you will be instructed to hold the bottle steady. When you are ready to begin, the experimenter will instruct you to tap the bottle cap in order to synchronise the sensor and video. The bottle should be held steady again after the tap.
    2. After five seconds, you will be instructed to **shake** the bottle. You should now begin shaking the bottle.
    3. After a further fifteen seconds, the experimenter will prompt you to stop shaking the bottle and hold the bottle steady. At this point, please cease shaking the bottle and keep it in the rest position for a few seconds until the experimenter indicates that the experiment is completed.
- You will be instructed to complete the shake agitation experiment three times.

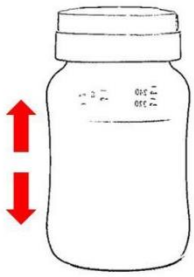

Figure 1 Shake agitation indicative illustration

Swirl Agitation:

- An infant bottle containing milk will be provided to you
- Figure 2 illustrates the swirl motion. It should be noted that this is only an indicative illustration. Your personal preferences will ultimately determine the details of the motion.
- During the experiment, the experimenter will instruct you on how to proceed:
    1. Initially, you will be instructed to hold the bottle steady. When you are ready to begin, the experimenter will instruct you to tap the bottle cap in order to synchronise the sensor and video. The bottle should be held steady again after the tap.
    2. After five seconds, you will be instructed to **swirl** the bottle. You should now begin swirling the bottle.
    3. After a further fifteen seconds, the experimenter will prompt you to stop swirling the bottle and hold the bottle steady. At this point, please cease swirling the bottle and keep it in the rest position for a few seconds until the experimenter indicates that the experiment is completed.
- You will be instructed to complete the swirl agitation experiment three times.

Figure 2 Swirl agitation indicative illustration

After you have repeated the Shake and Swirl agitation experiments as described above, the data collection from you will be completed.